MODELLING OF CONDENSATION HEAT TRANSFER IN A REACTOR CONTAINMENT

by

Moo-Hwan Kim

A thesis submitted in partial fulfillment of
the requirement for the degree of

DOCTOR OF PHILOSOPHY
(Nuclear Engineering)

at the
UNIVERSITY OF WISCONSIN-MADISON
1985

ACKNOWLEDGEMENT

I would like to express my best gratitude to my advisor Professor Michael L. Corradini. His patient guidance and continuous encouragement were invaluable for this work. The academic attitude I learned from him will be carried along with me throughout my life.

My special thanks go to Professor Gregory A. Moses and the RETRAN and KMC research groups for their valuable advice and cooperation.

I am grateful to J.J. Barry for his helpful assistance and continuous inspiration in this research. Faustino Gonzales was appreciated for providing good software to type this thesis and draw the figures.

My deep and heartly thanks go to my family; my wife, Hyunjoo, for her endless love, sacrifice and continuous support during this work; two sons, Bumjoon and Hongjoon, for being there.

My parents who sacrificed themselves for my being away from them, I cannot thank enough.

I gratefully acknowledge the financial support from Wisconsin Public Service, Westinghouse Electric Co. and the scholarship from Graduate School of University of Wisconsin-Madison

LIST OF TABLES

NOMENCLATURE

a	:	gravitational acceleration
A	:	wave amplitude
A^+	:	Van Driest Constant
C_f	:	friction coefficient
C_p	:	specific heat at constant pressure
D_{AB}	:	binary diffusivity for system A-B
f	:	friction factor
g	:	mass-transfer conductance
G	:	mass flux of x direction
Gr	:	Grashof number
h	:	heat transfer coefficient
i	:	enthalpy
k	:	turbulent kinetic energy
k^*	:	constant in universal velocity profile
k_s	:	equivalent "sand grain" roughness
K	:	thermal conductivity
L	:	length of plate
m^*	:	mass flux of y direction
M	:	molecular weight of A
Nu	:	Nusselt number
Pr	:	Prandtl number
Pr_t	:	turbulent Prandtl number
q^*	:	heat flux
Re	:	Reynolds number
Sc	:	Schmit number
Sc_t	:	turbulent Schmit number
Sh	:	Sherwood number
St	:	Stanton number
T	:	Temperature
u	:	velocity
x	:	distance down the plate
X	:	mass fraction of species i

Chapter 1
INTRODUCTION

During a postulated light water reactor accident (e.g. Loss of Coolant Accident), an important concern is how to predict the pressure-temperature response in the containment building. This is because the flashing high energy coolant released from the primary system can significantly contribute to a rise in the containment pressure, perhaps threatening its structural integrity. To reduce the steam pressure, both active and passive safeguard systems are used in current containment designs. The active systems include containment sprays, fan coolers, ice condensers and suppression pool cooling. The passive systems, which are the convective heat transfer to the containment wall and internal structural components, have an important role as an inherent safety feature. If the wall surface temperature is below the dewpoint, the heat transfer rate is able to be greatly increased by condensation, which is the subject of this report.

Even though condensation phenomena can be classified into dropwise and film condensation modes, dropwise condensation usually changes quickly to film condensation during the initial period of condensation and probably would not affect the final containment pressure-temperature response [1]. In this work we focus on film condensation heat transfer. Rates of heat transfer for film condensation can be predicted as a function of bulk and surface temperatures, total bulk pressure, surface and liquid film characteristics, bulk velocity and the presence of noncondensable gases. Even though film condensation has been investigated extensively, the majority of these studies were devoted to laminar film condensation (laminar bulk flow and laminar film). Since

air flow. The past work in condensation phenomena in a reactor containment are reviewed.

The simple model and two-dimensional model are described in chapter 3. The analyses are presented in chapter 4 by comparing these models to 'separate effects' experiments and integral test data. Finally, conclusions and recommendations are presented in chapter 5

the wavy interface, which is expected for vertically falling film, is investigated.

The model for the turbulent vapor-air flow and the effect of the turbulent flow on the condensation phenomena are presented, since the vapor-gas flow in the containment and the condensate film are supposed to be turbulent under some conditions.

After the review of condensation theories and experiments, the characteristics of a falling film and the model for the turbulent flow, the previous investigations of condensation phenomena in a reactor containment during a postulated accident are described.

2.2 Theoretical Developments of Condensation

2.2.1 Stationary Pure Vapor

For filmwise condensation of a "stationary" saturated vapor, Nusselt [5] presented the first analytical solution for heat transfer on a plane surface with the following assumptions [6]:

1) the flow of condensate in the film is laminar,
2) the fluid properties are constant,
3) subcooling of the condensate may be neglected,
4) momentum convective changes through the film are negligible,
5) the vapor is stationary and exerts no drag on the downward motion of the condensate,
6) heat transfer is by conduction only.

From a force balance on an element of film lying between y and δ in Fig. 2.1,

$$(\delta - y)\, dx\, (\rho_l - \rho_g)\, g \sin\theta = \mu_l \left(\frac{du_x}{dy}\right) dx \qquad (2.2.1\text{-}1)$$

Nusselt's assumptions. In particular, Bromley [7] considered the effects of subcooling within the liquid film and Rohsenow [8] also allowed the non-linear distribution of temperature through the film due to energy convection. The results indicated that the latent heat of vaporization, i_{fg}, in eq.(2.2.1-6) should be replaced by

$$i'_{fg} = i_{fg}\left[1 + 0.68\left(\frac{C_{pl}\Delta T_l}{i_{fg}}\right)\right] \qquad (2.2.1\text{-}8)$$

However, it should be noted that in most engineering applications, the value of $C_{pl}\Delta T/i_{fg}$ is small (typically less than 0.001) and can be neglected.

Sparrow and Gregg [9] removed assumption (4) and included inertia forces and a convection term within the condensate film by using a boundary layer treatment for the condensate film. The governing partial differential equations were reduced to ordinary differential equations by means of similarity transformations. For common fluids with Prandtl numbers around and greater than unity, inertia effects are negligible for values of $C_{pl}\Delta T/i_{fg}$ less than 2.0. For liquid metals with very low Prandtl numbers, however, the heat transfer coefficient falls below the Nusselt prediction with increasing $C_{pl}\Delta T/i_{fg}$ when $C_{pl}\Delta T/i_{fg}$ is greater than 0.001.

Poots and Mills [10] have looked at the effect of variable physical properties (assumption 2) on vertical plates.

More recently, Koh et al. [11] and Chen [12] included the influence of the drag exerted by the vapor on the liquid film. This interfacial shear stress also necessitated consideration of the vapor boundary layer. Both of them treated the condensate film and the vapor layer on the basis of boundary layer equations with appropriate conditions at the interface. Koh et al.

which means that the interfacial shear stress approaches the 'frictional' shear stress for single-phase flow over an impermeable plate for low condensation rates, while in the other extreme case of high condensation rates, it approaches the asymptotic value of momentum transfer rate of condensing vapor, τ_M.

$$\tau_M = \dot{m}'' (u_\infty - u_\delta) \qquad (2.2.2\text{-}3)$$

where u_δ was assumed to be zero in his own work. From these solutions, the local Nusselt number is given by

$$\frac{Nu}{\sqrt{Re}} \left(\frac{\nu}{\nu_v}\right)^{\frac{1}{2}} = \left(\frac{G_w''}{4}\right) \left(\left(\frac{\nu_v}{\nu}\right)^{\frac{1}{2}} \left(\frac{\rho_v}{\rho}\right) \left(\frac{Pr\ i_{fg}}{C_p\ \Delta T}\right)\right)^{\frac{1}{2}} \qquad (2.2.2\text{-}4)$$

where

G_w'' : tabulated value as a function of G_w, the suction parameter [14]

and the following asymptotic relations similar to Eq. (2.2.2-1) and (2.2.2-2) were derived

$$\frac{Nu}{\sqrt{Re}} \left(\frac{\nu}{\nu_v}\right)^{\frac{1}{2}} = 0.436 \left[\left(\frac{\nu_x}{\nu}\right)^{\frac{1}{2}} \left[\left(\frac{\rho_v}{\rho}\left(\frac{Pri_{fg}}{C_p\ \Delta T}\right)\right)\right]\right]^{\frac{1}{4}}$$

$$\text{for small } \left(\frac{\nu}{\nu_v}\right)^{\frac{1}{2}} \left(\frac{\rho}{\rho_v}\right) \left(\frac{C_p\ \Delta T}{Pr\ i_{fg}}\right) \qquad (2.2.2\text{-}5)$$

$$\frac{Nu}{Re} \left(\frac{\nu}{\nu_v}\right)^{\frac{1}{2}} = 0.5 \qquad \text{for large } \left(\frac{\nu}{\nu_v}\right)^{\frac{1}{2}} \left(\frac{\rho}{\rho_v}\right) \left(\frac{C_p\ \Delta T}{Pr\ i_{fg}}\right) \qquad (2.2.2\text{-}6)$$

Cess further suggested that it is permissible for $C_{pl}\Delta T/(Pr\ i_{fg}) \ll 30$ to neglect the inertia forces and for

This result corresponds to Eq. (2.2.2-6) which is Cess's result for high condensation rates when N is much less than 1. (This is generally true for non metallic liquids.) It means that Cess's assumption ($u_\delta = 0$) is valid for this case.

Shekriladze and Gomelauri also considered the case of an isothermal vertical plate with the same assumptions. (The effects of inertia forces and energy convection within the condensate film were neglected. In addition, the interfacial velocity u_δ was assumed to be zero for this calculation.) Only Eq. (2.2.2-7) is changed to

$$\frac{d^2 u_x}{dy^2} + \rho g = 0 \qquad (2.2.2\text{-}12)$$

with the same other equations and boundary conditions. The results are

$$h_{film}(x) = \frac{1}{2}\sqrt{\left(\frac{k_l^2 \rho_l u_\infty}{\mu_l x}\right)\left(\frac{1+\sqrt{\left(1+\frac{16ax}{u_\infty N}\right)}}{2}\right)} \qquad (2.2.2\text{-}13)$$

It was revieved that the interfacial shear stress, τ_I, has two asymptotic values, Eq. (2.2.2-1), vapor friction on the film, and Eq. (2.2.2-2) which is momentum drag as the vapor condenses on the slower moving film. Mayhew et. al. [16,17] attempted to expand Nusselt's simple approach to take account of both forms of drag by using a very simple interpolation formula,

$$\tau_I = \tau_F + \tau_M \qquad (2.2.2\text{-}14)$$

and

$$\mu\left(\frac{du_x}{dy}\right)dx = (\delta - y)(\rho_l - \rho_v)a\,dx + \tau_F dx + d\Gamma(u_\infty - u_\delta) \qquad (2.2.2\text{-}15)$$

comparison with the experimental data. It is interesting to note that the result of Shekriladze and Gomelauri corresponds to the case Dr = 0, ψ = 1 of Mayhew's calculation.

South and Denny [19] proposed an interpolation formula of the form for the interfacial shear stress,

$$\tau_I = (\tau_F^n + \tau_M^n)^{\frac{1}{n}} \qquad (2.2.2\text{-}19)$$

where n = 1.375 was suggested to give good agreement with the numerical results for both the flat plate and stagnation point flow over the entire range of the suction parameter as shown in Fig. 2.3. However, in view of the fact that the contribution of τ_F to τ_I is small except for very low condensation rates, such an interpolation formula would only lead to a small difference in the heat transfer with the result from $\tau_I = \tau_F$.

Jacobs [20] used an integral method to solve the boundary layer equation for the condensate film and the vapor boundary layer by matching the mass flux, shear stress, temperature and velocity at the interface. The inertia and convection terms in the boundary layer equations of the liquid film were neglected. The variation of the physical properties and the thermal resistance at the vapor-liquid interface were also neglected. Since Jacobs used an incorrect boundary condition for the vapor boundary layer ($u_y = 0$ instead of $\frac{\partial u_x}{\partial y} = 0$ at bulk), Fujii and Uehara [21] solved the same problem with the correct boundary condition. In addition, the velocity profile in the vapor layer was taken as a quadratic formula of $(y-\delta)$.

They presented the numerical results and their approximate expressions for the cases of free convection, forced convection, and combined free and forced convection. The results show good agreement with the

surface are restricted within some limitations and where Nu_L is smaller than 2×10^4. When the predicted Nu_L is larger than 2×10^4, the experimental Nu_L is about from 1.3 to 1.9 times as large as the predicted one except for the cases of small heat flux as shown in Fig. 2.4. These high Nu_L experimental data were reported by Goodykoontz and Dorsh [23,24] and Jacob et al. [22], who performed the experiments by condensing steam on the inner surface of a cylinder with a range of steam flow velocity of 10 - 60 m/s [22], 20-70 m/s [23] and 95-310 m/s [24]. The authors attributed this discrepancy to the turbulence in the liquid film from the very high vapor velocity.

2.2.3 Stationary Vapor with a Noncondensable Gas

Air, a noncondensable gas, exists in a containment and leads to a significant reduction in heat transfer during condensation. An air-vapor boundary layer forms next to the condensate layer and the partial pressures of air and vapor vary through the boundary layer as shown in Fig. 2.5. The build-up of noncondensable gas near the condensate film inhibits the diffusion of the vapor from the bulk mixture to the liquid film and reduces the rate of mass and energy transfer. Therefore, it is necessary to solve simultaneously the conservation equations of mass, momentum and energy for both the condensate film and the vapor-gas boundary layer together with the conservation of species for the vapor-gas layer. At the interface, a continuity condition of mass, momentum and energy has to be satisfied.

For a stagnant vapor-gas mixture, Sparrow and Eckert [25] and Sparrow and Lin [26] solved the mass, momentum and energy equations for laminar film condensation on an isothermal vertical plate by using a similarity

2.2.4 Moving Vapor with a Noncondensible Gas

For a laminar vapor-gas mixture case, Sparrow et. al. [29] solved the conservation equations for the liquid film and the vapor-air boundary layer neglecting inertia and convection in the liquid layer and assuming the streamwise velocity component at the interface to be zero in the computation of the velocity field in the vapor-gas boundary layer. Also a reference temperature was used for the evaluation of properties. The results showed that the effect of noncondensable gas for the moving vapor-gas mixture case is much less than for the corresponding stationary vapor-gas mixture. A moving vapor-gas mixture is considered to have a 'sweeping' effect, thereby resulting in a lower gas concentration at the interface (compared to the corresponding stationary vapor-gas mixture case). Also, the ratio of the heat flux with a noncondensable gas to that without a noncondensable gas was calculated to be independent of the bulk velocity (u_B). The computed results reveal that interfacial resistance has a negligible effect on the heat transfer and that superheating has much less of an effect than in the corresponding free convection case.

Koh [30] and Fujii et al. [31] solved this problem without the simplifying assumptions used in [29] except for uniform properties and showed good agreement with the approximate analysis.

Instead of solving a complete set of the conservation equations, Rose [32] used the experimental heat transfer result for flow over a flat plate with suction [33]

$$Nu_x Re_x^{-\frac{1}{2}} = \zeta \left(1 + a\beta_x^b Pr^c \right)^{-1} + \beta_x Pr \qquad (2.2.4\text{-}1)$$

where

simultaneously to give, for specified free stream conditions, the relationship between the vapor mass flux to the condensate surface and the composition at the interface. Eliminating either Z_x ($=Sh_x\ Re_x^{-\frac{1}{2}}$) or β_x he obtained

$$\omega = [\ 1 + \beta_x Sc\ (\ 1 + 0.941\ \beta_x^{1.14} Sc^{0.93})\ /\zeta]^{-1} \qquad (2.2.4\text{-}5)$$

or

$$Z_x + 0.941\ Sc^{-0.21}(\ 1 - \omega)^{1.14} Z_x^{2.14} - \zeta/\omega = 0 \qquad (2.2.4\text{-}6)$$

The results given by equation (2.2.4-5) were compared with the numerical solutions of Sparrow et. al. [29] for a given value of β_x and agreed very well as shown in Table 2.1. The results given by equation (2.2.4-6) were compared with the exact numerical solutions of Koh [30] and Fujii et. al. [31] as shown in Fig. 2.7. The good agreement between the exact numerical solutions and equation (2.2.4-6) confirms the validity of the simplifications made in his work.

Denny et. al. [34,35] also considered the case of downward vapor-gas mixture flow parallel to a vertical flat plate. They presented a numerical solution of similar mass, momentum and energy equations for a vapor-gas mixture by means of a forward marching technique. Interfacial boundary conditions at each step were extracted from a locally valid Nusselt type analysis of the condensate film. Locally variable properties in the condensate film were evaluated by means of the reference temperature concept, while those in the vapor-gas layer were treated exactly. Asano et. al. [36] treated the condensate film as in the Nusselt analysis but assumed the interfacial shear stress was the same as that for single-

and for the local vapor-side Sherwood number is

$$Sh_{x,g} = 0.332\, Re_x^{\frac{1}{2}} Sc_g^{\frac{1}{3}} g_1(B,Sc) \qquad (2.2.4\text{-}10)$$

where $g_1(B,Sc)$ can be understood as a high mass transfer correction factor which was tabulated to be a function of the dimensionless mass transfer driving force B. The numerical results showed good agreement with the numerical solution by Denny et al. for $u_\infty = 0.3$ m/s, L = 0.05 m.

The analytical model described above was solved using only a laminar vapor-gas (or pure vapor) boundary layer except for Mayhew [18]. All complete sets of the conservation equations were solved by assuming a laminar flow for both a condensate film and a vapor-gas layer. Whitley [37] proposed a simple method, which uses the analogy between heat and mass transfer for forced convection condensation of a turbulent mixture boundary layer by neglecting the interfacial velocity and treating the surface of the condensate film to be smooth. The local Nusselt number for a turbulent flow over a flat plate is

$$Nu_{x,g} = 0.0296\, Re_x^{0.8} Pr_g^{0.6} \qquad (2.2.4\text{-}11)$$

The local Sherwood number and mass transfer conductance are

$$Sh_{x,g} = 0.0296\, Re_x^{0.8} Sc_g^{0.6} \qquad (2.2.4\text{-}12)$$

$$g(x) = 0.0296\, c^*\, \rho_g\, u_\infty\, Re_x^{-0.2} Sc_x^{-0.4} \qquad (2.2.4\text{-}13)$$

where

$$c^* = \frac{\ln(1+B)}{B}$$

Mayhew and Aggarval [18] experimented with pure steam condensing on a flat surface. To avoid air in-leakage, the experiments were carried out at pressures slightly above atmospheric. Fig. 2.8 shows good agreement between the experimental results and the calculated values by their own theory (Eq. (2.2.2-17)). It is very interesting to note that the results for the counter-current flow cases are appreciably higher than those predicted by the authors' own model and indeed always higher than the corresponding co-current velocity vapor values. The reason was investigated and explained as follows in the original paper :

"An obvious explanation was provided by dye-injection tests which showed that, with counterflow, no laminar film flow could be achieved. The film was torn off the plate (i.e. flooding occurred) at quite moderate values of vapor velocity. Similar observations with parallel flow confirmed that the film was always both laminar and smooth. From work with noncondensing films it was expected that rippled flow would be encountered over part of the surface at the higher velocities used. In fact remarkably smooth films were observed suggesting that mass transfer, and possibly also surface tension effects on the non-isothermal film, must have had a stabilizing effect."

Recently Asano et al. [38] reported their data for the condensation of pure saturated vapors on a vertical flat copper plate and showed good agreement with the authors' own model (Eqs. (2.2.4-8, 2.2.4-9)).

2.3.3 Stationary Vapor with a Noncondensable Gas

Perhaps the earliest definitive experiment of the

active condensation length. The tube was mounted in a cylindrical pressure vessel 1.52 m O.D. by 3.35 m long. Saturated steam was supplied by an external source and allowed to diffuse to the tube resulting in steady-state, natural convection conditions. An expression, which is a function of ΔT, percent noncondensable gas by volume (Y%) and total pressure (P_{tot}), of the heat transfer coefficient was proposed from the experimental data.

$$h = 149.9\ (\Delta T)^{-1.11}(1-Y/100)^{2.59}(P_{tot})^{0.48} \qquad (2.3.3\text{-}1)$$

where $0.27 < P_{tot} < 0.70$ MPa
$0.0 < Y < 14.0$ %
$\Delta T < 40\ ^{o}C$

Even though this experiment was done over a good range of pressure for a containment analysis and showed a significant effect of pressure, the pipe geometry and length scale make it questionable to apply this correlation to a reactor containment analysis. Unfortunately, the experiment results were not compared with any other theoretical model.

2.3.4 Moving Vapor with a Noncondensable Gas

Rauscher, Mills and Denny [49] performed experiments of filmwise condensation from steam-air mixtures undergoing forced flow over a 0.74 in. O.D. horizontal tube. The heat transfer coefficient at the stagnation point was reported for bulk air mass fractions of 0 - 7 % and oncoming vapor velocity of 1 - 6 ft/s. The reduction in heat transfer for the steam-air mixture was found to be in excellent agreement with the theoretical analysis of Denny and South [50].

turbulence intensity and decreasing the viscous sublayer thickness similarly to the effects of a rough wall. Therefore, the understanding of the structure of the condensate liquid film and the interface on a long vertical wall is important to the study of condensation phenomena on a containment wall.

From the early experimental studies, three different flow regimes have been reported for the falling film on a vertical wall [51]:

1) At Reynolds numbers less than 20 to 30, there exists the usual viscous flow regime.
2) From Reynolds numbers between 30 to 80, a wave regime appears. In this flow regime, the gross flow rate does not deviate appreciably from the laminar parabolic description in spite of the presence of surface waves. Hence, it is sometimes called pseudo-laminar.
3) At Reynolds number larger than 1500 to 2000, the laminar region is replaced by turbulent motion.

Theoretically, there were many investigations made to obtain the analytic solution for the structure of the falling film. For example, Benjamin [52] developed a linear stability theory and Kapitza [53] attempted to solve the nonlinear equation which is derived from the boundary layer equation with kinematic surface condition and tangential and normal shear stress continuity condition. After that, many modifications or other attempts [54, 55, 56, 57] were made. Even though these theoretical analyses partially agreed with the experimental data, analysis generally can not describe the highly nonlinear wave motion with a few terms in a Fourier series.

force causes acceleration and thinning of the waves.

The following papers by Chu and Dukler [59,60] concluded that the small waves which cover the substrate in the falling film control the fluid resistance and transport processes in the gas boundary layer since the substrate is present for a large portion of time, while the large waves control these same processes in the liquid film since the large waves carry a large portion of liquid mass. Fig. 2.12 shows that the liquid flow rate has a strong effect on the probability density distribution of substrate thickness and the maximum peak value decreases rapidly with decreasing liquid flow rate. On the other hand, the gas flow rate has only a small effect on the maximum peak value and the spread of the curve. Also, Fig. 2.13 shows that increasing gas flow rate decreases the substrate thickness on the liquid film.

Fig. 2.14 shows that the probability densities of substrate wave amplitude f (A_s) is located remarkably near the same value, within 0.0128 mm, for all liquid rates in the absence of gas flow. From this phenomenon, it was suggested that the waves that are formed are all of same amplitude and that a process of dispersion or coalescence generates waves of other sizes. This dispersion and coalescence increases as the flow rate increases. The wave amplitude is insensitive to gas flow as shown at Fig. 2.15, even though the average substrate film thickness is sensitive as shown at Fig. 2.13.

On the other hand, probability density functions of large wave amplitudes display well defined multiple peaks except for the lowest film Reynolds number as shown in Fig. 2.16. This suggests the existence of several discrete large waves. At low liquid rates (Re_L < 700), one characteristic wave amplitude was presented with a modal value of about 0.05 mm. If Fig. 2.16 is compared with Fig.

strongly on the distance as well as the liquid and gaseous film Reynolds number. The critical Reynolds number, where the flow is supposed to change from laminar to turbulent, varies with the longitudinal distance as shown at Fig. 2.19. Fig. 2.20 shows a typical result of the longitudinal effect for Re_L = 576. In this figure, small amplitudes of less than 0.1 mm and high frequencies (100 Hz) were reported in the entrance region (0.1 m). This changed to ripple type waves of about 0.3 mm in amplitude and about 50 Hz frequency at 0.3 m. After 0.5 m, large waves (0.5 mm amplitude and 10 - 20 Hz frequency) were reported. These large waves and the substrates are similar to the two-wave system which was revieved before. Takahama also measured the increase of surface area due to interfacial waves and found that the increment is very small. This means that the promotion of heat and mass transfer between the two-phases is not due to an increase of the interfacial surface area but to the disturbance effect of the wavy motion.

Recently, the simulation of a vertical wavy film was solved analytically by using a finite-element method by P. Bach and J. Villadsen [63]. The computed result (Fig. 2.21) shows the characteristic features (the deep trough, the steep forefront and much smoother receding back of the wave) of a falling film wave which were reported by the previous experiment. Another important result of this calculation is the dramatic increase of y component velocity before the wave front (point E at Fig. 2.21 and Table 2.3). It means that a fluid particle, which is at a position quite close to the wall at that point, accelerates very rapidly out of the trough. It is swept towards the surface of the liquid and past the crest of the large wave before settling down in the smooth flow behind the wave. This phenomena must greatly enhance the

intensity and decreasing the viscous sublayer. This effect was correlated by comparing drag on the wavy surfaces to that on a roughened surface. As a conclusion, even though the numerical solution by P. Bach and J. Villadson recently, shows some possibility for solving for the wave motion, experimental correlation is still a better tool than numerical solution to represent the characteristics of the falling film and the effect of a wavy interface in promoting transport phenomena.

2.5 Turbulent Condensation

2.5.1 Turbulent film condensation

For long vertical surfaces, it is possible to obtain condensation rates such that the film Reynolds number exceeds the critical value at which turbulence begins. Kirkbride [67] found that the heat transfer coefficient is much greater than the value calculated from Nusselt's theory on this turbulent condensate film.

After his experiment, Colburn [68] reviewed the results of Kirkbride and developed the following correlation for the heat transfer coefficient of the turbulent condensate film by using the analogy with the flow of liquids through pipes under conditions where the liquid completely filled the pipe. In this work the critical film Reynolds number was taken as 2000.

$$\frac{h(x)}{K_l}\left[\frac{\mu_l^2}{\rho_l(\rho_l-\rho_g)g}\right]^{\frac{1}{3}} = 0.056\, Re_l^{0.2}\, Pr_l^{\frac{1}{3}} \qquad (2.5.1\text{-}1)$$

This analysis was extended by Carpenter and Colburn [69] to propose the following correlation which included the effect of vapor shear stress.

order of 10,000 with interfacial shear. Therefore, he suggested that neither true laminar nor fully developed turbulent flow exists in the film and the combined mechanism was considered at all points in the film. The Deissler equation near a solid boundary and Von-Karman's equation at the region of y^+ larger than 20 for the eddy viscosity were used to model the turbulent motion as follows:

$$\varepsilon = n^2 u y \left(1-\exp\left(-\frac{n^2 u y}{\mu_1/\rho_1}\right)\right) \quad \text{for } y^+ \ 20 \quad (2.5.1\text{-}3)$$

$$\varepsilon = X \left(\frac{du}{dy}\right)^3 \left(\frac{d^2u}{dy^2}\right)^2 \quad \text{for } y^+ \ 20 \quad (2.5.1\text{-}4)$$

where n and X are numerical constants.

This model was solved digitally by using a computer. It was found that the velocity distribution curve in the liquid film depends both on the interfacial shear and on the film thickness while the universal velocity distribution is usual in full pipe flow. The results agree well with Nusselt values at very low Reynolds number and with Carpenter's experimental data in the turbulent region. There is also good agreement with Seban's analysis at high Reynolds numbers and Prandtl numbers. Lee[73], however, pointed out that the fall-off in the heat transfer rate for small Prandtl numbers was greatly over-estimated since Dukler neglected the molecular thermal conductivity with respect to the eddy conductivity in defining the temperature profile at values of y^+ greater than 20. He has repeated Dukler's calculation using an improved velocity profile and considering the molecular conductivity term and obtained a solution which is very close to Dukler's results at high Prandtl numbers and to

C = wave celerity

The analogous dimensionless heat transfer equations are used by Bankoff [75] as follows:

$$Nu_t = 0.25\ Re_t\ Pr^{\frac{1}{2}} \quad \text{for } Re_t > 500 \qquad (2.5.1\text{-}8)$$

$$Nu_t = 0.7\ F\ Re_t^{\frac{1}{2}}\ Pr^{\frac{1}{2}} \quad \text{for } Re_t < 500 \qquad (2.5.1\text{-}9)$$

where the turbulent Nusselt number is given by $Nu_t = hl_t/k$. He used these correlations with $u_t = 0.3\ u_l$ and $l_t = \delta$ for the horizontal cocurrent steam-water flow and got a good fit of his own horizontal condensation experimental data and the value predicted by Eq (2.5.1-9).

H.J. Kim and S.G. Bankoff [76] presented another correlation as follows for countercurrent steam-water flow in an inclined channel, where the interface is expected to be more agitated by countercurrent flow and the inclined surface than the horizontal cocurrent flow.

$$Nu_t = 0.061\ Re_t^{1.12}\ Pr^{0.5} \qquad (2.5.1\text{-}10)$$

where, $u_t = \sqrt{\tau_I / \rho}$

$l_t = A$

As a conclusion, even though some theoretical predictions before 1970 agree well with the experimental data in some specific range, they do not consider the physical structure of the falling film. On the other hand, although the use of a turbulence-centered model appears to take into account the physical structure of the turbulent

$$\overline{-u'\rho'_i} = D_t \frac{\partial \overline{\rho}_i}{\partial x_j} \qquad (2.5.2\text{-}3)$$

The transport equation for $\overline{u_i u_j}$ is transformed to the turbulent kinetic energy equation by the contraction, j-i, which can be expressed as:

$$\frac{Dk}{Dt} = \frac{1}{\rho}\frac{\partial}{\partial x_k}\left[\frac{\mu_t}{\sigma_k}\frac{\partial k}{\partial x_k}\right] + \frac{\mu_t}{\rho}\left(\frac{\partial u_i}{\partial x_k} + \frac{\partial u_k}{\partial x_i}\right)\frac{\partial u_i}{\partial x_k} - \varepsilon \qquad (2.5.2\text{-}4)$$

Also, the turbulence dissipation equation can be derived in a similar way with some assumptions.

$$\frac{D\varepsilon}{Dt} = \frac{1}{\rho}\frac{\partial}{\partial x_k}\left[\frac{\mu_t}{\sigma_\varepsilon}\frac{\partial \varepsilon}{\partial x_k}\right] \qquad (2.5.2\text{-}5)$$

$$+ \frac{C_1 \mu_t}{\rho}\frac{\varepsilon}{k}\left(\frac{\partial u_i}{\partial x_k} + \frac{\partial u_k}{\partial x_i}\right)\frac{\partial u_i}{\partial x_k} - C_2\frac{\varepsilon^2}{k}$$

where the turbulent viscosity μ_t can be calculated by

$$\mu_t = \frac{C_\mu \rho k^2}{\varepsilon} \qquad (2.5.2\text{-}6)$$

The values of the constants appearing in Eqs. (2.5.2-4) - (2.5.2-6) were suggested as follows by Launder et al. [81].

assigned in the ordinary k-ε model, while C_μ and C_2 are to vary with turbulence Reynolds number according to the formulae:

$$C_\mu = C_{\mu o} \exp[-2.5/(1+Re_t/50.)] \qquad (2.5.2\text{-}9)$$

$$C_2 = C_{2o} \exp[1.0 - 0.3 \exp(-Re_t^2)] \qquad (2.5.2\text{-}10)$$

where

$$Re_t = \frac{k^2}{\nu\varepsilon}$$

where $C_{\mu o}$ and C_{2o} are the values assumed by C_μ and C_2 in the fully turbulent region.

Wall Function Method

In this method, the effective viscosity near the wall is deduced not from the k-ε model described above, but from the implications of the universal velocity profile. The fluxes of momentum and heat to the wall are calculated by the following correlations.

$$\frac{u_p}{(\tau/\rho)_w} C_\mu^{\frac{1}{4}} k_p^{\frac{1}{2}} = \frac{1}{k^*} \ln[E y_p \frac{(C_\mu^{\frac{1}{4}} k_p)^{\frac{1}{2}}}{\nu}] \qquad (2.5.2\text{-}11)$$

$$\frac{(T_p - T_w)\, C_p \rho\, C^{\frac{1}{4}}\, k_p^{\frac{1}{2}}}{q_w''} = \frac{Pr_t}{k^*} \ln[\frac{E\, y_p\, (C_\mu^{\frac{1}{4}} k_p)^{\frac{1}{2}}}{\nu}] + Pr_t \frac{\pi/4}{\sin \pi/4} (\frac{A^+}{k^*})^{\frac{1}{2}} (\frac{Pr}{Pr_t} - 1)(\frac{Pr}{Pr_t})^{-\frac{1}{4}} \qquad (2.5.2\text{-}12)$$

1) It is economical in computational time and storage. That is, it produces relatively accurate results with fewer node points within the boundary layer, since the wall effect is evaluated only in the numerical cells next to the wall. For example, Chieng and Launder [84] showed much slower convergence with a fine grid using the low Reynolds number model than that by using the near wall model on the calculation of turbulent heat transport downstream from an abrupt pipe expansion.
2) It allows the introduction of additional empirical information in special cases (for example: suction, blowing and rough wall, etc.). The extra empirical information can be expressed by way of the constants or functions k^+, E and A^+.

For normal steady flow like pipe flow, the above wall-function model showed good results [85]. It is frequently observed, however, that a disturbance in the main stream (separated, reattached or recirculating flows) has a significant effect on the wall boundary. Chieng and Launder [84] reported a numerical study of flow and heat transfer in the separated flow region created by an abrupt pipe expansion by using the k-ϵ model and the near wall model. In this calculation, a parabolic variation of the turbulent kinetic energy is assumed within the viscous sublayer, which means a linear increase of fluctuating velocity with distance from the wall. The turbulent kinetic energy varies linearly toward the outer node points. The turbulence shear stress is zero within the viscous sublayer and increases abruptly at the edge of the sublayer while varying linearly over the remainder of the cell. However, these local variations of turbulence quantities were not incorporated in the evaluation of both

The convective and diffusive terms are negligible near and on the wall. This is ensured in Eqs. (2.5.2-15a, 2.5.2-15b) by

$$\left.\frac{\partial k}{\partial y}\right|_w = 0 \qquad (2.5.2\text{-}17)$$

$$\left.\frac{\partial \varepsilon}{\partial y}\right|_w = 0 \qquad (2.5.2\text{-}18)$$

which corresponds to no diffusion of k and ε to the wall. With these distributions, the mean generation and destruction rates in the ε equation can be obtained as follows.

$$\overline{(C_1 \frac{\varepsilon}{k} P)} = \frac{\tau_w}{\rho} \frac{C_1}{k_v^{\frac{1}{2}} k^* C_1 y_n} [\tau_w (\frac{k_v^{\frac{1}{2}}}{y_v} - \frac{k_n^{\frac{1}{2}}}{y_n} + \frac{b}{2}\lambda) + \frac{\tau_n - \tau_w}{y_n}(2(k_n^{\frac{1}{2}} - k_v^{\frac{1}{2}}) + a\lambda)] \qquad (2.5.2\text{-}19)$$

$$+ \frac{C_1}{C_1 y_n}[\tau_w (2(k_n^{\frac{1}{2}} - k_v^{\frac{1}{2}}) + a\lambda) + \frac{2}{3}\frac{\tau_n - \tau_w}{y_n}\frac{1}{b}(k_n^{\frac{3}{2}} - k_v^{\frac{3}{2}})]\frac{\partial v}{\partial x}$$

$$\overline{(C_2 \frac{\varepsilon^2}{k})} = C_2 \frac{12}{n_v}(\frac{k_v}{Re_v})^2 + \frac{1 - y_v/y_n}{C_1^2}(\frac{a^2}{y_v y_n} + \frac{2ab}{y_n - y_v}\ln\frac{y_n}{y_v} + b^2) \qquad (2.5.2\text{-}20)$$

where

$$\lambda = \frac{1}{a^{\frac{1}{2}}} \ln[\frac{(k_n^{\frac{1}{2}} - a^{\frac{1}{2}})(k_v^{\frac{1}{2}} + a^{\frac{1}{2}})}{(k_v^{\frac{1}{2}} - a^{\frac{1}{2}})(k_n^{\frac{1}{2}} + a^{\frac{1}{2}})}] \quad \text{for} \quad a > 0$$

low-Reynolds number model described in section 2.5.2 was used to consider the laminalization near the interface for the k-ϵ model. A modified Nusselt approximation was used for the liquid film.

The results show that Cebeci's model agrees best with the measured Stanton number of heat and mass transfer and the profiles of velocity, temperature and concentration in the three version of the Prandtl mixing length model. Even though the predicted profiles from the k-ϵ model were in reasonable agreement with the measured value, this model underpredicted the condensation rate for the higher condensation rate case.

Recently, by comparing the ratio of the experiment value to the computed one with the film Reynolds number as shown Fig. 2.27, Renz and Odenthal [92] attributed the discrepancy between the experiments and the computation results to the influence of the condensate film waves. The increase in the condensation rate by a wavy interface is supposed to be due to the influence of the waves on the turbulence structure of the vapor-gas side, since the contribution of the transfer resistance of the condensate film to the overall resistance is calculated to be less than 5 percent in this experiment.

By assuming the condensate film as a sinusoidal wave form, the instantaneous values of the x and y components velocity at the film surface were calculated by Gollan and Sideman's [56] statement. Also, the amplitude of the waves is assumed to be of the order of 30 to 80 percent of the average film thickness. The value of the turbulent kinetic energy of the gas boundary layer was calculated with these velocities and amplitudes.

Fig. 2.28 shows the distribution of the turbulent kinetic energy in the boundary layer. The thickly drawn curve shows the computed results for an incompressible

typical containment following a loss of coolant accident can vary by about 4 - 7 psi at the end of blowdown [1] and up to 23 psi at maximum [37] depending on the assumptions made for the condensation heat transfer coefficient.

An experiment of condensation phenomena in a reactor containment was started by Jubb [94]. Steam was supplied to a large boiler (8 ft 3in dia, 30 ft long). Both the heat transfer coefficient for the forced convection portion (during blowdown) and for the free convection portion (post blowdown) were simulated. In the forced convection period, Jubb correlated the heat transfer rate as

$$St\ Pr^{0.5} = 0.0576 / (Re\ P)^{0.25} \qquad (2.6\text{-}1)$$

and in the natural convection portion, the heat transfer rate was correlated as

$$h = 0.0152\ \rho\ \Delta T^{0.25} \qquad (2.6\text{-}2)$$

In the calculation of the Reynold's number, the velocity is calculated for steam at the end of the blowdown pipe, and the influence of this velocity on the air-vapor boundary layer is characteristic of this particular boiler. That is, the velocity along the condensing wall is needed to calculate a condensation rate at any position in a containment. Also, the dependence of ΔT was presented rather than the fundamental condensation theory of the dependence of $(1/\Delta T)$. Kolflat [95] reported a containment experiment where the containment was simulated by a steel tank 8 feet high and 10.5 feet in diameter. Steam entered from an external pressure tank at 1000 psia and was injected into the containment through a pipe located under a baffle plate. The authors concluded that

the time to reach the maximum coefficient decreased, and the maximum heat flux increased. The maximum heat transfer coefficient was expressed by Slaughterbeck [1]

$$h_{max} = C \left(\frac{Q}{V\, t_p}\right)^{0.62} \qquad (2.6\text{-}3)$$

where

h_{max} : the maximum heat transfer coefficient during blowdown (cal/sec-cm-^{o}C or Btu/hr-ft-^{o}F)

C : a constant equal to 0.185 for metric units or 72.8 for English units

Q : the total energy released from the primary during blowdown (cal or Btu)

V : the free volume of the containment vessel

t_p : the time interval until peak pressure (sec).

and the heat transfer coefficient for the transition period to the maximum was recommended to be

$$h = h_{max} \left(\frac{t}{t_p}\right) \qquad (2.6\text{-}4)$$

where

t : time (sec)

Fujii et al. showed the following correlation which was presumably derived from same experimental data

$$q''_p \propto \left(\frac{Q}{V\, t_p}\right)^{1.3} \qquad (2.6\text{-}5)$$

orifice plates of various sizes and types. The BTP C-series tests involved geometrically complex containment configuration with a blowdown source of saturated liquid that resulted in the introduction of a two-phase blowdown mixture into the containment. The D-series test configurations were geometrically simpler than the C-series configurations and were characterized by a single-phase blowdown of saturated steam. The independent variables of both series are the blowdown mass flow rate, blowdown location, number of compartments involved in the test and the connectivity of the subcompartments.

The HDR experiments are an extension of the containment analysis from the small scale facility of BTP and should shed more light on the feasibility of extrapolating results to real plant scale. This facility has a 75 m^3 reactor which was filled with saturated water and steam at a pressure of 110 bar. As shown in Fig. 2.31, total containment consisted of 34 compartments and most of the facility data was presented in terms of these zones.

Kanzleiter [97] showed that the measured maximum internal pressure of the BTP test amounted to only 60 percent of the internal pressure calculated without heat transfer to the cold concrete and steel structures. The good agreement was achieved between the results of this experiment (subcompartment R9 of experiment C1) and calculations using a constant heat transfer coefficient of 1300 $w/m^{2o}K$ as shown in Fig. 2.32. The author attributed the big difference in the pressure to the higher ratio of inner surface area to volume and that the influence of heat transfer to the cold structure is much greater in a scale model containment than in a full scale plant. Schwan and Aust [98] presented the experiment for the break compartment with high steam flow. The heat tranfer coefficient was reported to be the order of 10^4 $w/m^{2o}K$

cold wall and other time dependent effects, however, the condensation heat transfer coefficient data have not been systematically examined for these experiments.

2.7 Summary and Concluding Remarks

Condensation phenomena can be classified by the presence of noncondensable gas, the gas mixture velocity, the flow characterization (laminar or turbulent) of the gas mixture and the condensate film and the interface condition as shown in Table 2.4, which shows the summary of the theoretical and experimental investigations revieved.

For all cases except the turbulent vapor-air mixture boundary layer and the wavy interface of both the pure vapor and the vapor-air mixture case, it is seen that exact numerical solutions of the conservation equations and approximate solutions agree well with the corresponding experimental work. For the analysis of condensation phenomena in a reactor containment, however, the effect of the turbulent vapor-air flow and the wavy interface is supposed to be important, since the structure of a falling film is covered by very unsymmetric waves and this wavy interface is supposed to have some effect on the transport phenomena through both the vapor-air boundary layer and the condensate film. Whitley's model for the turbulent vapor-air mixture boundary layer was only applied to a containment analysis assuming the velocity of vapor-air flow and comparing the calculated containment pressure response with the experimental data.

As a conclusion, theoretical development and experiments for turbulent flow with a wavy interface are needed to predict condensation phenomena in a reactor

Table 2.1 Reproduced from Rose [32]

Table 1. Condensation on a flat plate. Comparison of numerical solutions of Sparrow *et al.* [3] for $Sc = 0.55$ with values given by equation (9)

	ϕ	
β_s	Sparrow	Equation (9)
0.025	0.951	0.951
0.05	0.905	0.905
0.075	0.863	0.863
0.1	0.823	0.824
0.125	0.787	0.788
0.15	0.752	0.753
0.175	0.720	0.721
0.2	0.690	0.691
0.225	0.662	0.663
0.25	0.635	0.637
0.3	0.587	0.588
0.35	0.543	0.545
0.5	0.438	0.439
0.75	0.319	0.318
1.0	0.241	0.240
1.5	0.149	0.149
2.0	0.100	0.100
2.5	0.0717	0.0713
3.5	0.0532	0.0532
5.0	0.0216	0.0217

Table 2.2 Experimental Results of Mills and Seban [41] and Slegers and Seban [42]

Investigator	fluid	T_∞(°C)	ΔT(°K)	$\dot{Q}''$(kw/m^2)	$\dot{Q}''/\dot{Q}''_{Nu}$
[41]	steam	7.2 - 10.0	4.4 - 6.1	31.4 - 34.6	0.9 - 1.1
[42]	n-butyl alcohol	29.5 - 38.2	3.9 - 5.6	25.1 - 34.6	0.98 -1.02

Table 2.4 Theoretical and Experimental Investigation of Condensation

Presence of noncondensable gas	Pure vapor			Vapor - noncondensable gas			
Vapor-gas boundary layer condition	Stationary vapor	Moving vapor[a]		Stationary[b] vapor-gas	Moving vapor-gas		
					Laminar	Turbulent	
Interface condition	Smooth	Smooth	Wavy[c]	Smooth	Smooth[d]	Smooth	Wavy
Solution of conservation equations	Sparrow & Gregg [9] Koh et. al. [11] Chen [12]	Cess [13]	-----	Sparrow & Eckert [25] Sparrow & Lin [26] Minkowycz & Sparrow [27]	Sparrow et. al. [29] Koh [30] Denny et. al. [34] Anand et. al. [36]	Jones & Renz [38]	-----
Approximate solution	Emmert [3]	Shekriladze & Gomelauri [15] Mayhew et. al. [16]	-----	Rose [28]	Rose [32]	Whitley [37]	-----
Experimental work	Nitto & Sabin [41] Shigeru & Sabin [42]	Mayhew & Aggarwal [18] Gandyhamata & Burab [22,23] Jacobs et. al. [24]		Othmer [43] Hampson [44] Akers et. al. [45] Shigeru & Sabin [46] Al-Diwany & Rose [47] DuVauss & Christensen [48]	Nitto & Denny [49] Anand et. al. [36]	Baltuoyar [39]	-----

(a) Since there is no heat resistance in a pure vapor boundary layer, the classification of a laminar or turbulent moving vapor are not needed.

(b) For the case of the presence of noncondensable gas, the natural convection flow will be generated from the temperature and the concentration difference on the air-vapor boundary layer.

(c) Even though the wavy interface does not mean the turbulent condensate film, both phenomena enhance the condensation.

(d) The wavy interface with laminar moving vapor-gas mixture is not considered.

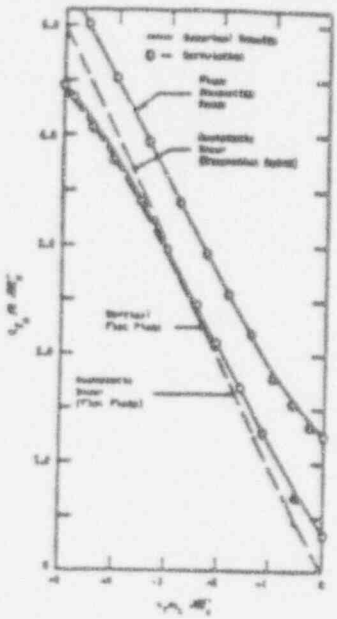

Fig. 2.3 Comparison of Dimensionless Shear with Numerical Results for Laminar Film Condensation down a Vertical Flat Plate and a Horizontal Cylinder, Reproduced from South and Denny [19]

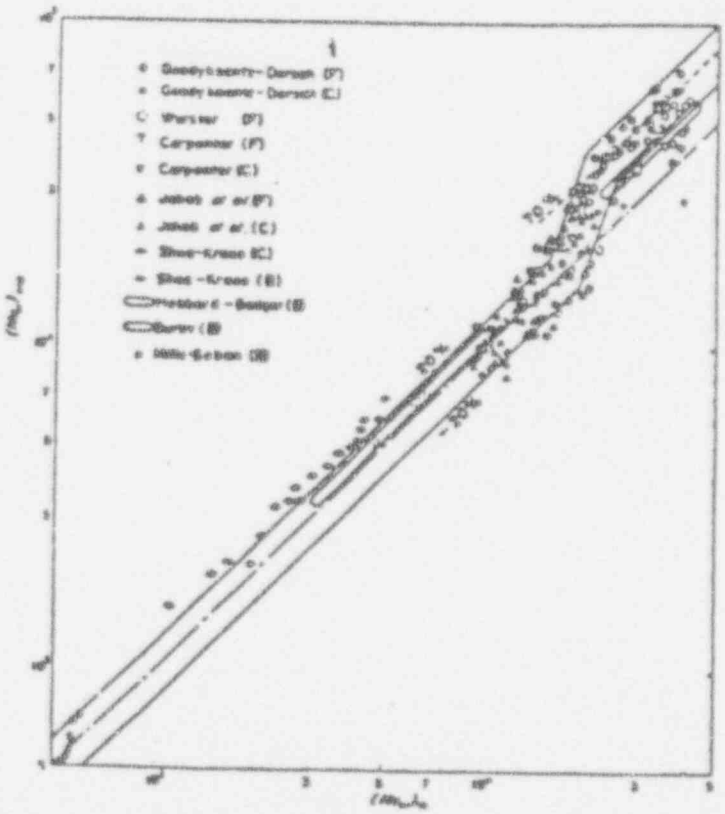

Fig. 2.4 Correlation between Experimental Nu_L and Theoretical Nu_L Predicted from Eq. (2.2.2-21) for Water, Reproduced from Fujii and Uehara [21]

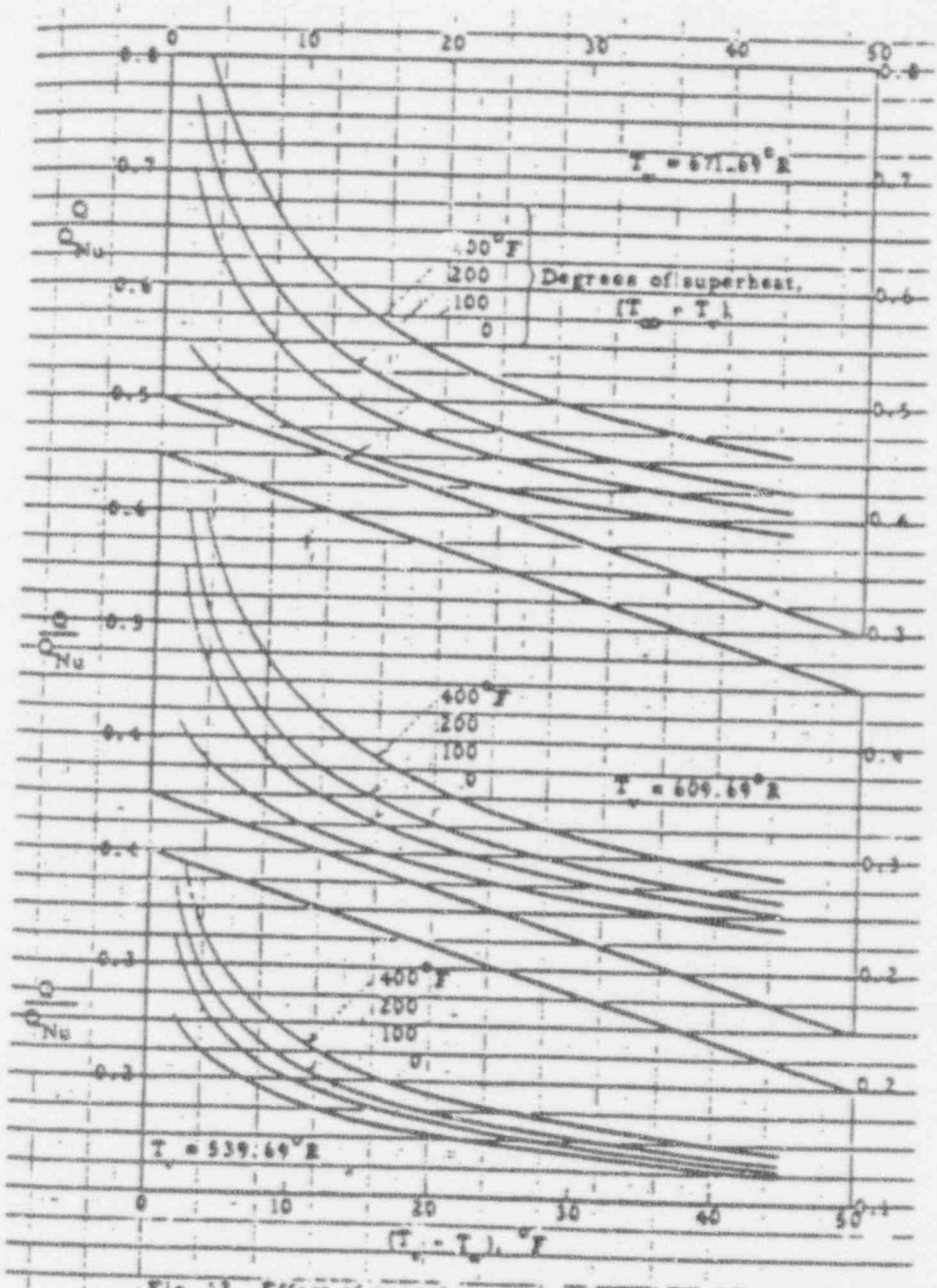

Fig. 12 Effect of superheating for various prescribed values of T_∞ and for W_∞ = 0.005 (no interfacial resistance)

Fig. 2.6 Reproduced from Minkowycz [27]

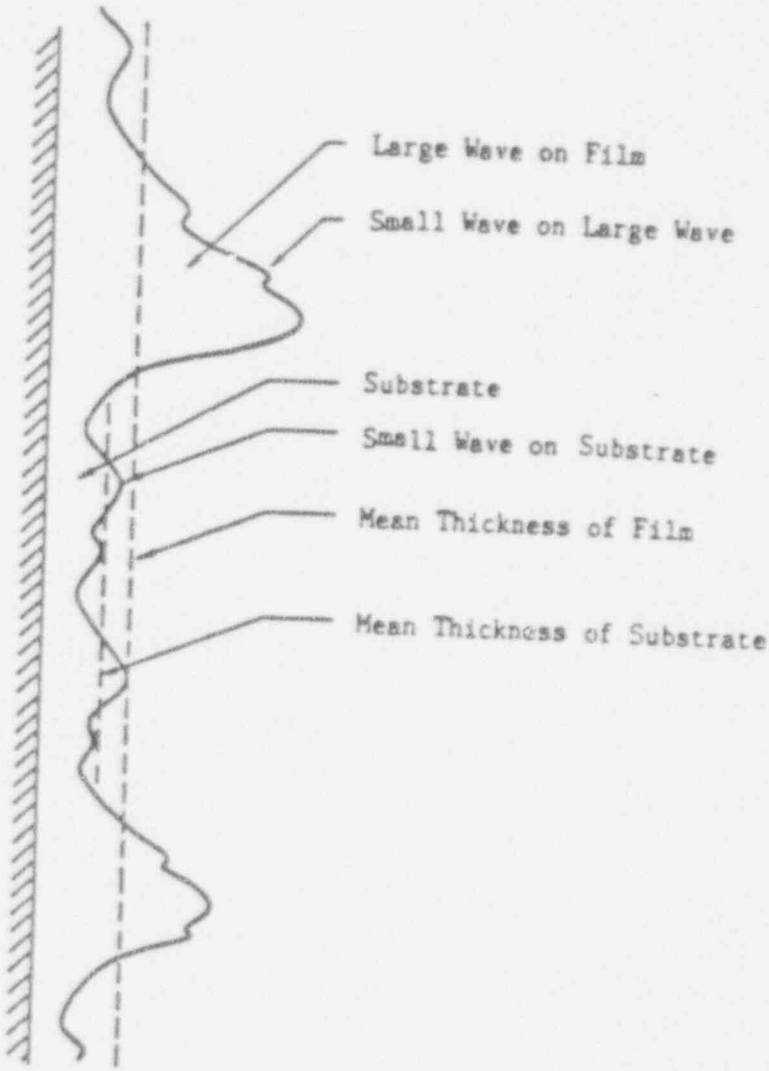

Fig. 2.9 Identification of the Structure of a Falling Film,
Reproduced from Chu and Dukler [59]

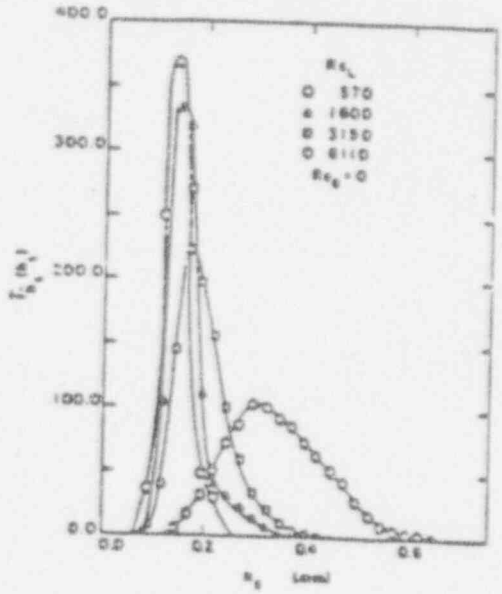

Fig. 2.12 Probability Density of Substrate Thickness: Effect of the Film Reynolds Number, Reproduced from Chu and Dukler [59]

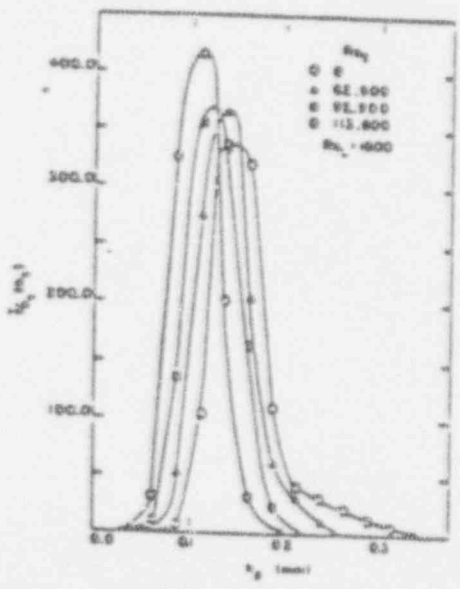

Fig. 2.13 Probability Density of Substrate Thickness: Effect of the Gas Reynolds Number, Reproduced from Chu and Dukler [59]

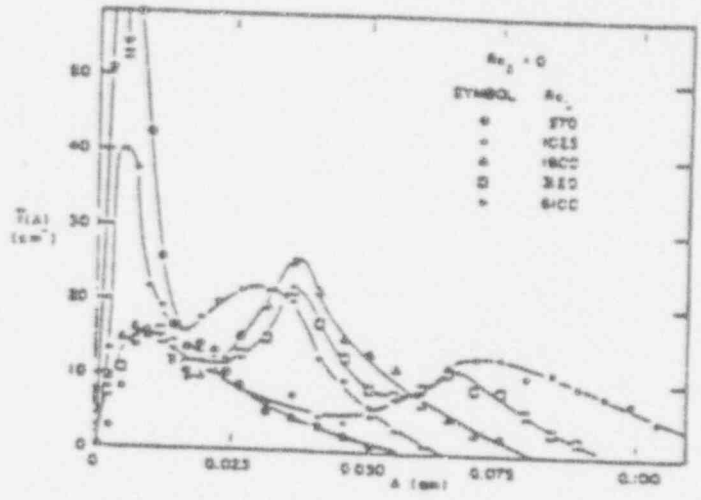

Fig. 2.16 Probability Density of Wave Amplitude, Re_g = 0: Varying Liquid Rates
Reproduced from Chu and Dukler [60]

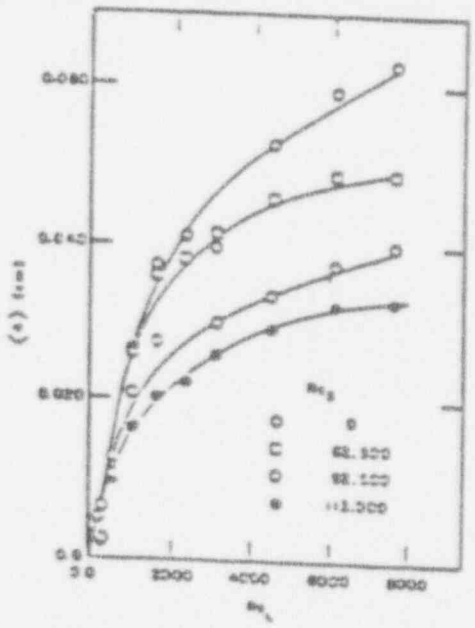

Fig. 2.17 Mean Deviation of Large Wave Amplitude
Reproduced from Chu and Dukler [60]

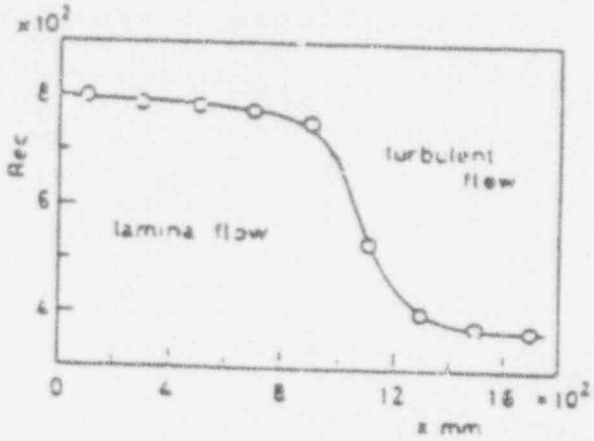

Fig. 2.19 Longitudinal Change of Critical Reynolds Number. Reproduced from Takahama[62]

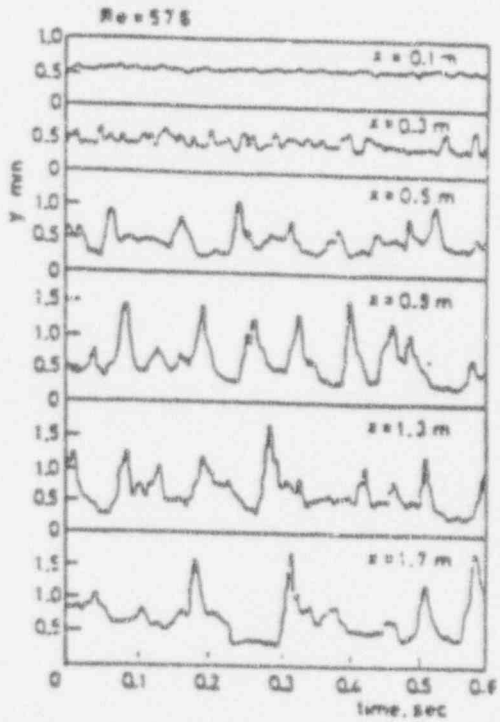

Fig. 2.20 Longitudinal Developing Process of Interfacial Wave Form. Reproduced from Takahama[62]

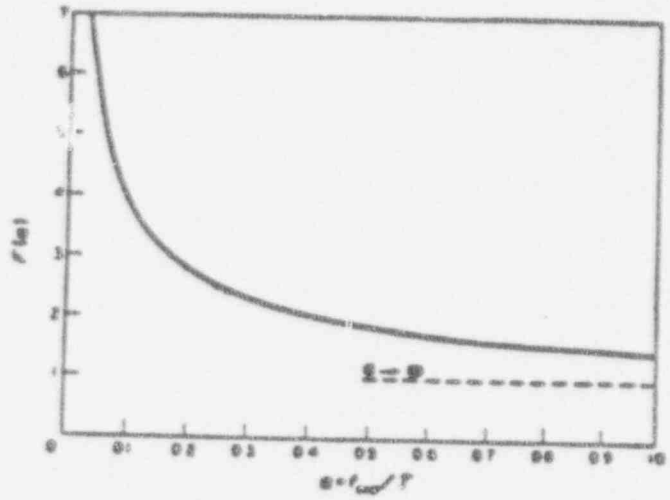

Fig. 2.23 The Function F,
Reproduced from Brumfield [74]

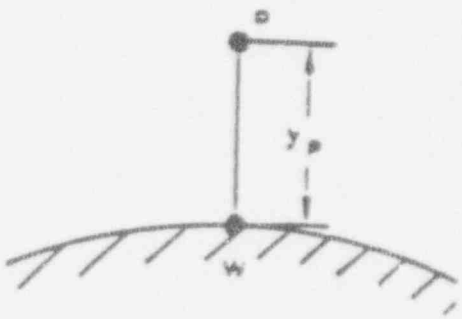

Fig. 2.24 The Near-Wall Nodes W and P

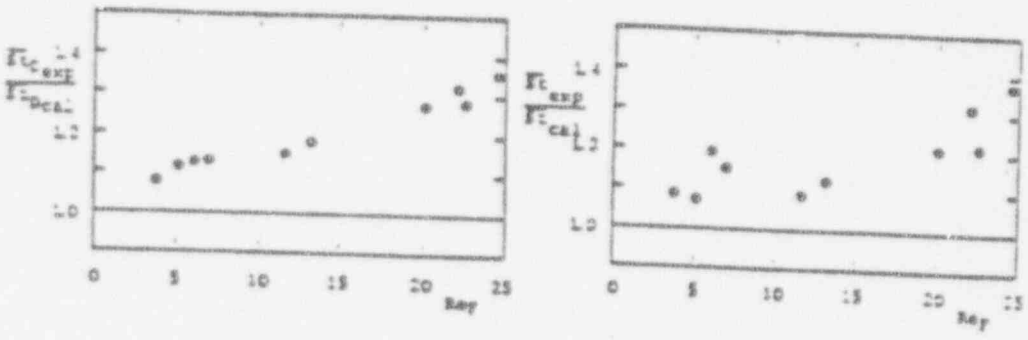

Fig. 2.27 Ratio of Experimental and Theoretical Stanton Number for Heat and Mass Transfer, Reproduced from Renz and Odenthal [92]

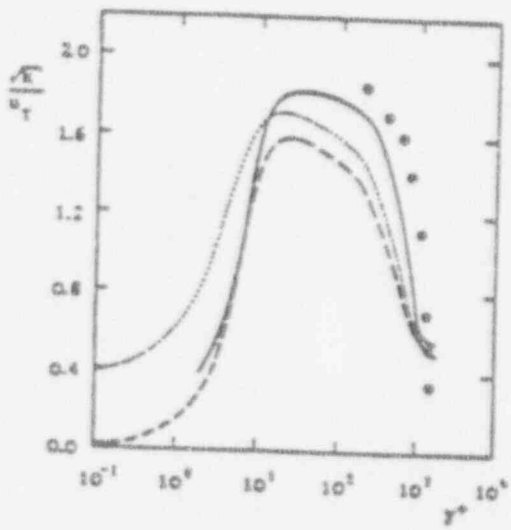

Fig. 2.28 Numerical Prediction of the Influence of Film Waves on the Turbulence Energy Distribution in the Boundary Layer for $Re_\tau = 95$.
(— Incompressible Boundary Layer, --- Boundary Layer with Condensation and Wave-Free Film, ··· Boundary Layer with Condensation and Wavy Film (A/ δ = 0.5) Measurements of Archaya [93], Incompressible Boundary Layer), Reproduced from Renz and Odenthal [92]

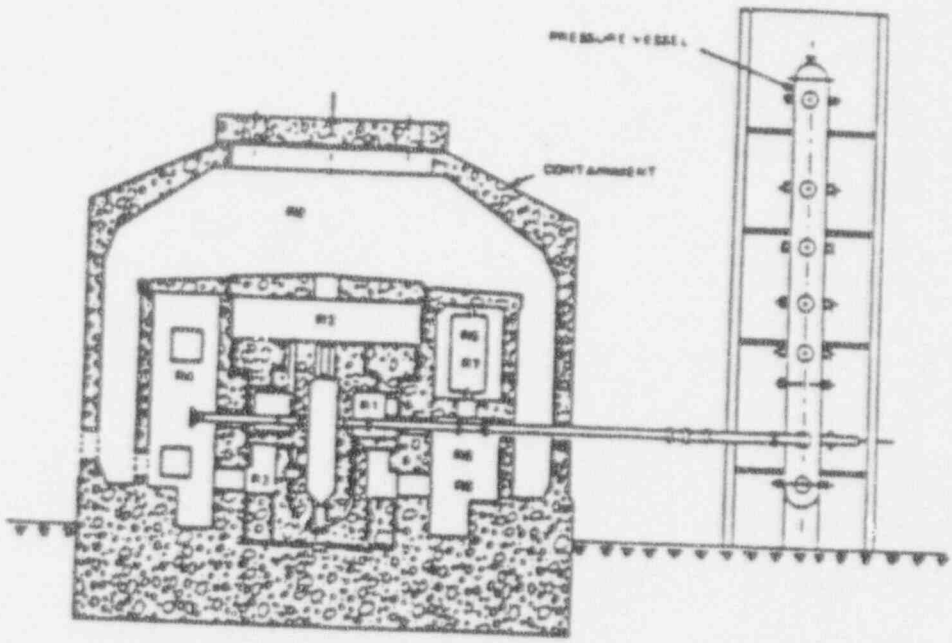

Fig. 2.30 BTF Containment Test System

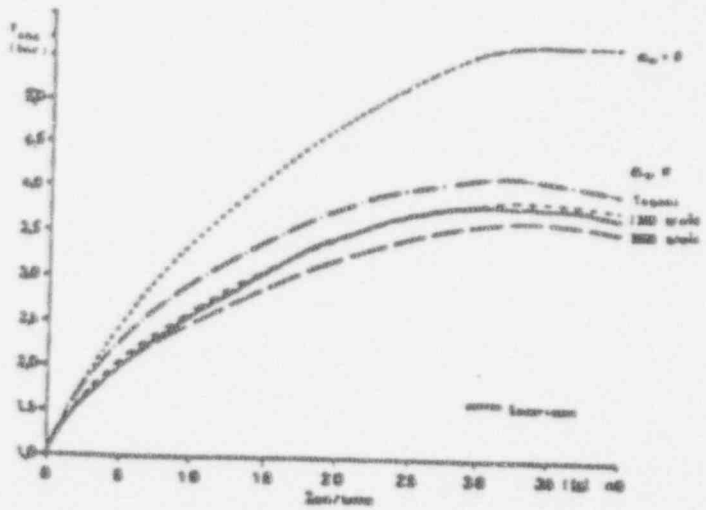

Fig. 10. Absolute pressure: experimental and theoretical results.

Fig. 2.32 Reproduced from Kanzleiter [54]

$$h_{film} = 0.943 \left(\frac{\rho_l(\rho_l - \rho_g)\, ai_{lg}\, K_l^3}{\mu L (T_I - T_w)}\right)^{1/4} \qquad (3.1.1\text{-}3)$$

where L is the vertical length of the cold surface and h_{film} is the average heat transfer coefficient. As mentioned previously, a number of modifications were suggested to this model. In addition, the surface of the liquid film will eventually become wavy and the liquid film will be turbulent as the wall length increases and as obstacles on the wall disturb the film flow. The detailed model for the condensate film with these conditions is to be presented in section 3.3. However, when noncondensable gases are present the film heat transfer coefficient is larger than that of the vapor-air layer coefficient, and therefore is usually negligible or can be estimated by Nusselt's method with little error on the overall heat transfer coefficient except under special conditions, which will be explained in section 4.3.3. If the film becomes turbulent, this assumption becomes even more valid.

The heat transfer coefficient in the vapor-air boundary layer is composed of three contributions:

1) convective heat transfer from the vapor-air mixture to the film, h_{conv}.
2) condensation of the steam onto the liquid film, h_{cond}.
3) radiation heat transfer from the air-vapor mixture, h_{rad}.

$$h_{gas} = h_{conv} + h_{cond} + h_{rad} \qquad (3.1.1\text{-}4)$$

condition (vertical-horizontal, plate-tube, forced-natural and laminar-turbulent), the condensation heat transfer coefficient could be calculated easily without any specific condensation experiment correlation. For the turbulent flow, the above equations become

$$\tau = \mu \frac{\partial U_x}{\partial y} - \rho \overline{U_x' U_y'} \qquad (3.1.1\text{-}10)$$

$$q = - K \frac{\partial T}{\partial y} + \rho C_p \overline{T' U_y'} \qquad (3.1.1\text{-}11)$$

$$j = - \rho D_{AB} \frac{\partial X_A}{\partial y} + \rho \overline{X_A' U_y'} \qquad (3.1.1\text{-}12)$$

The bar is omitted for simplicity except for the correlation terms. In analogy to molecular transport coefficients, Boussinesq suggested the introduction of eddy diffusivities by the definitions

$$\overline{U_x' U_y'} = - \epsilon_M \frac{\partial U_x}{\partial y} \qquad (3.1.1\text{-}13)$$

$$\overline{T' U_y'} = - \epsilon_H \frac{\partial T}{\partial y} \qquad (3.1.1\text{-}14)$$

$$\overline{X_A' U_y'} = - \epsilon_D \frac{\partial X_A}{\partial y} \qquad (3.1.1\text{-}15)$$

Now the Reynolds shear stress is replaced by the eddy diffusivity ϵ_M for momentum and Reynolds heat and mass

of meters per second [2,96]. If the length of the containment wall and some obstacles to disturb the flow were considered with the above velocity, the vapor-air boundary layer has to be considered as turbulent.

Since the Chilton-Colburn analogy applies for fully turbulent flow inside tubes, and for flow parallel to plane surfaces at low mass transfer rates [106], it can be used to calculate the convective heat transfer coefficient near the containment wall,

$$\frac{h_{conv}}{\rho_g C_p u_g} = \frac{f}{2} E_H \qquad (3.1.2\text{-}1)$$

$$E_H = Pr_t^{-1} = Pr^{-2/3} \qquad (3.1.2\text{-}2)$$

where E_H is the ratio of the turbulent eddy diffusivity of heat ϵ_H to momentum ϵ_M. This analogy cannot apply to any other geometry (e.g. streamline tubes or flow across tube and tube bank) however. Now, for a wall the local skin-friction factor is given by [107]

$$\frac{f}{2} = 0.0296\, Re_x^{-0.2} \qquad (3.1.2\text{-}3)$$

for Reynolds numbers between 5×10^5 and 10^7. When this is combined with Eq. (3.1.2-1), the resultant local convective heat transfer coefficient is

$$Nu_x = \frac{h_{conv}\, x}{K} = 0.0296\, Re_x^{0.8}\, Pr^{1/3} \qquad (3.1.2\text{-}4)$$

Since the Reynolds number is a function of x, the average turbulent convective heat transfer coefficient for the

$$\dot{m}'' = g \frac{X_I - X_B}{1 - X_I} \qquad (3.1.2\text{-}11)$$

and the condensation heat transfer coefficient is then given by

$$h_{cond} = \frac{g \frac{X_I - X_B}{1 - X_I} (i_B - i_I)}{(T_B - T_I)} \qquad (3.1.2\text{-}12)$$

Recently, a lot of effort has been given to predict the turbulent Prandtl/Schmidt number [108]. The most interesting analytical results were derived from transport equations for the turbulent kinetic energy, for the turbulent heat flux, and the turbulent mass flux by Jischa and Rieke [109].

$$Pr_t = C_1 + \frac{C_2}{P_r} \qquad (3.1.2\text{-}13)$$

$$Sc_t = C_1 + \frac{C_2}{Sc} \qquad (3.1.2\text{-}14)$$

The two constants C_1 and C_2 were fitted on experimental data

$$C_1 = 0.85 \qquad (3.1.2\text{-}15)$$

C_2 = 0.012 to 0.05 for $Re = 2 \times 10^4$

the same functional form.

Since Eqs. (3.1.2-13) and (3.1.2-14) agree well with the experimental data for a wide range of Prandtl and Schmidt number, these equations are to be implemented in Eqs. (3.1.2-2) and (3.1.2-7). The resultant local heat and mass transfer coefficients are calculated from

$$Nu_x = \frac{0.0296\ Re_x^{0.8}\ Pr}{(0.85 + 0.01/Pr)} \qquad (3.1.2\text{-}20)$$

$$Sh_x = \frac{0.0296\ Re_x^{0.8}\ Pr}{(0.85 + 0.01/Sc)} \qquad (3.1.2\text{-}21)$$

As the mass transfer rate (condensation rate) increases, the momentum, thermal and mass transfer boundary layers will be reduced in size because of the apparent suction effect of the condensation process. This reduction in the boundary layer thickness will further increase the temperature and concentration gradients near the wall and increase the heat and mass transfer coefficients. To consider this effect, the following correction factors [112, 113] can be used

Momentum transfer:

$$\frac{f^*}{2} = \frac{\ln(1 + B_f)}{B_f}\frac{f}{2} \qquad (3.1.2\text{-}22)$$

$$B_f = \frac{\dot{m}'' / G_\infty}{f/2}$$

Heat transfer:

$$St^* = \frac{\ln(1 + B_h)}{B_h} St \qquad (3.1.2\text{-}23)$$

$$B_h = \frac{\dot{m}'' / G_\infty}{S_t}$$

$$Re_k = \frac{u_\tau k_s}{\nu} \qquad (3.1.3\text{-}1)$$

where u_τ is the shear velocity. For the solid rough surface, three regimes are identified as smooth surface ($Re_k < 5.0$), transitional roughness ($5.0 < Re_k < 70.0$) and fully rough region ($Re_k > 70.0$). Since the interface of a falling film changes quickly to be a highly unsymmetric wave, it is hard to define and model the transitional region for the wavy interface. Therefore, the wavy interface is assumed to be the fully rough region if a wave is formed. Collier [6] presented that the shear stress increases progressively by the wavy interface at a film Reynolds number greater than 100, which will be used for the critical Reynolds number for the wavy interface in this work.

In the fully rough regime, the viscous sublayer is expected to disappear entirely and the momentum is transmitted to the wall (liquid falling film) by the impact or pressure drag on the rough element (wave). Therefore, the eddy diffusivity and mixing length must be finite at the wall surface (interface) and can be represented as

$$\ell = k^*(y + \delta y_o) \qquad (3.1.3\text{-}2)$$

rather than the mixing length model for smooth surfaces:

$$\ell = k^* y \qquad (3.1.3\text{-}3)$$

where ℓ goes to zero at the wall.
In Eq (3.1.3-2), δy_o can be correlated to k_s as a nondimensional form

$$v_o^+ = \frac{v_o}{\sqrt{\tau_w/\rho}} \qquad (3.1.3\text{-}8c)$$

$$p^+ = \frac{\mu(\frac{dp}{dx})}{(\rho^{\frac{1}{2}}\tau_w^{\frac{1}{2}})} \qquad (3.1.3\text{-}8d)$$

This equation is reduced for the case of no pressure gradient and mass transfer to the wall

$$\tau_o = \rho(\nu + \varepsilon_M)\frac{d\bar{u}}{dy} \qquad (3.1.3\text{-}9)$$

For the fully turbulent region, the molecular viscosity can be neglected relative to the eddy viscosity ε_M.

$$\tau_o = \rho\varepsilon_M \frac{d\bar{u}}{dy} = \rho\ell^2 (\frac{d\bar{u}}{dy})^2 \qquad (3.1.3\text{-}10)$$

$$= \rho k^{*2} [y^+ + (\delta y_o)^+]^2 (\frac{d\bar{u}}{dy})^2$$

By introducing the nondimensional form, we obtain

$$\frac{du^+}{dy} = \frac{1}{k^* [y^+ + (\delta y_o)^+]} \qquad (3.1.3\text{-}11)$$

Since there is no viscous subl yer in the fully rough region, the lower limit of integration of this differential equation must be extended to $y^+ = 0$.

boundary layer, the friction coefficient becomes

$$\frac{C_f}{2} = \frac{0.168}{\ln (864\ \delta_2/k_s)^2} \qquad (3.1.3\text{-}15)$$

Now, it is worthwhile to notice that the friction coefficient depends only on boundary layer thickness and the roughness size, not on the viscosity or velocity of the fluids. This friction coefficient is used to calculate the shear stress on the interface and the film thickness.

The effective roughness k_s is correlated by using Wallis's suggested correlation [65] as described in section 2.5.

$$k_s = 4\delta \qquad (3.1.3\text{-}16)$$

where δ is the mean film thickness, which is calculated by the model for the condensate liquid film presented in section 3.3. As described in section 2.4, the substrate in a falling film plays an important role in the transport phenomena through the vapor-air boundary layer. The substrate film thickness or the wave amplitude of the substrate, therefore, seems to be more plausible for the correlation of the friction coefficent for a falling film than the average film thickness. The experimental data of the friction coefficient for a falling film by Chu and Dukler [59, 60] was compared with the ratio of the substrate film thickness to the diameter. Fig. 3.2 shows a very similar correlation with Eq. (2.4-1)

$$(C_f)_I = 0.005 * (1 + 750\ \frac{\delta_s}{D}) \qquad (3.1.3\text{-}17)$$

It means that the substrate film thickness is proportional

correlations for the heat and mass transfer are required for the wavy interface. For the thermal boundary layer at the wall without pressure gradient and mass transfer, the dimensionless temperature profile is expressed from the conservation equation of energy with the Couette flow approximation as follows:

$$T^+ = \int_0^{y^+} \frac{dy^+}{1/Pr + \epsilon_M/\nu} \qquad (3.1.3\text{-}19)$$

where

$$T^+ = \frac{(T_w - \bar{T})\sqrt{\tau_w/\rho}}{q_w''/\rho C_p} \qquad (3.1.3\text{-}20)$$

Since there is no viscous sublayer at the rough wall, the eddy conductivity ϵ_M is assumed to be much larger than the molecular conductivity for all the way down to $y^+ = 0$ except very small Prandtl numbers. The temperature difference across the interface by conduction is represented by δy_o^+. Thus Eq. (3.1.3-20) becomes

$$T^+ - T_o^+ = \int_0^{y^+} \frac{dy^+}{\epsilon_H/\nu} \qquad (3.1.3\text{-}21)$$

To calculate ϵ_H, the turbulent Prandtl number and Eq. (3.1.3-2) are used

$$\frac{\epsilon_H}{\nu} = \frac{1}{Pr_t}\frac{\epsilon_M}{\nu} = \frac{k^*}{Pr_t}(y^+ + \delta y_o^+) \qquad (3.1.3\text{-}22)$$

where Eq. (3.1.3-15) is used to calculate $C_f/2$. Since St_k is a function of Prandtl number, the resistance for heat transfer by the molecular conduction is included. The Nusselt number for the convective heat transfer is calculated from the following equation.

$$Nu = \frac{C_f/2 \; Re \; Pr}{Pr_t + \sqrt{C_f/2} \; / \; St_k} \qquad (3.1.3\text{-}28)$$

Stanton number for the mass transfer is derived by analogy between the heat and mass transfer.

$$St_{AB} = \frac{C_f/2}{Sc_t + \sqrt{C_f/2} \; / \; St_{ABk}} \qquad (3.1.3\text{-}29)$$

where

$$St_{ABk} = C \; Re_k^{-0.2} \; Sc^{-0.44} \qquad (3.1.3\text{-}29a)$$

The Sherwood number for the condensation heat transfer is correlated as;

$$Sh = \frac{C_f/2 \; Re \; Sc}{Sc_t + \sqrt{C_f/2} \; / St_{ABk}} \qquad (3.1.3\text{-}30)$$

These equations will be used to compute the heat and mass transfer through the vapor-gas boundary layer with a wavy interface.

3.1.4 Natural Convection Model

$(10^4 < Gr\ Pr < 10^8)$

$Nu = 0.13\ (Gr\ Pr)^{1/3}$: Transition flow range (3.1.4-4)
$(10^8 < Gr\ Pr < 10^{10})$

$Nu = 0.021(Gr\ Pr)^{2/5}$: Turbulent flow range (3.1.4-5)
$(10^{10} < Gr\ Pr)$

We have generalized the original condensation mass transfer model by using a similar approach. Table 3.1 shows the analogies between heat and mass transfer at low mass transfer rates. For the laminar flow range, the mass transfer correlation was derived by merely substituting Sh for Nu and Sc for Pr. For the other range, one can derive a simple formulation by using the Chilton-Colburn analogy which is valid for turbulent flow.

$Sh = 0.56\ (Gr\ Sc)^{1/4}$ Laminar flow range (3.1.4-6)
$(10^4 < Gr\ Pr < 10^8)$

$Sh = 0.13\ (Gr\ Sc)^{1/3}$: Transition flow range (3.1.4-7)
$(10^8 < Gr\ Pr < 10^{10})$

$Sh = 0.021(Gr^{2/5}\ Sc^{1/3}\ Pr^{1/15})$:
Turbulent flow range (3.1.4-8)

$= 0.021(Gr\ Pr)^{2/5}$ $(10^{10} < Gr\ Pr)$ (3.1.4-9)

Since $(Sc/Pr)^{1/15}$ of vapor-air is almost 1.0, Eq. (3.1.4-9) could be used instead of Eq. (3.1.4-8) for a simpler consistent form.

The high mass transfer correction factors can also be used with this natural convection model.

A staggered grid system is associated with every grid node, while the vector quantities (velocity components) are displaced in space relative to the scalar quantities. This grid system has advantages in solving the velocity field since the pressure gradients are easy to evaluate and velocities are conveniently located for the calculation of the convective fluxes. The discretization equation of eq (3.2.1-1) can be written for the two-dimensional geometry as shown in Fig.3.3,

$$a_P\phi_P = a_E\phi_E + a_W\phi_W + a_N\phi_N + a_S\phi_S + b \qquad (3.2.1\text{-}3)$$

where

$$a_E = D_e A(|P_e|) + MAX(-F_e, 0) \qquad (3.2.1\text{-}3a)$$

$$a_W = D_w A(|P_w|) + MAX(-F_w, 0) \qquad (3.2.1\text{-}3b)$$

$$a_N = D_n A(|P_n|) + MAX(-F_n, 0) \qquad (3.2.1\text{-}3c)$$

$$a_S = D_s A(|P_s|) + MAX(-F_s, 0) \qquad (3.2.1\text{-}3d)$$

$$a_P = a_E + a_W + a_N + a_S + a_P^\circ - S_P^\circ \Delta x \Delta y \qquad (3.2.1\text{-}3e)$$

$$b = Sc\Delta x\Delta y + a_P^\circ \phi_P^\circ \qquad (3.2.1\text{-}3f)$$

$$a_P^\circ = \frac{\rho_P^\circ \Delta x \Delta y}{t} \qquad (3.2.1\text{-}3g)$$

and ϕ_P° and ρ_P° refer to the known values at time t, while all other values are unknown at time t+Δt. Also the flow rates F and conductances D are defined by

$$F_e = (\rho u)_e \Delta y \qquad (3.2.1\text{-}4a)$$

field to correct the velocity field. After that, the remaining ϕ's are solved and the whole process is repeated until convergence.

3.2.2 Near Wall Model for Smooth Interface

As described at section 2.5.2, the effective viscosity near the wall is calculated by using the universal velocity profile of turbulent flow over a flat plate as follows [113];

$$u^+ = 2.44 \ln y^+ + 5.0 \qquad (3.2.2\text{-}1)$$

which corresponds to the Eqs. (2.5.2-11) and (2.5.2-12) with

$$k^* = 0.41 \qquad (3.2.2\text{-}2)$$

$$E = 7.76 \qquad (3.2.2\text{-}3)$$

Also, the Van Driest's constant is recommended as 25.0 for the external boundary layer over the flat plate. The effective diffusivities are calculated from Eqs (2.5.2-11) and (2.5.2-12)

$$\mu_{eff} = \frac{\mu \delta y^+}{k^* \ln(E \delta y^+)} \qquad \text{for u and v} \quad (3.2.2\text{-}4)$$

$$\frac{k_{eff}}{C_p} = \frac{\mu \delta y^+}{Pr_t [k^* \ln(E \delta y^+) + PFN]} \qquad \text{for T} \quad (3.2.2\text{-}5)$$

$$\rho D_{eff} = \frac{\mu \delta y^+}{Sc_t [k^* \ln(E \delta y^+) + SFN]} \qquad \text{for m}^* \quad (3.2.2\text{-}6)$$

(3.1.3-23), the second term of Eq. (2.5.2-12), which contains A^+, can be replaced by the second term of Eq. (3.1.3-23) with the modification of k^+ and E described above. It corresponds to the change of PFN in Eq. (3.2.2-5) to

$$PFN = \frac{Re_k^{0.2} \, Pr^{0.44}}{Pr_t} \qquad (3.2.3\text{-}3)$$

The analogy between heat and mass transfer is used again for the eddy diffusivity for mass. SFN in Eq. (3.2.2-6) becomes

$$SFN = \frac{Re_k^{0.2} \, Sc^{0.44}}{Sc_t} \qquad (3.2.3\text{-}4)$$

Akai et al. [119] used a k-ϵ turbulence model with near wall model to solve a horizontal stratified two-phase flow system. Fig. 3.4 shows the velocity profile shifted downward nearly parallel with increasing gas phase Reynolds number, which is expected for the horizontal flow at section 2.5. The universal velocity profile for near wall model, therefore, was modified to match their own experimental velocity profile with the wavy interface as follows

$$u^+ = \frac{1}{0.4} \ln \frac{8 \, \delta v^+}{A^+} \qquad (3.2.3\text{-}5)$$

where A^+ : dimensionless wave amplitude

and showed good agreements as shown at Fig. 3.5. Also, the

For the laminar condensate film, the velocity distribution is calculated from the balance of forces

$$\tau dx = \mu\left(\frac{du}{dy}\right)dx = (\delta-y)(\rho_l-\rho_g)\, g\, dx + \tau_\delta dx + \psi\, dm\,(u_g-u_\delta) \qquad (3.3.1\text{-}1)$$

where each term of the right side represents the forces arising from gravity, friction at the surface, and momentum drag by mass transfer through the interface and ψ is a multiplying factor. This factor was suggested to be 0.75 by Mayhew, since the vapor crossing at the interface is not supposed to be at exactly the same velocity as the main vapor. Even though this factor seems to vary with the condition of the gas flow pattern and interface, the suggested value, 0.75, will be used. Since the condensation rate, dm must be same as the heat transfer rate through the condensate film as shown

$$dm = \frac{K\,(T_I-T_W)}{i'_{fg}\,\delta}\,dx \qquad (3.3.1\text{-}2)$$

Eq. (3.3.1-1) can be rewritten with the assumption of $\rho_l \gg \rho_g$.

$$du = \frac{\rho_l g}{\mu}(\delta-y)dy + \frac{\tau_\delta}{\mu}dy + \frac{K\,(T_I-T_W)(u_g-u_\delta)}{\mu\, i'_{fg}\,\delta}\,dy \qquad (3.3.1\text{-}3)$$

Integrating this equation with respect to y, with u = 0 at y = 0, gives

interface at film Reynolds numbers less than the critical value.

With the mean film thickness calculated from the above equation, the heat transfer coefficient through the condensate film can be calculated by

$$h = \frac{k_l}{\delta} \qquad (3.3.1\text{-}8)$$

3.3.2 Model for a Turbulent Condensate Film

The condensate film is supposed to change from laminar flow to turbulent flow at the critical Reynolds number, which is widely suggested to lie between 1000-3000. Takahama, however, reported it as a function of the longitudinal distance without gas flow. In the current work, 2000 is temporarily chosen for the critical Reynolds number.

The universal velocity profile for the external boundary layer is used, since the shear stress on the interface is large due to the large vapor-gas velocity and wavy surface.

$$u^+ = y^+ \qquad \text{for } y^+ < 10.8 \quad (3.3.2\text{-}1)$$

$$u^+ = 2.44 \ln y^+ + 5.0 \qquad \text{for } y^+ > 10.8 \quad (3.3.2\text{-}2)$$

With these distributions, the mass flow rate can be calculated by using Eq. (3.3.1-5) for $y^+ < 10.8$

$$\Gamma = \frac{\mu \delta^{+2}}{2} \qquad (3.3.2\text{-}3)$$

for $y^+ > 10.8$

Table 3.1 Analogies between Heat and Mass Transfer at Low Mass-Transfer Rates

	Heat-Transfer	Binary Mass-Transfer
Profiles	T	x_A
Diffusivity	$\alpha = \frac{k}{\rho C_p}$	$\mathscr{D}_{AB}$
Transfer rate	Q	$\mathscr{N}''_A - x_{A0}(\mathscr{N}''_A + \mathscr{N}''_B)$
Transfer coefficient	$h = \frac{Q}{A\,\Delta T}$	$k_x = \frac{\mathscr{N}''_A - x_{A0}(\mathscr{N}''_A + \mathscr{N}''_B)}{A\,\Delta x_A}$
Dimensionless groups which are the same in both correlations	$Re = \frac{DV\rho}{\mu} = \frac{DG}{\mu}$ $Fr = \frac{V^2}{gD}$ $\frac{L}{D}$	$Re = \frac{DV\rho}{\mu} = \frac{DG}{\mu}$ $Fr = \frac{V^2}{gD}$ $\frac{L}{D}$
Basic dimensionless groups which are different	$Nu = \frac{hD}{k}$ $Pr = \frac{C_p\mu}{k} = \frac{\nu}{\alpha}$ $Gr = \frac{D^3\rho^2 g\beta\,\Delta T}{\mu^2}$ $St = \frac{Nu}{RePr} = \frac{h}{\rho C_p V}$	$Nu_{AB} = \frac{k_x D}{c\mathscr{D}_{AB}}$ $Sc = \frac{\mu}{\rho\mathscr{D}_{AB}} = \frac{\nu}{\mathscr{D}_{AB}}$ $Gr_{AB} = \frac{D^3\rho^2 g(\Delta x_A}{\mu^2}$ $St_{AB} = \frac{Nu_{AB}}{ReSc} = \frac{k_x}{cV}$
Special combinations of dimensionless groups	$Pé = RePr = \frac{DV\rho C_p}{k}$ $j_H = NuRe^{-1}Pr^{-1/3}$ $= \frac{h}{\rho C_p V}\left(\frac{C_p\mu}{k}\right)^{2/3}$	$Pé_{AB} = ReSc = \frac{DV}{\mathscr{D}_{AB}}$ $j_D = Nu_{AB}Re^{-1}Sc^{-1/3}$ $= \frac{k_x}{cV}\left(\frac{\mu}{\rho\mathscr{D}_{AB}}\right)^{2/3}$

Table 3.3 Summary of ϕ, Γ and S in Eq. (3.2.1-1) for the Axisymmetric Cylindrical Coordinate

Equation	ϕ	μ_{eff}	S
Continuity	1	0	0
X Momentum	u	μ_{eff}	$-\frac{\partial P}{\partial x} + \frac{\partial}{\partial x}(\mu_{eff}\frac{\partial u}{\partial x}) + \frac{1}{r}\frac{\partial}{\partial r}(r\mu_{eff}\frac{\partial v}{\partial x})$
Y Momentum	v	μ_{eff}	$-\frac{\partial P}{\partial r} + \frac{\partial}{\partial x}(\mu_{eff}\frac{\partial u}{\partial r}) + \frac{1}{r}\frac{\partial}{\partial r}(r\mu_{eff}\frac{\partial v}{\partial r}) - \frac{2\mu_{eff}v}{r^2}$
Energy	T	$\frac{K_{eff}}{C_p}$	0
Mass Concentration	X	ρD_{eff}	0
Turbulent Energy	k	$\frac{\mu_t}{\sigma_k}$	$\rho P - \rho\varepsilon$
Energy Dissipation	ε	$\frac{\mu_t}{\sigma_\varepsilon}$	$C_1\frac{\rho\varepsilon P}{k} - C_2\frac{\rho\varepsilon^2}{k}$

where

$$P = \nu_t\left[\left(\frac{\partial u}{\partial r} + \frac{\partial v}{\partial x}\right)^2 + 2\left(\frac{\partial u}{\partial x}\right)^2 + 2\left(\frac{\partial v}{\partial r}\right)^2 + 2\left(\frac{v}{r}\right)^2\right.$$

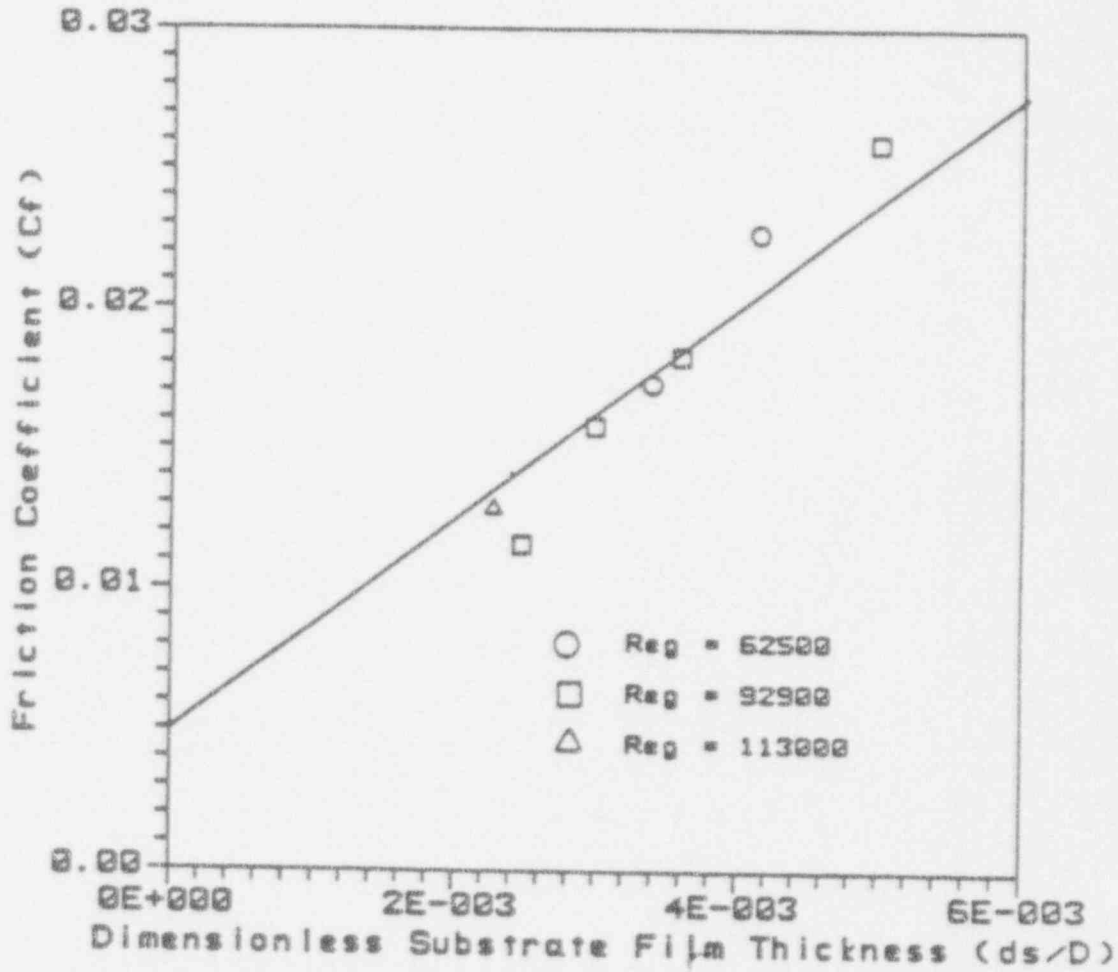

Fig. 3.2 Comparison between Eq. (3.1.3-17) for the Friction Coefficient and Chu and Dukler Experiment [59,60]

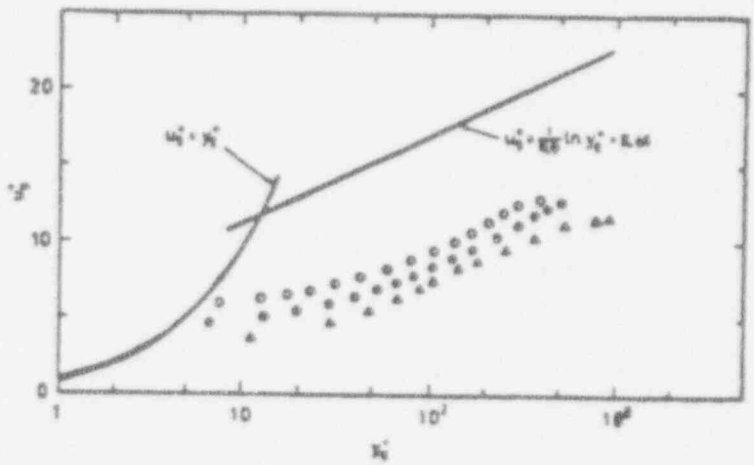

Fig. 3.4 Mean Gas Velocity Profiles for Interfacial Region
(Re_L = 8.04x10^3; o, Re_G = 6.52x10^3; •, Re_G = 8.54x10^3;
▲, Re_G = 1.32x10^4; ——, Universal Velocity Profile)

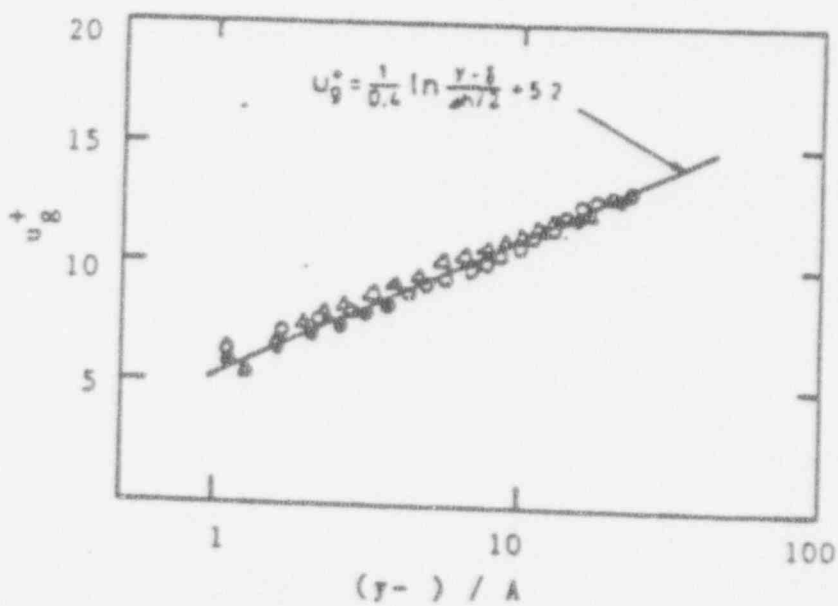

Fig. 3.5 Rough Surface Correlation for Gas Velocity
(Re_L = 8.04x10^3; o, Re_G = 6.52x10^3; •, Re_G = 8.54x10^3
▲, Re_G = 1.32x10^4; ——, Correlation Line)

Chapter 4
COMPARISON WITH EXPERIMENTAL DATA

4.1 Analysis with the Condensation Heat Transfer Model and Verification

4.1.1 Analysis with the Simple Model

The condensation heat transfer models were incorporated into a computer program to compare with the experimental data. This program separately calculates the heat flux through the liquid film by using the model described in section 3.3 and the heat flux through the air-vapor boundary layer by using the model in section 3.1 with an assumed interface temperature (T_I). The program then iterates on the heat flux by modifying T_I until the heat fluxes converge within a specified accuracy as shown in Fig 4.1.

Since the shear stress is a function of the distance along the wall and the characteristics of the condensate film change along the wall, the wall is divided into a finite number of control nodes and the condensate rate and the other values are calculated at each node along the direction of the condensate film flow. For countercurrent flow, the momentum boundary thickness of the vapor-air flow is guessed at the starting point of the condensate film and is subtracted at each node. At the end of the calculation for the whole length, the momentum boundary thickness is checked and will be iterated to obtain the proper momentum boundary layer thickness.

When these heat and mass transfer coefficients were calculated, the transport properties at the vapor-air boundary layer were evaluated at a reference temperature and mass fraction suggested by Sparrow et al. [29] as

$$T_{R1} = T_W + \frac{(T_I - T_W)}{3} \qquad (4.1.1\text{-}7)$$

4.1.2 Condensate Film

The model for the condensate film was compared with the pure vapor experimental data of J.E. Goodykoontz and R.G. Dorsh [23]. One should remember that for pure vapor the condensate film controls the heat transfer. The purpose of comparison to this data is to verify that the model for the condensate is reasonable when compared to tests in which the film controls the heat transfer. This data showed that the experimental heat transfer coefficient is 1.3 to 1.9 times as large as the value predicted by the laminar model of Fujii and Uehara as shown in Fig. 2.4. Fujii and Uehara attributed this discrepancy to the turbulence in the film due to the very high vapor velocity. The effect of the wavy interface and the turbulent model of the condensate film were, therefore, investigated. The following values of k^+, E and A^+ were chosen from the expeimental data for pipe flow in a tube, where the experiments were done, and were used with Eqs. (2.5.2-11) and (2.5.2-12)

$$k^+ = 0.4 \qquad (4.1.2\text{-}1)$$

$$E = 9.0 \qquad (4.1.2\text{-}2)$$

$$A^+ = 26.0 \qquad (4.1.2\text{-}3)$$

This experiment was done with a range of the steam inlet velocity from 10 to 80 m/sec and the condensate film should change from a laminar film to a turbulent film with

The dimensionless shear stress at the high inlet velocity, however, is calculated to be much higher than 10, and in this case the critical film Reynolds number is considered to be less than 100 in Fig. 2.22. Therefore, two criteria will be used for the change from laminar flow to turbulent flow as follows :

a) A critical Reynolds number : 2000

b) A dimensionless critical shear stress of 10 with the critical film Reynolds number of 100.

3) The wavy interface affects the heat transfer rate by increasing the shear stress and decreasing the film thickness. The calculation shows about a 10 percent increase in the heat transfer coefficient at the entrance region for the laminar flow. In this model, for laminar flow, although the wavy interface reduces the film thickness by increasing the shear stress, it is not considered that it increases the heat transfer by the turbulent motion of the wavy layer. It results in a small increase of the heat transfer rate by the wavy interface for laminar flow. This effect seems to disappear at the end of the tube, since more vapor was condensed at the entrance region and the velocity at the end region is calculated to be much slower than that of the case of a smooth interface. In addition to the decrease of the condensate film thickness, the eddy diffusivity of heat for the turbulent flow is modelled to increase with the shear stress. The effect of the wavy interface is, therefore, larger than that on the laminar flow as shown by Figs. 4.2 and 4.5.

4.1.3 Verification of Simple Model with Laminar Flow

Asano comes from the high mass transfer correction factor, since Asano used a tabulated value from mass transfer experiments rather than the value calculated from Eq. (3.1.2-24). The origin of Asano's tabulated values for high mass transfer was not given in the original paper nor referenced in the bibliography.

4.1.4 Verification of Two-Dimensional Model with Laminar Flow

A two dimensional calculation was done with the SIMPLER algorithm for the vapor-air phase and calculated the condensation rate on the assumed interface temperature. The perpendicular velocity (y direction velocity) at the condensate interface is assigned as the boundary condition from the condensate rate calculated.

$$v_{gI} = m'' / \rho \qquad (4.1.4\text{-}1a)$$

The other boundary conditions for the condensate interface are

$$u_{gI} = u_l(\delta) \qquad (4.1.4\text{-}1b)$$

$$T_{gI} = T_l(\delta) \qquad (4.1.4\text{-}1c)$$

$$X_{vI} = \frac{P_{vI}*M_v}{P_{vI}*M_v + P_{vI}*M_v} \qquad (4.1.4\text{-}1d)$$

where the partial pressure of the steam at the interface is set equal to the saturation pressure at the interface temperature calculated. The following boundary conditions for the other side wall are imposed

Since the perpendicular velocity is set at the interface, the correction term for high mass transfer rates is not needed and is included within the theory of the two-dimensional calculation. The results, therefore, show very good agreement with the experiments for the wide range of the vapor mass fractions as shown in Fig. 4.8.

4.2 Comparison with Dallmeyer's Experiment

The Dallmeyer experiment was also compared with the calculated results from the simple model developed for turbulent vapor-gas flow and with the two dimensional k-ϵ model. This experiment was chosen because it was the only forced convection 'separate effects' test available for turbulent flow of the vapor-gas mixture. The condensate film is considered to be in laminar flow with a smooth interface, since the film was maintained to be laminar by sucking off the condensate at intervals of 100 and 200 mm along the plate. Moreover, the film Reynolds number without considering the suction is calculated to be less than 100.

The thermophysical properties of CCL_4 were evaluated from tabulated values [121]. In the two dimensional calculation, the boundary conditions for velocity, temperature and mass fraction at the interface were evaluated by Eqs. (4.1.4-1a) - (4.1.4-1d) and the turbulent kinetic energy and dissipation were calculated by the local equilibrium condition of Eqs. (2.5.2-13) and (2.5.2-14). The following boundary conditions for the centerline of the apparatus are imposed

$$u = u_B \qquad (4.2\text{-}1)$$

4.3 Comparison with CVTR Experiment

4.3.1 CVTR Experiment

The only large scale integral containment experiments which have been performed in the United States, are the Carolinas Virginia Tube Reactor (CVTR) test series, where slightly superheated steam was injected from a nearby fossil power plant into a full scale containment of a decommissioned nuclear reactor. This steam was injected through a diffuser which consisted of a 10 ft section of 10 inch diameter pipe mounted vertically with 128 1 inch diameter holes drilled in its wall. The base elevation of the diffuser was 335 ft, which was 10 ft higher than the operating floor. Only one experiment of the three in the test series (Test 3) was conducted without an active spray system, which was used for the other two experiments. Table 4.3 shows the injected steam condition of Test 3.

The CVTR containment is a reinforced concrete cylindrical structure with a hemispherical top dome, having an internal diameter of 17.66 m. The operating floor is also of reinforced concrete (see Fig. 4.12). The communication between the operating region and basement is via the circumferential space between the containment wall and the edge of the operating floor and through the stairways [122].

The most reliable method of measuring the heat transfer coefficient through the containment wall utilized two heat transfer assemblies (heat plugs), which were installed in the operating floor (elevation of 330 ft and 350°) and Heat Plug 2 some 23 ft higher on the wall (elevation of 348 ft and 315°). These measured the temperature profile

The K-FIX computer code [123] which calculates the transient dynamics of two-dimensional, two-fluid flow with interfacial exchange, was used to obtain an estimate of the velocities along the surface of the heat plugs. The six field equations for the two fluids couple through mass, momentum, and energy exchange and are solved using an Eulerian finite difference technique [124].

For the velocity field calculation of the CVTR test, air was treated as one fluid and steam was assumed as the other. No condensation or evaporation for either phase was assumed and the same velocity and temperature for air and steam was calculated by setting a large interfacial friction coefficient and heat transfer coefficient. As shown in Fig. 4.14, the total containment (total volume = 64.8 m^3, height = 25.9 m , radius = 8.83 m) was divided into 388 cells by using the axis of symmetry; i.e. the r-direction was divided into 20 nodes, the z-direction was done by 21 nodes and 62 cells were used for the internal obstacles which simulated the hemispherical dome and the operating floor. The communication between the operating region and the basement is allowed only via the circumferential gap between the containment wall and the edge of the operating floor. The steam was assumed to be injected homogeneously and horizontally through a 10 ft high inflow boundary opening as an approximation to the horizontally oriented holes in the diffuser. The injected steam conditions at the inflow opening were estimated by using choked flow calculations as shown in Table 4.4.

Since a small time step was required (2 msec), the velocity fields in the containment could not be simulated during the whole blowdown period (166.4 sec). They were calculated at the beginning of steam injection (BOSI) and the end of steam injection (EOSI) by assuming a quasi steady-state. This method is a good assumption given the

model, the vapor-air boundary layer is developed from 340 ft for both directions and the countercurrent effect is considered.

The heat transfer coefficient along the wall at 110 sec after the blowdown was calculated and is shown in Fig 4.18. The calculation estimated that the condensate film develops waves at 385 ft, where the film Reynolds number exceeded 100. The effect of the wavy interface is expected to increase the heat transfer coefficient about 10 percent at the position of Heat Plug 2 and agrees well with the experimental data. Figure 4.19 shows that the heat resistance through the condensate film cannot be neglected for this condition, even though the early investigators [37, 116] insisted that the condensate film could be neglected in computing the total heat transfer coefficient for condensation with a noncondensable gas. The conditions are different as follows:

1) Asano's experiment and analysis [36] was done in laminar vapor-air flow, where the heat and mass transfer rates through the vapor-air boundary layer are much lower than that in turbulent vapor-air flow.
2) Even though the turbulent vapor-air flow is considered by Corradini's analysis, he neglected the vapor mass fraction at interface (X_I at Eq. (3.1.2-12)) to calculate the heat transfer by condensation. At 110 sec after a blowdown, however, the temperature of the containment wall rises to the saturation temperature of the atmosphere and the vapor mass fraction is not negligible at the interface. Figure 4.20 shows that the heat transfer coefficient with X_I is almost 1.6 times as large as that without it.
3) The velocity of the vapor-air mixture is higher

condensation will not occur any more given this condition, and only forced convection heat transfer occurs at the surface. This transition is not represented in the present model.

The results of the heat transfer coefficients calculation at Heat Plug 1 (lower plug) overestimated the experiment data with the parallel velocity calculated by K-FIX as shown in Fig. 4.24.

Finally, the two-dimensional model results for the vapor-air flows are compared as shown in Fig. 4.25 to the experimental data. The vapor-air flow conditions calculated from K-FIX are used as the boundary condition in the two-dimensional calculation as shown in Fig. 4.26. The calculation results show the following discrepancies with that of the simple model:

1) The two dimensional calculation estimated a lower heat transfer coefficient than the simple model near the stagnation point. This seems to be reasonable, since it is supposed to come from the laminarization by the strong stabilization effect of acceleration. This same effect was found in the turbulent impinging jet experiment on a plate by C. O. Popiel et al. [125] for the ratio of the distance from the nozzle to the nozzle diameter (z/d) less than 4 (at this calculation z/d = 1). By a limitation of the wall function model, which is that the nearest node should be remote from the wall for y^+ to be larger than 10.8, the calculation result is not expected to be accurate at the node of the stagnation point, where y^+ is less than 10.8. This is because the τ_I is calculated to be very small due to the small parallel velocity to the wall.
2) The velocity at Heat Plug 2 is used as the velocity along the wall for the whole upper wall (from 340 ft

coefficient agrees well with the experimental data and the two-dimensional calculation at the point of Heat Plug 1 (9.2 m). Even though this velocity may not be correct, it is used for the whole period of the experiment to include the effect of the two dimensional flow and stair way. Fig 4.24 shows good agreement for the whole period. After 110 sec, the upper wall is not expected to have a condensate film, and the condensate film is assumed to start at 340 ft (stagnation point). Also, near the time of the steam shutoff, the temperature difference between the bulk and the wall surface are small (5-10°C). Small temperature difference uncertainties, which were estimated to be about 1.1°C in the report [2], result in large heat transfer coefficient uncertainties from Eq. (4.3.2-1) (see error bar in Fig. 4.24). These two reasons cause the differences between the model and experiment after 110 sec.

As a conclusion, the calculated results of the simple model agree fairly well with the experimental data and the detailed two-dimensional calculation except for the narrow stagnation area. Since the velocity of the vapor-air flow is one of the most important factors in estimating the heat transfer coefficient, a more reliable computing method for predicting the vapor-air flow in a containment, which may consider the effect of three dimensional geometry and turbulent vapor-air flow, is required to make more reliable estimates.

4.4 Natural Convection Model with Tagami Experiment

4.4.1 Tagami Experiment

The Tagami experiment, which measured the condensation heat transfer coefficient at the steady-state, was

condensation heat transfer was measured to be slightly dependent on the surface height [3]. It agrees well with the natural convection model of the transition region, where the heat transfer coefficient is independent of the surface length. Therefore, Tagami's experiment was analyzed by using the natural convection model. Figs. 4.27 and 4.28 show good agreement of the calculated heat transfer coefficients with experiment. Also, the results of the turbulent and laminar model calculation show that the turbulent region model is useful to predict results for the case beyond this transition region. From this analysis, it is concluded that the developed natural convection models are useful to predict a post-blowdown accident by choosing the appropriate model from the (Gr Pr) number.

4.5 Precalculation of the Future Experiment

Using the simple model, parametric studies were done to predict the result of the condensation experiment with a noncondensable gas, which is under way in this laboratory. The dimensions of the apparatus are shown at Fig. 4.29. The turbulent vapor-air flow is injected into the rectangular flow channel (100 mm x 100 mm) and the water is injected onto the surface to model the thick film condition, which is expected from a long containment wall.

No condensation is assumed in the inlet section (1.245 m) but the boundary layer of the vapor-air is developed in this section. The temperature of the condensing wall is about 20°C and the total pressure is maintained to be about atmospheric. The mass ratio of the air to the vapor is controlled by changing the bulk temperature, which is the saturation temperature at the partial vapor pressure.

Table 4.1 The Effect of the Distance of the Nearest Node to the Wall at the Two-Dimensional Calculation of Asano Experiment

X_{vB}	T_B(°C)	$(Q/Q_{Nu})_{Exp}$	Two-Dimensional Calculation (Q/Q_{Nu})					
			2.0E-4*	1.0E-4	5.0e-5	2.7e-5	1.2e-5	5.0e-6
0.97	65.0	0.7	0.471	0.517	0.550	0.564	0.575	0.578
0.95	65.0	0.5	0.345	-	0.400	0.410	0.417	0.420
0.85	37.0	0.23	0.189	0.207	0.218	0.224	0.227	-
0.80	37.0	0.19	0.150	-	-	0.173	0.171	-
0.70	17.0	0.13	0.115	0.118	0.119	-	-	-
0.50	17.0	0.047	0.062	0.064	-	-	-	-
0.40	17.0	0.037	0.047	0.047	-	-	-	-

* : The Distance of the Nearest Node to the Wall

\- : Not Calculated

Table 4.4 Inflow Steam Condition for K-FIX

Pressure (MPa)	0.6307 (1.1660) [a]
Temperature (^{o}C)	122.08 (186.67)
Density (kg/m^{3})	3.4972 (5.5570)
Mass Flow Rate (kg/sec)	47.879
Velocity (m/sec)	214.58
Inflow Area (m^{2}) [b]	0.0638

[a] () repersents the values before choked,

[b] Inflow area is calculated by summation of the areas of 126 1 inch diameter hole.

Table 4.5 Results of Estimated Velocity from K-FIX

	BOSI (0-- 10 sec)	EOSI (160 - 166 sec)
Heat Plug 1 (m/sec)	7.9	6.1
Heat Plug 2 (m/sec)	10.2	8.0

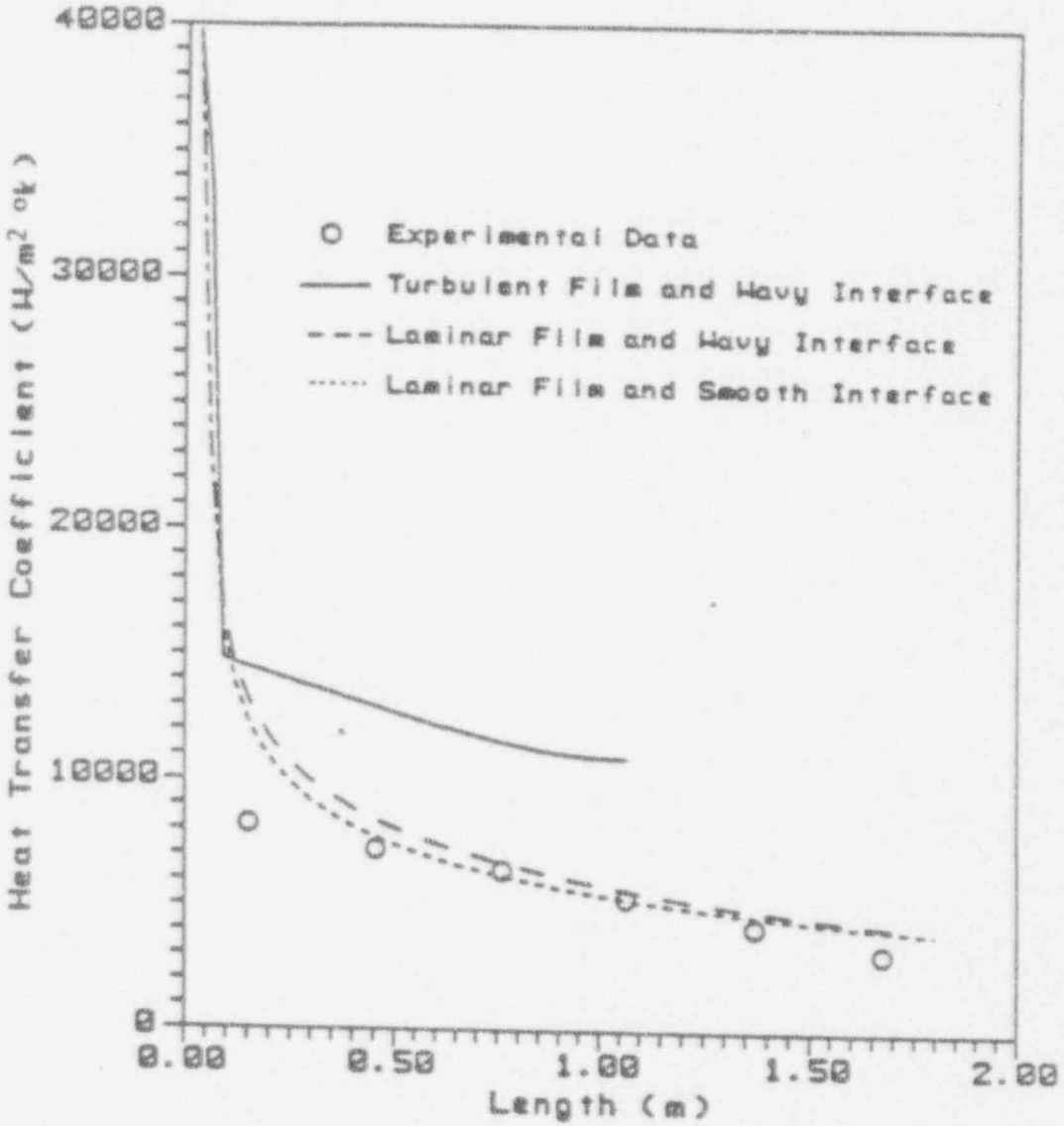

Fig. 4.2 Calculation Results from the Models Developed and Goodykoontz and Dorsh's Experiment Data at Uin = 19.9 m/sec

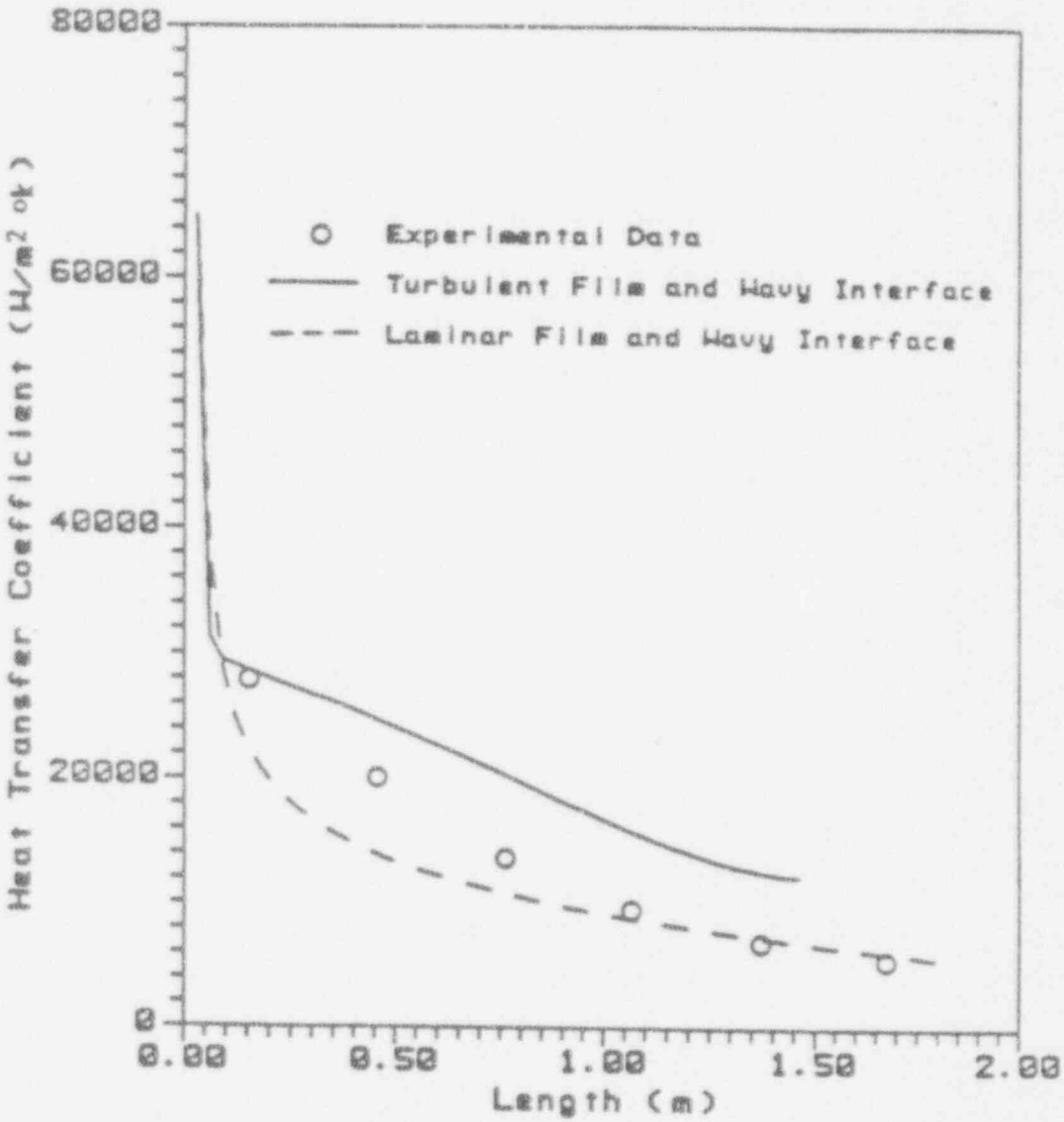

Fig. 4.4 Calculation Results from the Models Developed and Goodykoontz and Dorsh's Experiment Data at Uin = 47.9 m/sec

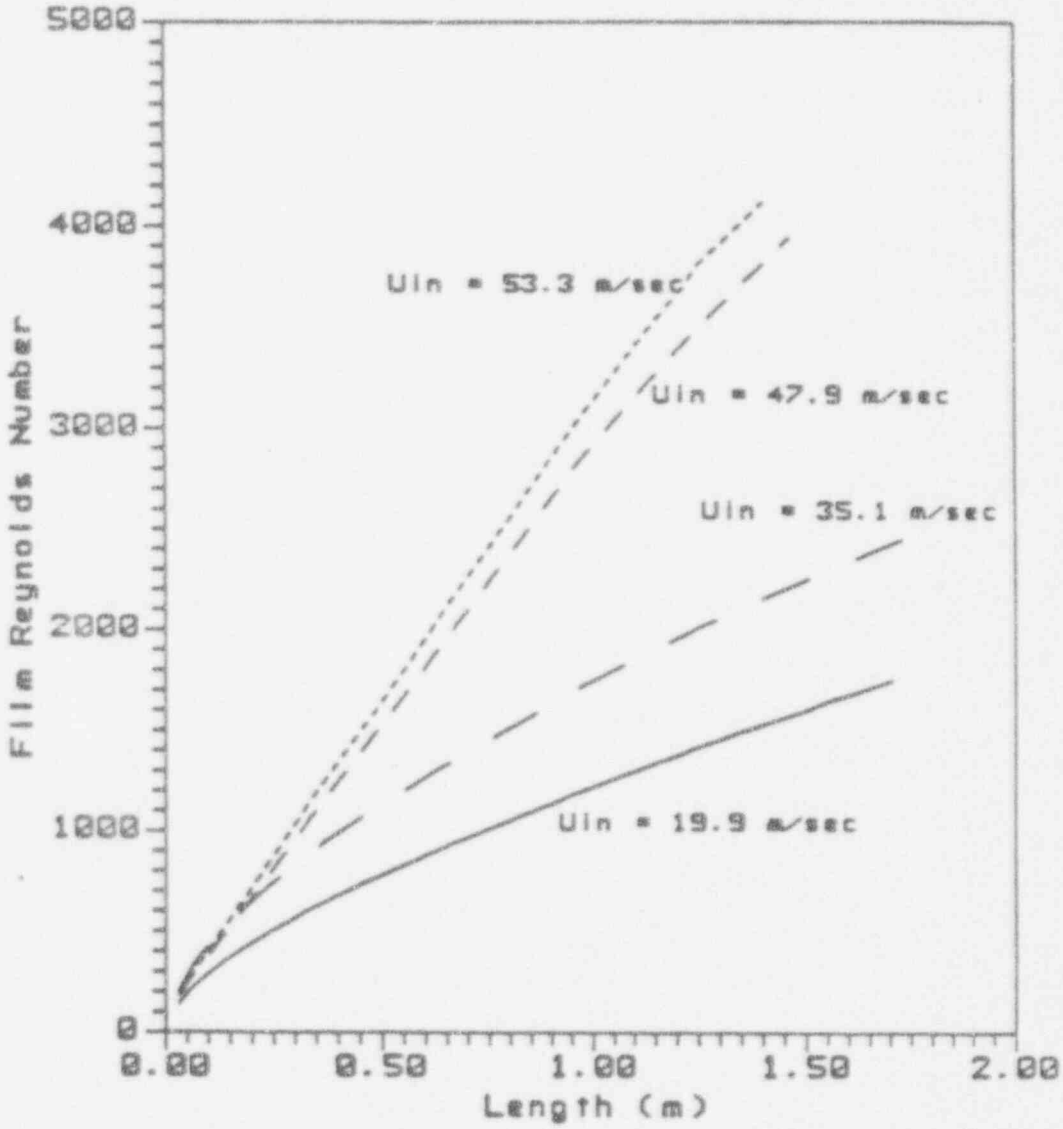

Fig. 4.6 Calculated Film Reynolds Number

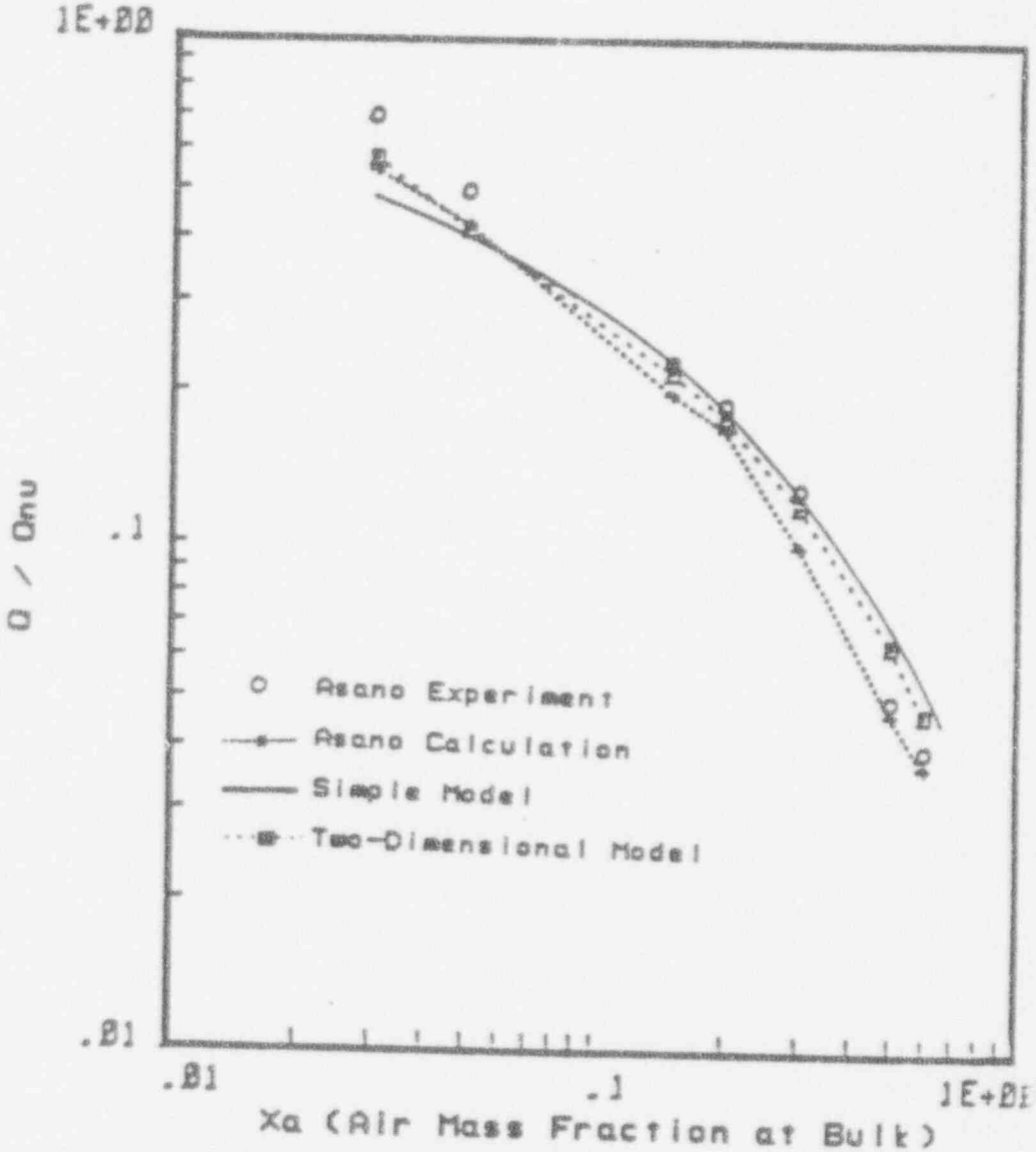

Fig. 4.8 Calculation Results of Simple Model and Two-Dimensional Model with Asano Experimental Data [36]

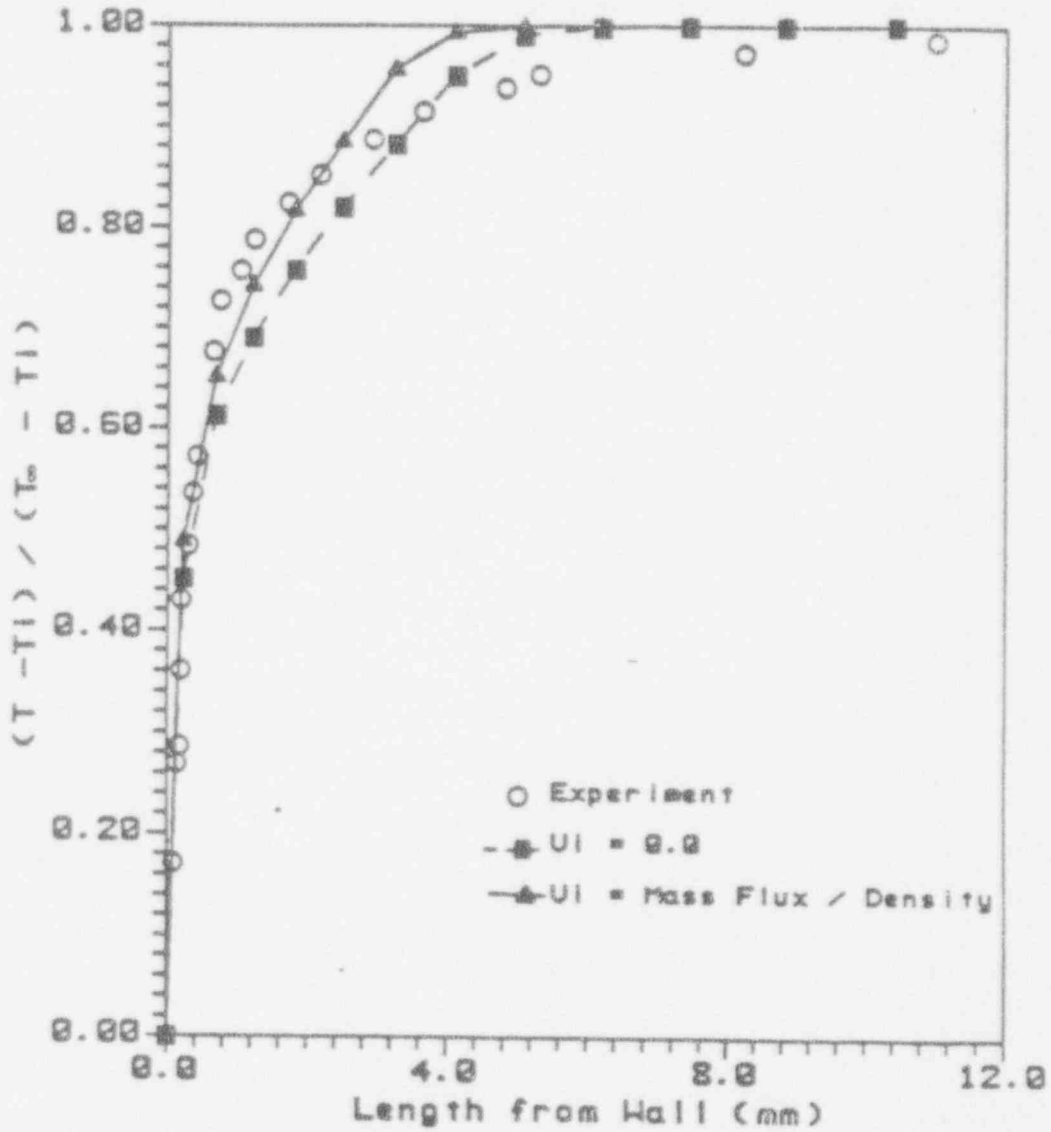

Fig. 4.10 Comparison of the Temperature Profile between the Two-Dimensional Calculation Results and Dallmeyer Experimental Data

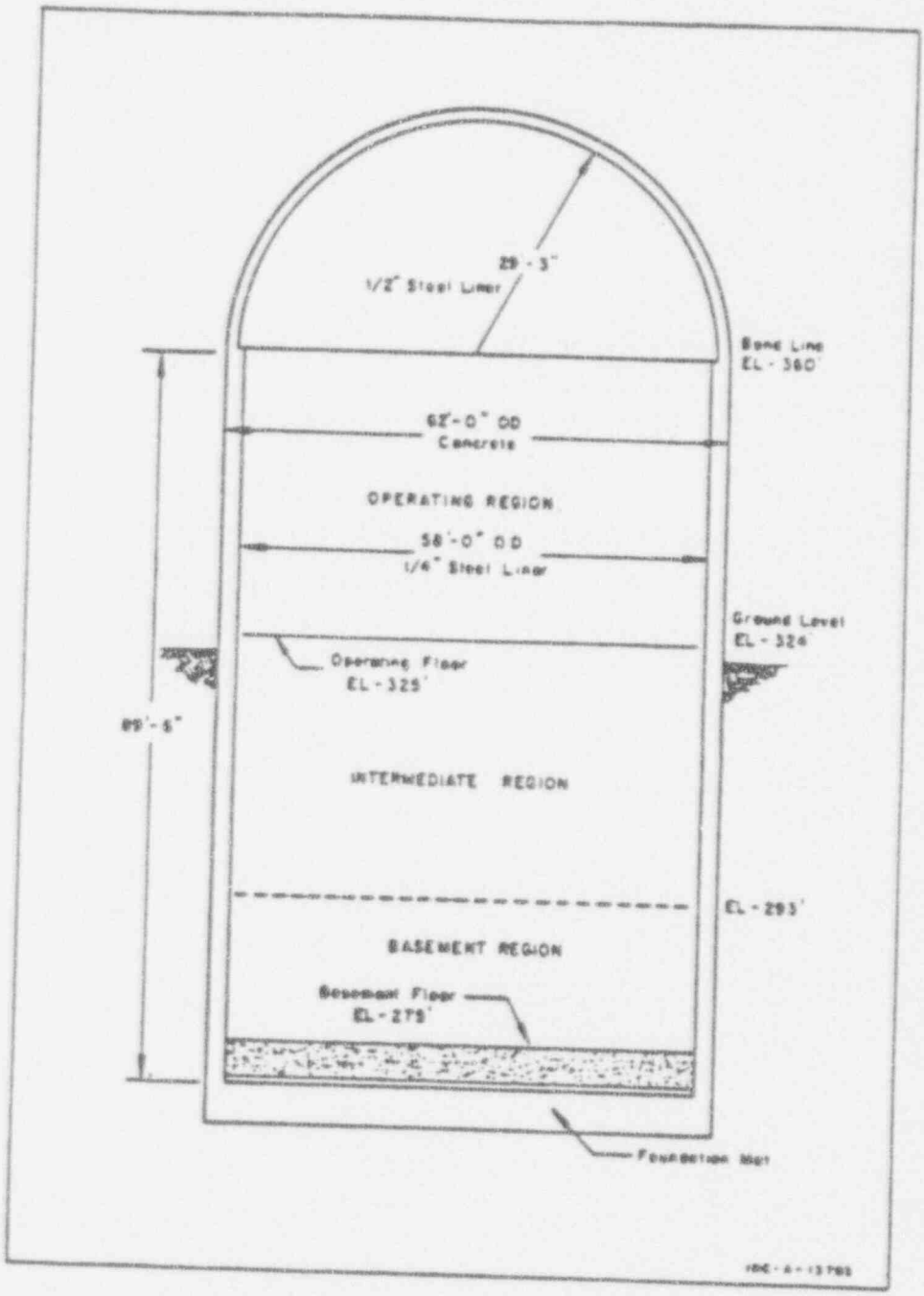

Fig. 4.12 CVTR Containment Structure

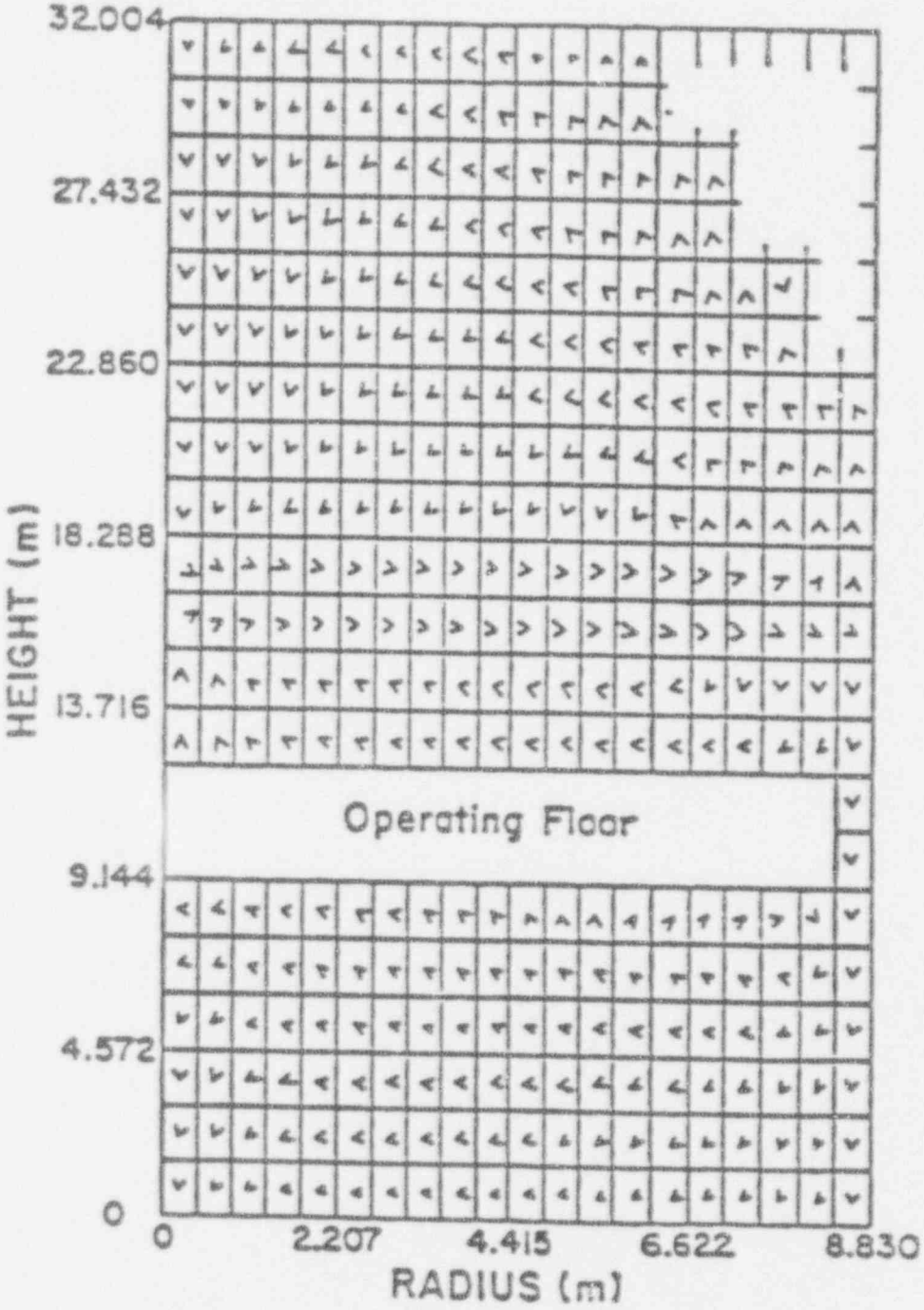

Fig. 4.14 Flow Distribution Calculated from K-FIX at 5 sec for CVTR test

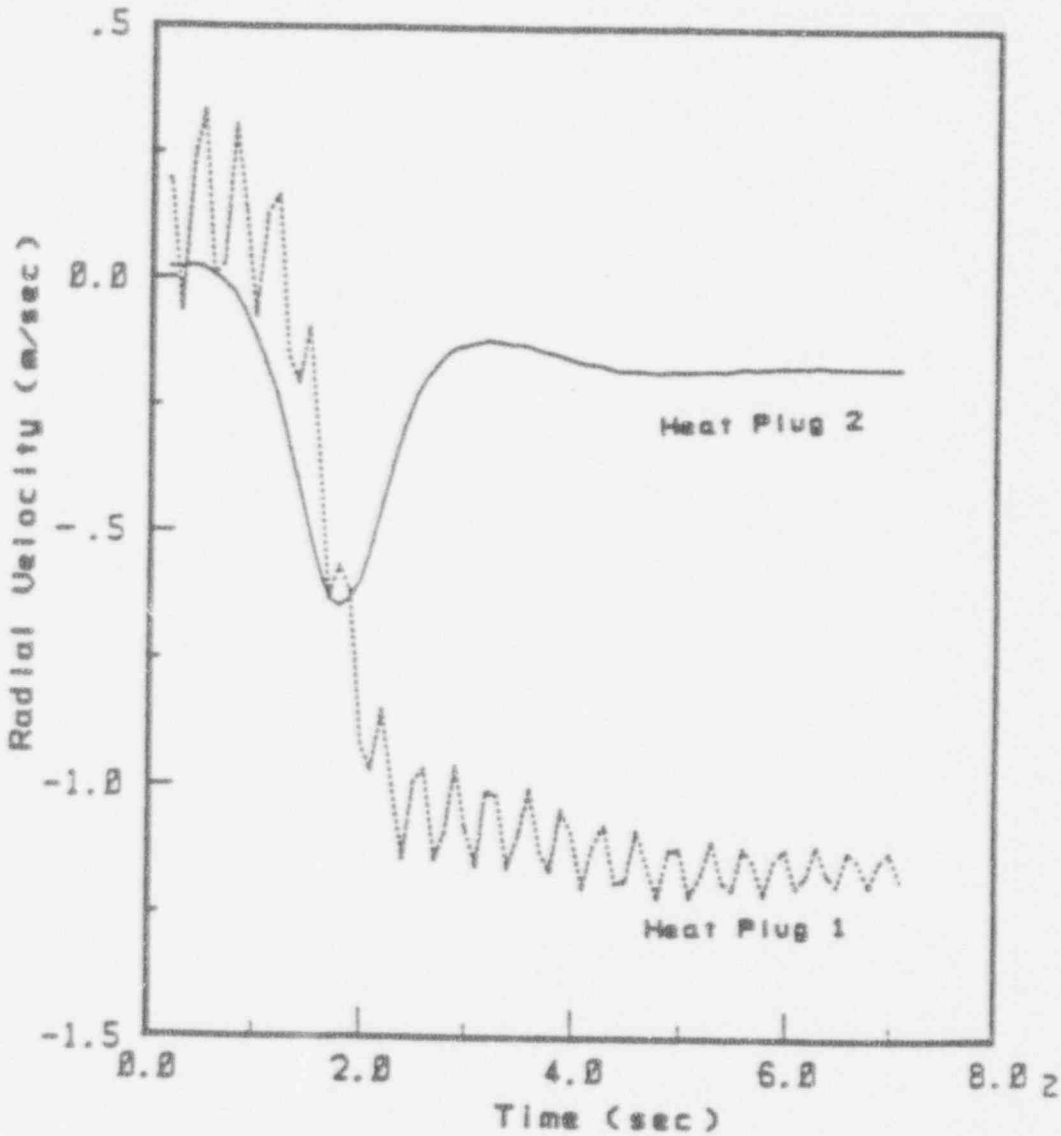

Fig. 4.16 Radial Velocity Calculated at BOSI (0-8 sec)

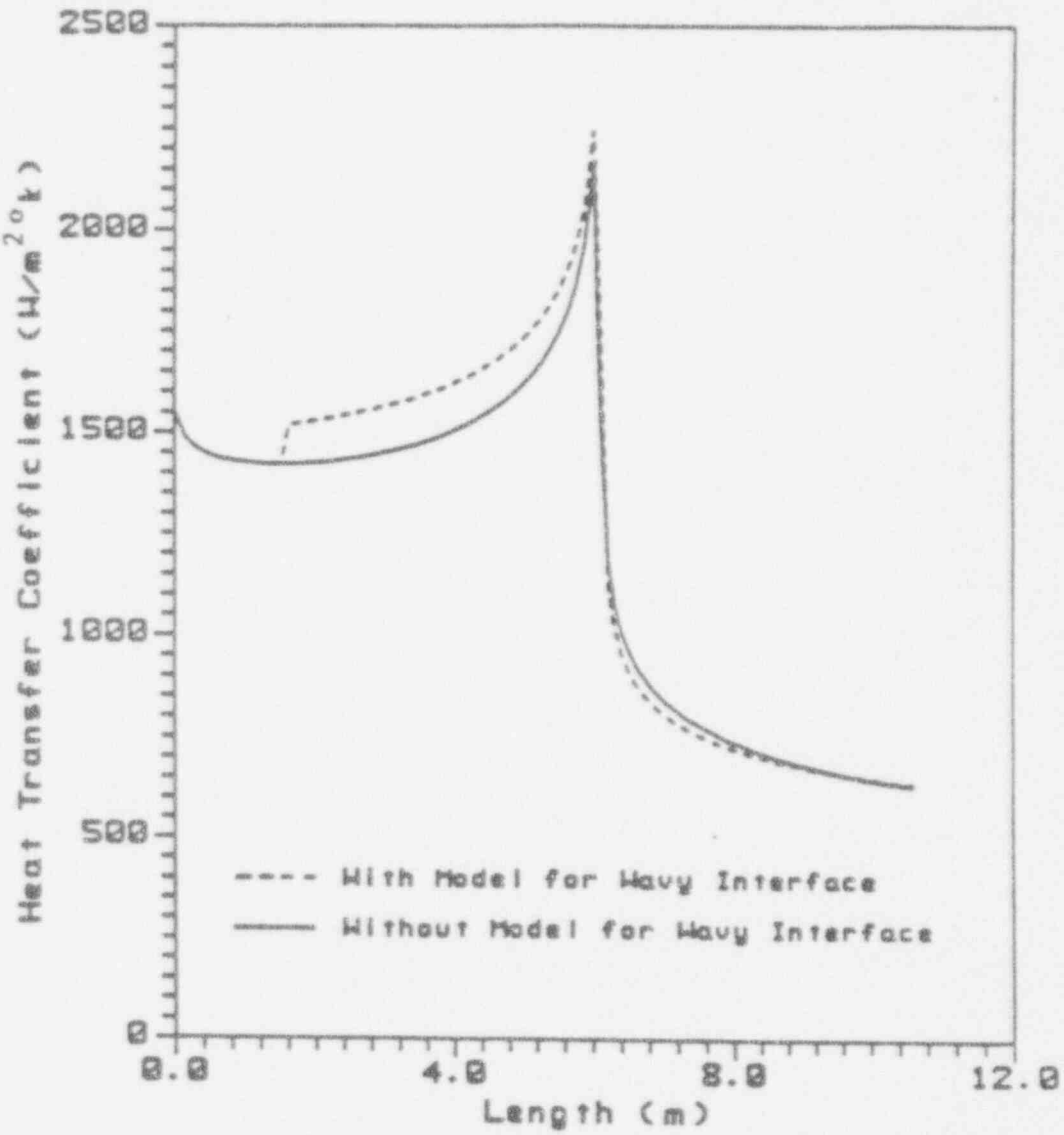

Fig. 4.18 Heat Transfer Coefficient along the Wall at 110 sec after a Blowdown

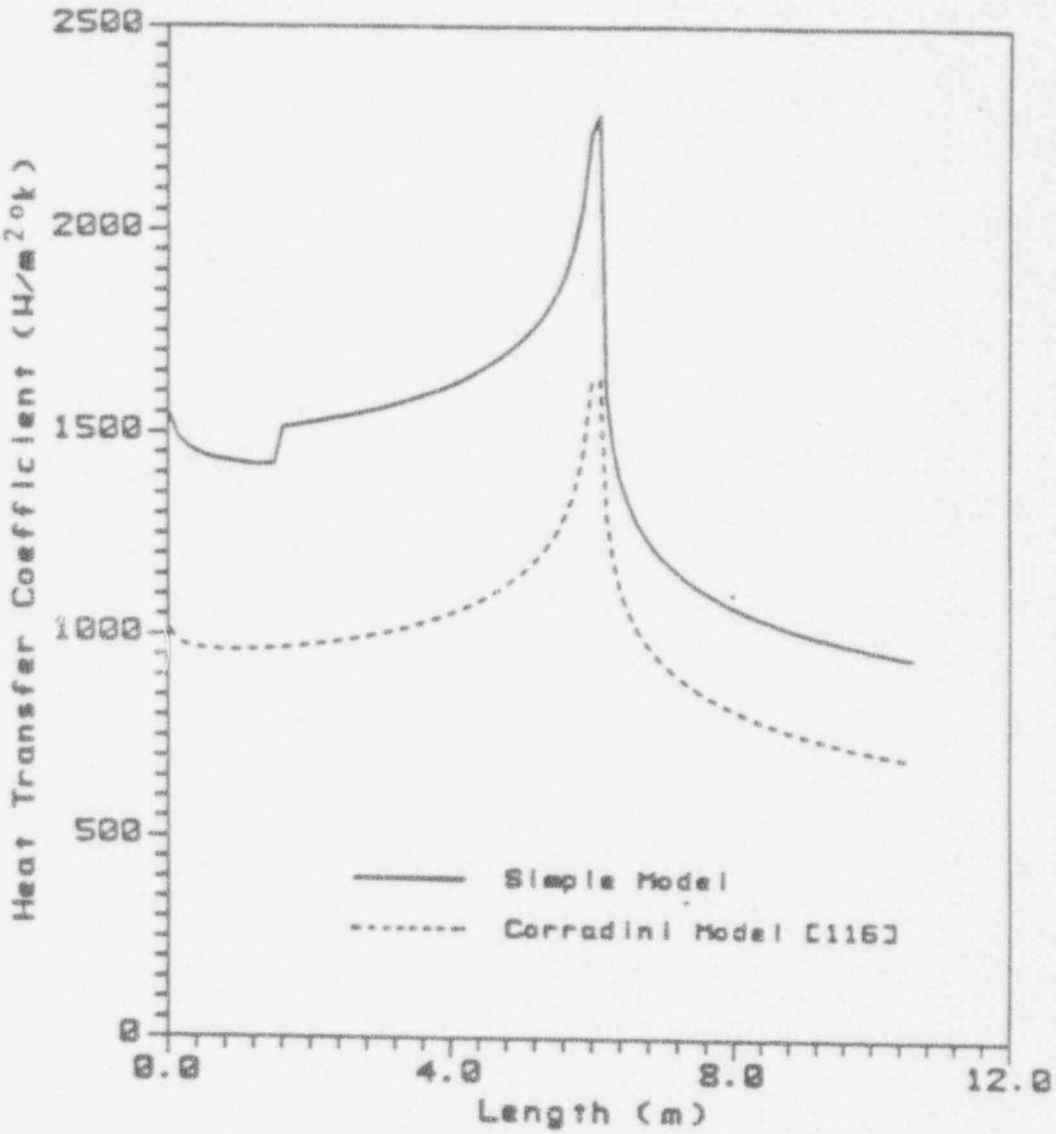

Fig. 4.20 Comparison between the Simple Model and Corradini Model

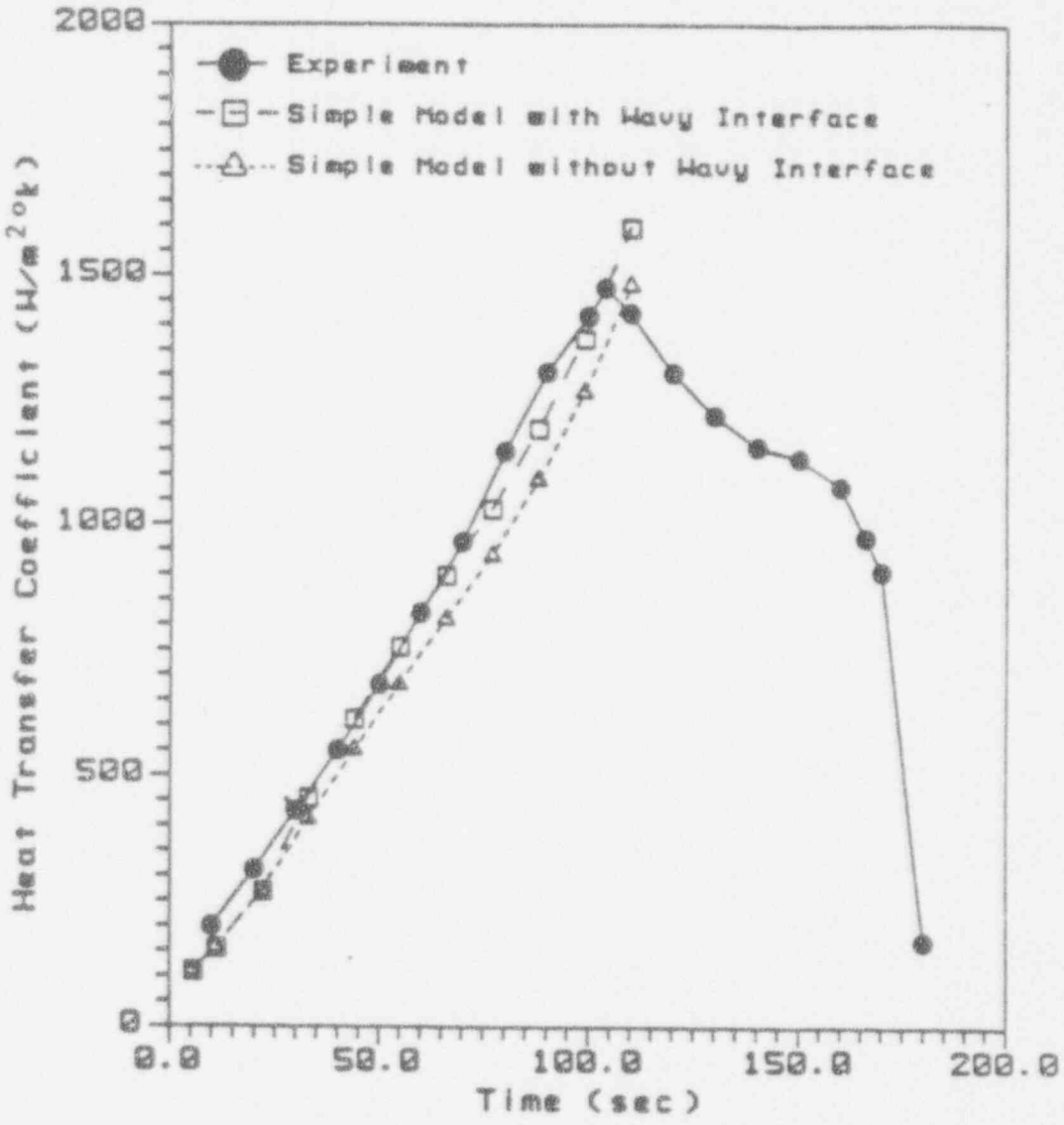

Fig. 4.22 Condensation Heat Transfer Coefficient at Heat Plug 2

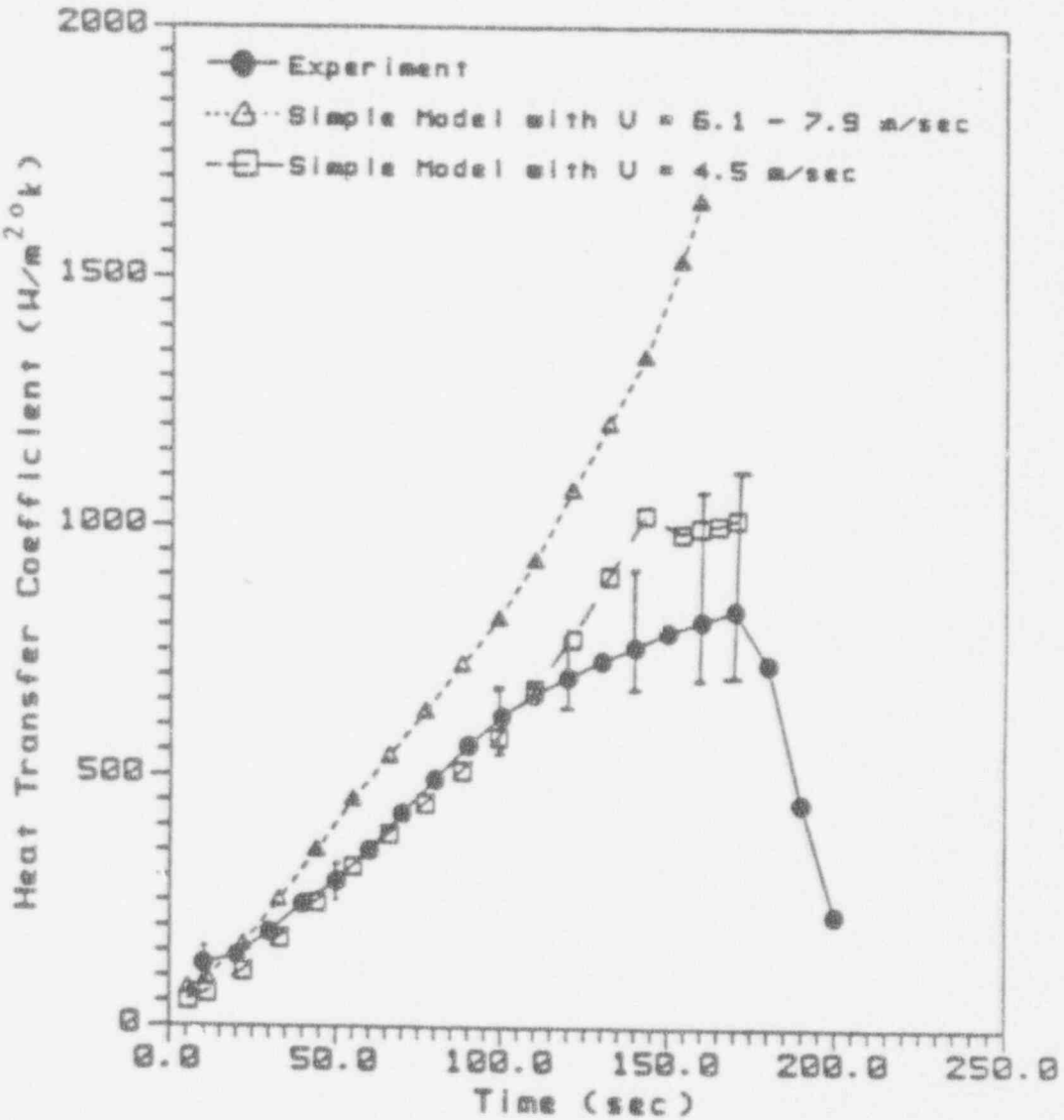

Fig. 4.24 Condensation Heat Transfer Coefficient at Heat Plug 1

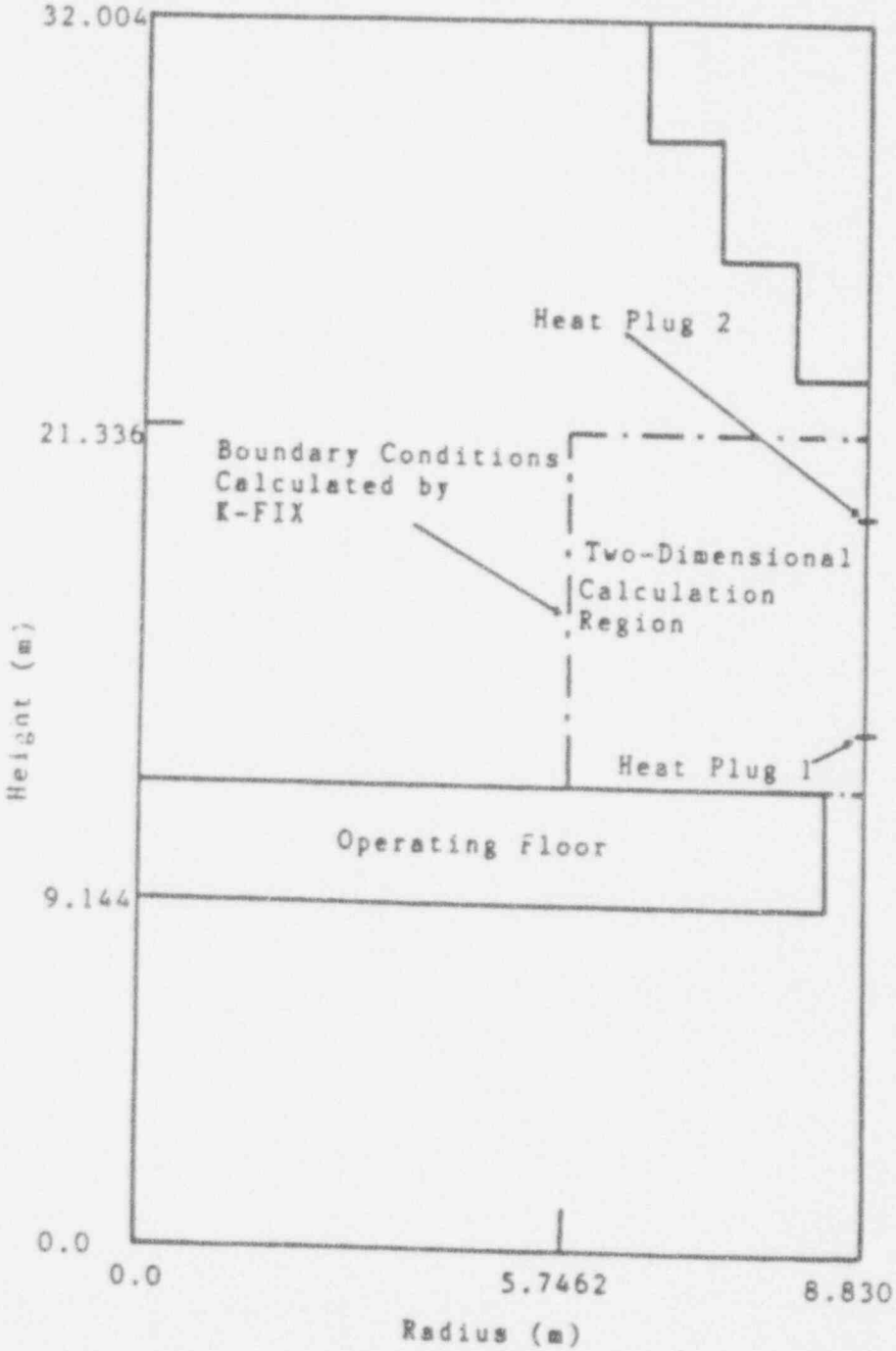

Fig. 4.26 The nodes used at Two-Dimensional Calculation of CVTR Test with the Boundary Conditions Calculated by K-FIX

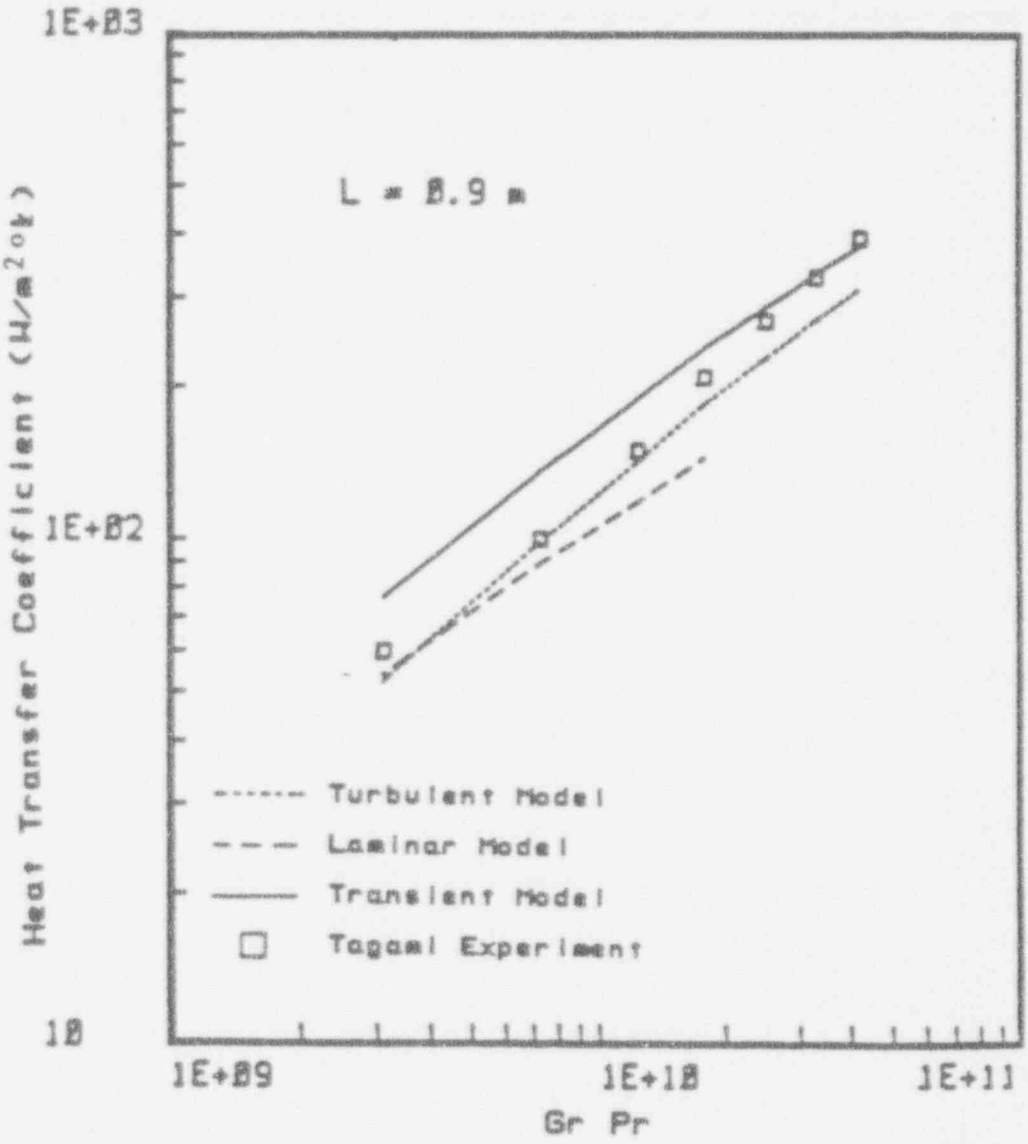

Fig. 4.28 Natural Convection Model vs. Tagami Experiment (L = 0.9 m)

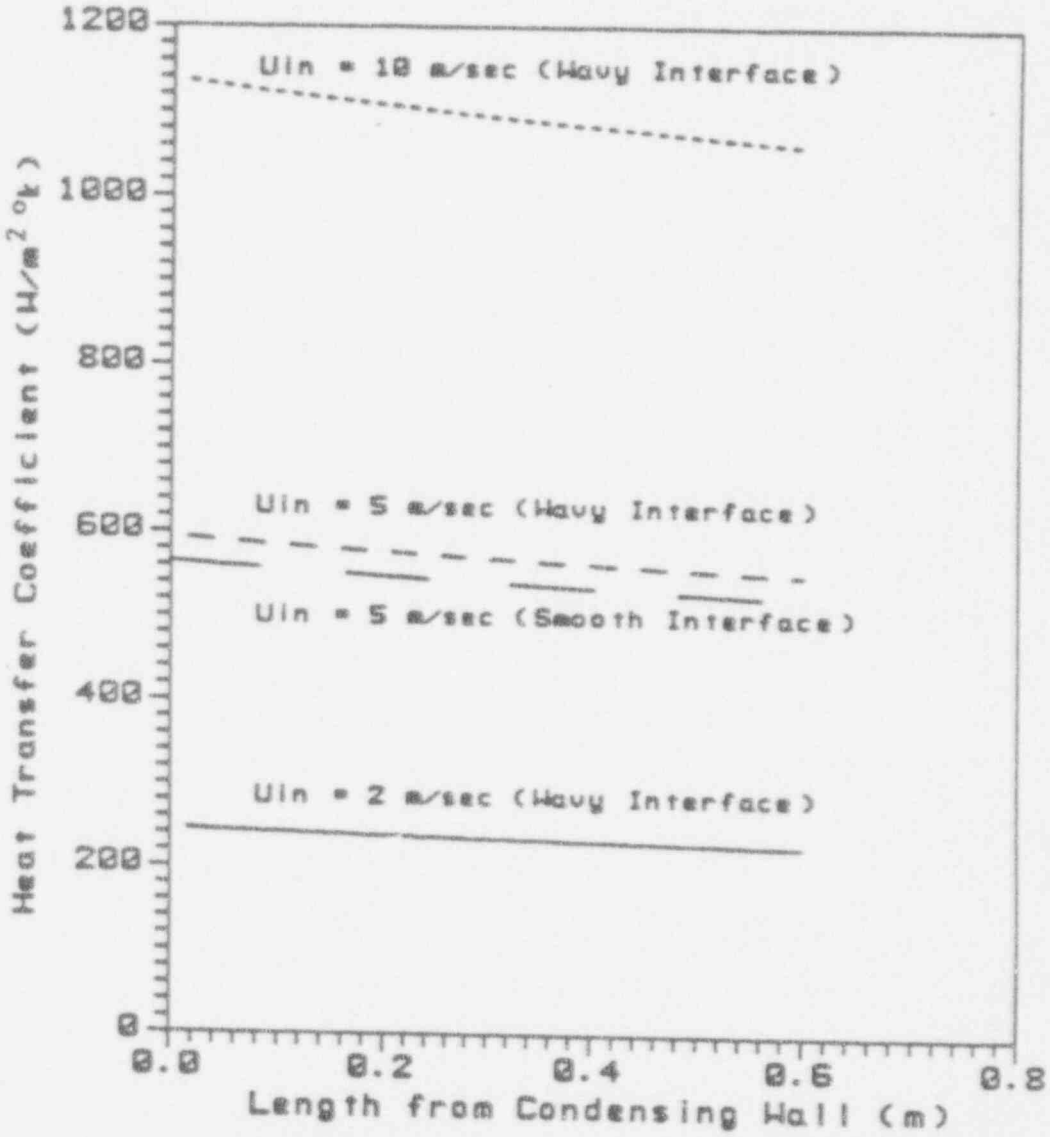

Fig. 4.30 The Effect of Inlet Velocity
(Mass Ratio of Air to Vapor = 0.684)
(Injected Film Thickness = 0.5 mm)
(Temperature Difference = 70 °C)

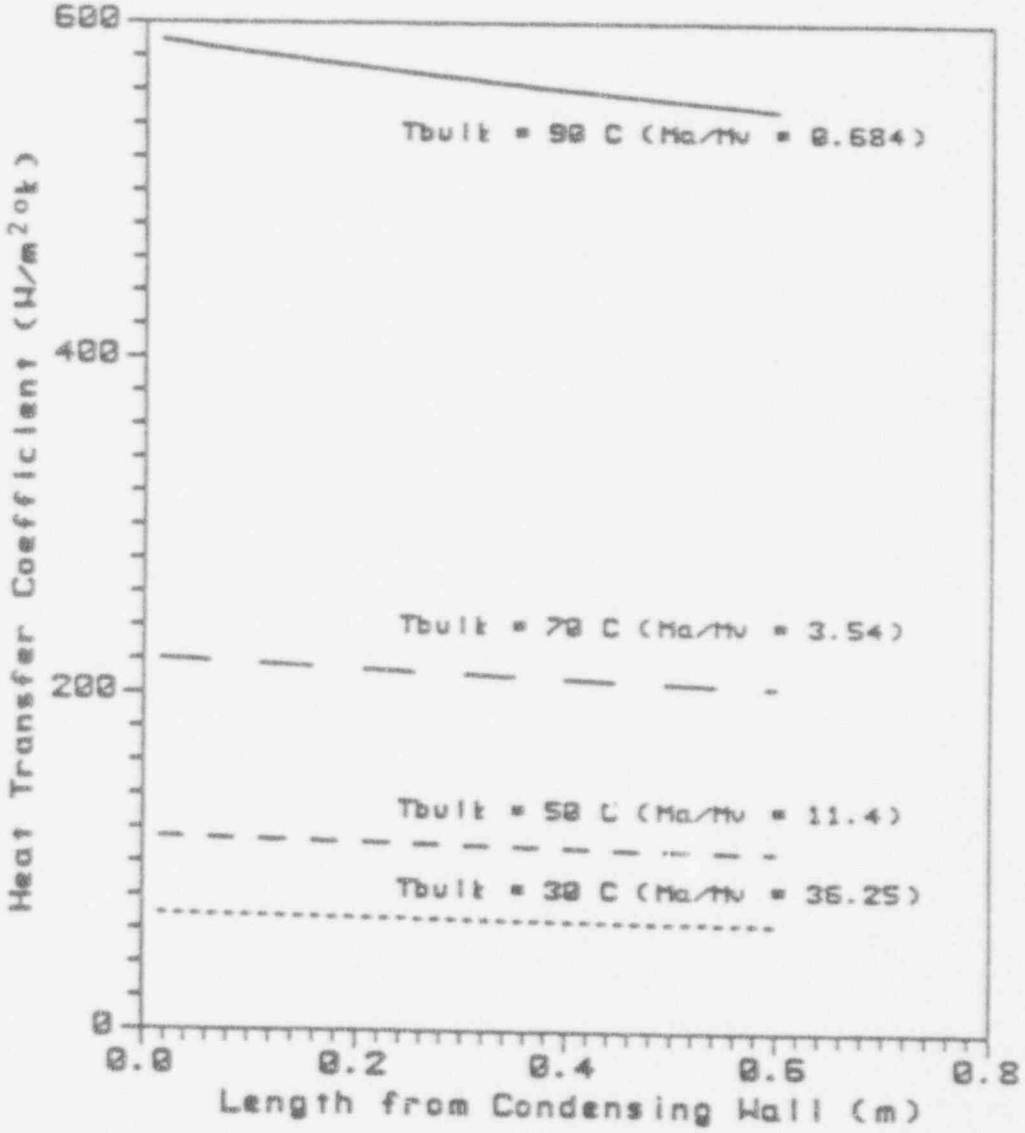

Fig. 4.32 The Effect of Mass Ratio of Air to Vapor
(Injected Film Thickness = 0.5 mm)
(Injected Gas Velocity = 5 m/sec)

- Asano experiment
  (laminar vapor-air flow)
- Dallmeyer experiment
  (turbulent vapor-air flow with laminar condensate film and smooth interface)
- CVTR experiment (Heat Plug 2)
  (turbulent vapor-air flow with laminar condensate film and wavy interface)
- Tagami experiment
  (natural convection)

2) The effect of the wavy interface on the vapor-air boundary layer shows about a 10 percent increase in the heat transfer rate at Heat Plug 2 for the CVTR test. The increased rate is a function of the wave height as shown in the prediction of the future experiments.

3) Usually, the heat transfer resistance through the condensate film in the presence of noncondensable gas is much smaller than that through the vapor-air boundary layer and can be neglected. The heat transfer coefficient of the condensate film, however, should be considered under the following conditions:
   (a) The temperature difference between the bulk and the wall is small,
   (b) The heat transfer coefficient of the vapor-air boundary is large enough due to the high velocity of the vapor-air or the high wall temperature, since the high wall temperature causes the vapor mass fraction at the interface to be large.

4) The two-dimensional calculation with a k-ϵ model shows good agreement with the separate effects' data and the simple model. In particular the computations

vapor. No experiment of condensation with noncondensable gas which investigated the structure of the interface, the critical condition for the generation of a wavy interface or the structure of the turbulent condensate film, has been reported.

4) The correlation for a rough wall surface is used to model the effect of a wavy interface. Since the structure of a wavy surface is apparently different than that of sand roughness or a rough solid wall, the correlation can be modified from future condensation experimental data.

5) Two dimensional calculations with a k-ϵ model for the turbulent flow and a wall function model for the wavy interface can be combined with a multi-dimensional turbulent containment analysis code for a better overall estimate of the pressure-temperature response after a postulated accident.

```
C |  DESCRIPTION OF PARAMETERS (SI UNITS)                                    |
C |                                                                          |
C |   ACF2    : FRICTION COEFFICIENT                                         |
C |   AKA     : THERMAL CONDUCTIVITY OF AIR AT Tref                          |
C |   AKS     : THERMAL CONDUCTIVITY OF STEAM AT Tref                        |
C |   ALEHG   : LENGTH OF THE WALL                                           |
C |   ALEHGO  : LENGTH OF THE TOP WALL FOR THE CONTINUOUS CALCULATION        |
C |   AMFA    : MASS FRACTION OF AIR AT Tref                                 |
C |   AMFS    : MASS FRACTION OF STEAM AT Tref                               |
C |   AMUA    : VISCOSITY OF AIR AT THE REFERENCE TEMPERATURE (Tref)         |
C |   AMUG    : VISCOSITY OF MIXED VAPOR (AIR & STEAM) AT Tref               |
C |   AMUL    : VISCOSITY OF LIQUID (WATER) AT Tref                          |
C |   AMWA    : MOLECULAR WEIGHT OF AIR                                      |
C |   AMWS    : MOLECULAR WEIGHT OF WATER                                    |
C |   CI      : MOLAR CONCENTRATION OF STEAM AT INTERFACE                    |
C |   CONSTE  : CONSTANT IN THE UNIVERSAL VELOCITY PROFILE (E IN EQUATION)   |
C |   CONSTK  : CONSTANT IN THE UNIVERSAL VELOCITY PROFILE (k+ IN EQUATION)  |
C |   CONSTV  : CONSTANT FOR THE CONTRIBUTION OF THE MASS TRANSFER           |
C |             TO THE SHEAR STRESS IN THE LIQUID FILM CALCULATION           |
C |   CONTFI  : FLAG FOR THE CONTINUOUS CALCULATION                          |
C |                        *** CONTINUOUS CALCULATION ***                    |
C |                                                                          |
C |                        VAPOR-AIR FLOW          CONDENSATE FLOW           |
C |                                                                          |
C |                        CALCULATION 1   UP      DOWN                      |
C |                        CALCULATION 2   DOWN    DOWN                      |
C |                                                                          |
C |   COUNTC  : FLAG FOR THE COUNTERCURRENT FLOW                             |
C |   CPA     : SPECIFIC HEAT OF AIR AT Tref                                 |
C |   CPS     : SPECIFIC HEAT OF STEAM AT Tref                               |
C |   CRTRE1  : CRITICAL FILM REYNOLDS NUMBER FOR THE TURBULENT FILM (2900)  |
C |   CRTRE2  : CRITICAL FILM REYNOLDS NUMBER WITH SHEAR STRESS (CRTTAU)     |
C |             FOR THE TURBULENT FILM (100)                                 |
C |   CRTTAU  : CRITICAL DIMENSIONLESS SHEAR STRESS WITH CRTRE2              |
C |             FOR THE TURBULENT FILM (10)                                  |
C |   CRWERE  : CRITICAL FILM REYNOLDS NUMBER FOR THE WAVY INTERFACE         |
C |   CS      : MOLAR CONCENTRATION OF STEAM AT BULK                         |
C |   CSTAR   : COEFFICIENT FOR HIGH MASS TRANSFER RATE                      |
C |   DAB     : DIFFUSION COEFFICIENT                                        |
C |   DEL2    : MOMENTUM BOUNDARY LAYER THICKNESS OF VAPOR-AIR FLOW          |
C |   DELTAX  : INCREMENT (LENGTH OF EACH NODE)                              |
C |   DENSA   : DENSITY OF AIR AT Tref                                       |
C |   DENSAB  : DENSITY OF AIR AT Tbulk                                      |
C |   DENSL   : DENSITY OF LIQUID (WATER)                                    |
C |   DENSM   : DENSITY OF MIXED VAPOR AT Tref                               |
C |   DENSMB  : DENSITY OF MIXED VAPOR AT Tbulk                              |
C |   DENSS   : DENSITY OF STEAM AT Tref                                     |
C |   DENSSB  : DENSITY OF STEAM AT Tbulk                                    |
C |   GAM     : MASS FLOW RATE OF CONDENSATE PER UNIT WIDTH                  |
C |   GRAGO   : GRAVITATIONAL ACCELERATION COEFFICIENT                       |
C |   HFILM   : CONDENSATION HEAT TRANSFER COEFF. THROUGH CONDENSATE FILM    |
C |   HGAS    : CONDENSATION HEAT TRANSFER COEFF. THROUGH VAPOR-AIR B. L.    |
C |   HOVER   : TOTAL CONDENSATION HEAT TRANSFER COEFFICIENT                 |
C |   HPRIM   : ENTHALPY DIFFERENCE BETWEEN VAPOR AND CONDENSATE WATER       |
```

```
166           OPEN(10,FILE=FNAME,STATUS='OLD')
167     C
168           WRITE(*,'(A\)')' OUTPUT FILE NAME FOR PARAMETERS?'
169           READ(*,'(A)') FNAME
170           OPEN(21,FILE=FNAME,STATUS='NEW')
171     C
172           WRITE(*,'(A\)')' OUTPUT FILE NAME FOR GENERAL RESULTS I?'
173           READ(*,'(A)') FNAME
174           OPEN(22,FILE=FNAME,STATUS='NEW')
175           WRITE(22,400)
176       400 FORMAT('   xleng', 4X, 'xfirst', '  wave length', 3X, 'tauio',
177          *       , 6X, 'refl1m', 5x, 'tl', 9x, 'del', 5X, 'resumk', 6X,
178          *       'kflim', 4X, 'kgeo', 7X, 'kover')
179     C
180           WRITE(*,'(A\)')' OUTPUT FILE NAME FOR GENERAL RESULTS II?'
181           READ(*,'(A)') FNAME
182           OPEN(23,FILE=FNAME,STATUS='NEW')
183           WRITE(23,401)
184       401 FORMAT('  XLENG', 8X, 'XLLENG', 6X, 'XGLENG', 5X, 'COUNTC',
185          *         1X, 'CONTFI', 1X, 'REMAN', 6X, 'XXS', 7X, 'DEL2',
186          *         7X, 'CF2',    6X, 'VELDIF')
187     C   ------------------------
188     C    Loop for each data set
189     C   ------------------------
190     C
191     C Read input data and set the initial conditions
192     C
193       201 READ (10,*) ICASE, PTOTAL, TWALL, TS, VG, ALENG, ITNODE, INATU
194           WRITE(22,21) ICASE, PTOTAL, TWALL, TS, VG
195        21 FORMAT(1H1,    'ICASE=', I5, '  PTOTAL=', E12.5, '  TWALL=',
196          1       E12.5,  '  TS=', E12.5,  '  VG= ', E12.5,//)
197           IF (ICASE .EQ. 999) THEN
198            GO TO 10
199           END IF
200           IF (ABS(ICASE) .EQ. ABS(ICASED)) THEN
201            CONTFI = .TRUE.
202           ELSE
203            CONTFI = .FALSE.
204           END IF
205           LSTOP = .FALSE.
206           TIME = ICASE * 5.5
207           CALL SAT (TS, PS, DPS)
208           PA = PTOTAL - PS
209           RATIO = AMRA * PA / (AMPS * PS)
210           DELTAX = ALENG / (1.*ITNODE)
211           ICCITE = 1
212     C
213     C Initialization for concurrent flow
214     C
215           IF (ICASE .LT. 0) THEN
216            COUNTC = .FALSE.
217            LSTOP = .TRUE.
218            TIME = -1. * TIME
219            IF (CONTFI) THEN
220             VELDIF = VG - VDELTA
```

```
            XLLDMG = XLDMG
            XGLDMG = ALDMG - XLDMG
          ELSE
            XLLDMG = XLDMG
            XGLDMG = XLDMG
          END IF
          IF (CONTFI) THEN
            XLLDMG = ALDMGO + XLDMG
          END IF
C
C First guess of the interface temperature at each node
C
          IF (ICCITE .NE. 1) THEN
            TI = TII1(IMODE)
          ELSE IF (IMODE .EQ. 1) THEN
            TI = (TWALL +TS) / 2.
           ELSE
            TI = TI
          END IF
          ITER = 1
          TLOW = TWALL
          THIGH = TS
C
C   ------------------------------------------------------------
C    Iteration loop for the interface temperature
C   ------------------------------------------------------------
C
C Calculate the heat transfer coefficient through the vapor-air
C   boundary layer and condensate film
C
  284 CALL PARAM
          THETAS = TI - TWALL
          REYNUM = DENSGB * VELDIF * XGLDMG / AMUG
          IF (NFIRST) THEN
            DEL2 = DELO2
            DELM2 = 0.0
            CALL FORCE(WAVE,COUNTC)
            CALL FILMIN(COUNTC)
            GO TO 285
          END IF
          DEL = DELI
          DEL2 = DEL2I
          DELM2 = DELM2I
          VDELTA = VDELTI
          IF (LAMINA) THEN
            CALL FILMLA(WAVE,COUNTC)
          ELSE
            CALL FILMTU(COUNTC)
          END IF
          CALL FORCE(WAVE,COUNTC)
C
C Calculate the new interface temperature to match the heat flux
C   through the vapor-air boundary layer and the condensate film
C
  285 QFILM = HFILM * (TI-TWALL) * DELTAX
```

```
            WRITE(23,404) XLENG, XOLENG, XLLENG, COUNTC, CONTFI,
     1                    RENUM, XX3, DEL2, ACF2, VELDIF
           END IF
           XLENG = XLENG + DELTAX
           NFIRST = .FALSE.
           INODE = INODE + 1
           IF (LSTOP) THEN
            IF (INODE .LE. ITNODE) THEN
             GO TO 283
            ELSE
             GO TO 287
            END IF
           ELSE IF (INODE .LE. ITNODE) THEN
            GO TO 283
           END IF
       403 FORMAT(f10.5, 3L8, 8(e10.3, 1x))
       404 FORMAT(3(F10.5, 1X), 2L8, 8(E10.3, 1X))
C
C End of the calculation for the whole length
C
           IF (COUNTC) THEN
            ERDEL2 = ABS ((DELN2 - DEL02) / DELN2)
            IF (ERDEL2 .LE. 1.0E-3) THEN
             WRITE(28,*) 'CONVERGE COMPLETELY AND GO TO THE NEXT TIME STEP'
             CALL OUTPUT(COUNTC, CONTFI)
             LSTOP = .TRUE.
             DEL2 = DELN2
            ELSE IF (WAVE) THEN
              DEL2 = 0.7*DEL02 + 0.3*DELN2
             ELSE
              DEL2 = DELN2
             END IF
            ICCITE = ICCITE + 1
            GO TO 282
           END IF
C End of the calculation of one data set
       287  IF (COUNTC) THEN
            ELSE
             CALL OUTPUT(COUNTC, CONTFI)
            END IF
            ALENGO = ALENG
           ICASEO = ICASE
           GO TO 281
       288 WRITE(*,*) 'CONVERGE FAIL FOR FINDING THE INTERFACE TEMP.'
           WRITE(*,*) 'HFILM, HGAS, QFILM, QGAS, EPS',
          1            HFILM, HGAS, QFILM, QGAS, EPS
        10 STOP
           END
C
C-----------------------------------------------------------------------
           SUBROUTINE FORCE(WAVE, COUNTC)
C-----------------------------------------------------------------------
C
C  THIS SUBROUTINE CALCULATES THE CONDESATION HEAT TRANSFER COEFFICIENT
C  OF THE VAPOR-AIR BOUNDARY LAYER BY USING THE ANALOGY BETWEEN MOMENTUM .
```

```
      RETURN
      END
C
C-----------------------------------------------------------------------
      SUBROUTINE NATU
C-----------------------------------------------------------------------
C
C   THIS SUBROUTINE CALCULATES THE CONDENSATION HEAT TRANSFER COEFFICIENT
C   BY USING THE MODEL DEVELOPED FOR THE NATURAL CONVECTION
C
$INCLUDE: 'CWNG.CMN'
      IF (GRLPR .LE. 1.0E8) THEN
       AG = 0.56 * (GRL * SCNUM) ** (1./4.) * DAB / ALENG
       HCONV = 0.56 * (GRL * PRNUM) ** (1./4.) * AKG / ALENG
      ELSE IF (GRLPR .LE. 1.0E10) THEN
       AG = 0.13 * (GRL * SCNUM) ** (1./3.) * DAB / ALENG
       HCONV = 0.13 * (GRL * PRNUM) ** (1./3.) * AKG / ALENG
      ELSE
       AG = 0.021 * (GRL * SCNUM) ** (2./5.) * DAB / ALENG
       HCONV = 0.021 * (GRL * PRNUM) ** (2./5.) * AKG / ALENG
      END IF
      HCOND = AG * AMPS * (CS - CI) * (HDIFF + HEVAP) / (TS - TWALL)
     *        + AHCONV
      HCOND = CSTAR * HCOND
      HCONV = CSTAR * HCONV
      HGAS = HCOND + HCONV
      RETURN
      END
C
C-----------------------------------------------------------------------
      SUBROUTINE FILMIN(COUNTC)
C-----------------------------------------------------------------------
C
C  THIS SUBROUTINE IS PROGRAMED TO CALCULATE THE HEAT TRANSFER
C  COEFFICIENT OF THE CONDENSATE FILM AT THE FIRST NODE
C
$INCLUDE: 'CWNG.CMN
      LOGICAL NFIRST, WAVE, LAMINA, COUNTC, CONTFI
      AMAKTH = AMUL * AKL * THETAS
      SM = DENSL**2. * GRAVG * HPRIM * XLLENG**3. / (4.*AMAKTH)
      ACF2 = 0.0256 / REYNUM**0.2
      IF (COUNTC) THEN
       ACF2 = -ACF2
      END IF
      DR =  DENSL * ACF2 * DENSGB * VG**2 * HPRIM * XLLENG**2. / AMAKTH
      RETP = DENSL * CONSTV * VG * XLLENG / AMUL
      IITER = 1
      IF (ITER .EQ. 1) THEN
       X = 1.0E-7
      END IF
   40 Y = SM * X**4 + DR * X**3 / 3. + RETP * X**2 / 4. - 1.
      ERY = ABS (Y)
      DERIV = 4.*SM*X**3 + DR*X**2 + RETP*X/2.
      DX = Y / DERIV
      X = X - DX
```

```
      DEL = DEL + DELTAD
      RETURN
      END
C
C-----------------------------------------------------------------------
      SUBROUTINE FILMTU(COUNTC)
C-----------------------------------------------------------------------
C
C    THIS SUBROUTINE IS PROGRAMED TO CALCULATE THE HEAT TRANSFER
C    COEFFICIENT OF THE TURBULENT CONDENSATE FILM
C
$INCLUDE: 'COMMO.CMN'
      LOGICAL  MFIRST, WAVE, LAMINA, COUNTC, CONTFI
  101 ODEL = DEL
      OTAUB = TAUB
      OVDELT = VDELTA
      ITER = ITER + 1
      IF (COUNTC) THEN
       VELDIF = VG + VDELTA
      ELSE
       VELDIF = VG - VDELTA
      END IF
      ACF2 = 0.158 / (ALOG(884.*DEL2/XKS))**2.
      IF (COUNTC) THEN
       ACF2 = -ACF2
      END IF
      TAUIB = ACF2 * DENSGB * VELDIF**2
      TAUIC = DELTAM * CONSTV * VELDIF
      TAUI = TAUIB + TAUIC
      TAUIA = GRAVG * (DENSL-DENSGB) * DEL
      TAUB = TAUIA + TAUI
      VTAU = (TAUB/DENSL)**0.5
      DELP = DEL * DENSL / AMUL * (TAUB/DENSL)**0.5
      ODELP = DELP
  102 IF (DELP .LE. 10.8) THEN
       DELP = (GAM*2./AMUL)**0.5
      ELSE
       DELP = (GAM/AMUL+32.84)/(2.44*ALOG(DELP)+2.56)
      END IF
      ERROR = (DELP - ODELP) / DELP
      ODELP = DELP
      IF (ABS(ERROR) .GT. 1.0E-4) GO TO 102
      DEL = DELP / DENSL * AMUL / (TAUB/DENSL)**0.5
      IF (DELP .LE. 10.8) THEN
       VDELTA = (TAUB/AMUL) * DEL
      ELSE
       VDELTA = (2.44 * ALOG(DELP) + 5.0) * VTAU
      END IF
      ERROR = ABS(DEL - ODEL) / DEL
      IF (ERROR .GT. 1.0E-4) GO TO 101
      IF (DELP .LT. 10.8) THEN
       AKTL = AKL
      ELSE
       PRNUML = CPL * AMUL / AKL
       PRTL = 0.55 + 0.61 / PRNUML
```

```
      CALL SAT (TREF1, PSREF1, DPSAT)
C
C Calculate density
C
      DENSS = 1. / SVSD (TREF1)
      DENSSB = 1. / SVSD(TS)
      DENSA = (PTOTAL-PSREF1)*1.0E6 * AMWA / (8314.*(TREF1 + 273.))
      DENSAB = (PTOTAL-PS) * 1.0E6 * AMWA / (8314. * (TS + 273.))
      DENSG = DENSS + DENSA
      DENSGB = DENSSB + DENSAB
      DENSL = 1. / 0.001
C
C Calculate viscosity
C
      AMUS = 8.84E-6 + 4.07E-8 * TREF1 - DENSS * (1.858E-7 - 5.9E-10
     1       *TREF1)
      AMUA = AMUAD(TREF1)
      PISA = (1 + (AMUS / AMUA)**0.5 * (AMWA / AMWS)**0.25)**2 /
     1       (8 * (1 + AMWS / AMWA))**0.5
      PIAS = (1 + (AMUA / AMUS)**0.5 * (AMWS / AMWA)**0.25)**2 /
     1       (8 * (1 + AMWA / AMWS))**0.5
      AMFS = PSREF1 * AMWS / (PSREF1 * AMWS + (PTOTAL - PSREF1) * AMWA)
      AMFA = 1 - AMFS
      AMOLES = AMFS / AMWS
      AMOLEA = AMFA / AMWA
      XS = AMOLES / (AMOLES + AMOLEA)
      XA = AMOLEA / (AMOLES + AMOLEA)
      AMUG = XS * AMUS / (XS + XA*PISA) + XA * AMUA / (XA + XS*PIAS)
      AMUL = AMULD (TREF2)
C
C Calculate conductibity
C
      AKS = AKSD (TREF1)
      AKA = AKAD (TREF1)
      AKG = XS * AKS / (XS + XA * PISA) + XA * AKA / (XA + XS * PIAS)
      AKL = AKLD(TREF2)
C
C Calculate specific heat
C
      CPS = CPSD (TREF1)
      CPA = CPAD (TREF1)
      CPG = AMFS * CPS + AMFA * CPA
      CPL = CPLD (TREF2)
C
C Calculate diffusion coefficient
C
      TCA = 132.
      PCA = 36.4
      TCB = 647.3
      PCB = 218.01
      P = PTOTAL * 0.9892
      DAB = 3.64E-6 * ((TREF1+273.)/(TCA*TCB)**0.5)**2.334 * (PCA*PCB)
     1      **(1./3.) * (TCA*TCB)**(5./12.) * (1/AMWA + 1/AMWS)**0.5 / P
C
C Calculate enthalph difference
```

```
C   THIS SUBROUTINE CALCULATES THE CORRECTION FACTOR OF HIGH MASS TRANSFER
C
$INCLUDE: 'COMMO.COMM'
C
      AMFSB = PS * AMWS / (PS * AMWS + (PTOTAL - PS) * AMWA)
      AMFAB = 1 - AMFSB
      AMOLESB = AMFSB / AMWS
      AMOLEAB = AMFAB / AMWA
      XSB = AMOLESB / (AMOLESB + AMOLEAB)
      XAB = AMOLEAB / (AMOLESB + AMOLEAB)
      AMFSI = PI * AMWS / (PI * AMWS + (PTOTAL - PI) * AMWA)
      AMFAI = 1 - AMFSI
      AMOLESI = AMFSI / AMWS
      AMOLEAI = AMFAI / AMWA
      XSI = AMOLESI / (AMOLESI + AMOLEAI)
      XAI = AMOLEAI / (AMOLESI + AMOLEAI)
      R = (XSI - XSB) / (1 - XSI)
      CSTAR = ALOG(R+1)/R
C
      IF (ICCITE .EQ. 1 .AND. INODE .EQ. 1 .AND. ITER .EQ. 1) THEN
      WRITE(21,100) ICASE, RATIO, PTOTAL, TWALL, DELTAX
      WRITE(21,200) VG, ALEMG, AMFSI, AMFSB
      WRITE(21,300) XSI, XSB, R, CSTAR
      END IF
  100 FORMAT(' I=', I2, ' RATIO =', E15.7, '   PTOTAL=', E15.7
     1                '   TWALL =', E15.7, '   DELTAX=', E15.7)
  200 FORMAT(5X, 'VG    =', E15.7, '   ALEMG =', E15.7,
     1       '   AMFSI =', E15.7, '   AMFSB =', E15.7)
  300 FORMAT(5X, 'XSI   =', E15.7, '   XSB   =', E15.7,
     1       '   R     =', E15.7, '   CSTAR =', E15.7)
      RETURN
      END
C
C-----------------------------------------------------------------------
      SUBROUTINE SAT (TSAT, PSAT, DPSAT)
C-----------------------------------------------------------------------
C
C   THIS SUBROUTINE CALCULATES SATURATION PRESSURE WITH RESPECT TO
C   SATURATION TEMPERATURE.
C
      DIMENSION F(8)
      DATA F / -741.9242, -29.721, -11.55286, -0.8665638, 0.1014098,
     1         0.438893, 0.2520656, 0.05210684 /
      SUM = 0.
      DSUM = 0.
      X = 0.68 - 0.01 * TSAT
      TAU = 1000. / (TSAT + 273.15)
      DELT = 374.136 - TSAT
      DO 1 I = 1, 8
      J = 9 - I
      IF (J .EQ. 1) GO TO 1
      DSUM = DSUM * X + (J - 1) * F(J)
    1 SUM = SUM * X + F(J)
      RES = TAU * 1.E-05 * DELT *SUM
      PSAT = EXP(RES) * 22.088
```

```
      1       * (A(ISUB+1) - A(ISUB))
       RETURN
       END
C  ------------------------------
       FUNCTION AKSD(TEMP)
C  ------------------------------
C  CALCULATION OF THERMAL CONDUCTIVITY OF STEAM
C
       DIMENSION  A(15)
       DATA A    / 19.9,    19.6,    18.2E-3, 18.8E-3, 19.5E-3,
      1            20.2E-3, 20.9E-3, 21.6E-3, 22.4E-3, 23.2E-3,
      2            24.0E-3, 24.9E-3, 25.8E-3, 26.7E-3, 27.6E-3 /
       ISUB = 3. + (TEMP -A(2)) / A(1)
       B = ISUB - 3
       TLOW = A(2) + B * A(1)
       THIGH = TLOW + A(1)
       AKSD = A(ISUB) + (TEMP - TLOW) / (THIGH - TLOW)
      1       * (A(ISUB+1) - A(ISUB))
       RETURN
       END
C  ------------------------------
       FUNCTION AMUAD(TEMP)
C  ------------------------------
C  CALCULATION OF VISCOSITY OF AIR
C
       DIMENSION  A(11)
       DATA A/20.,  0., 0.01718, 0.01813, 0.01906, 0.01999, 0.02087,
      1       0.02173, 0.02258, 0.02343, 0.02428/
       ISUB = 3. + (TEMP -A(2)) / A(1)
       B = ISUB - 3
       TLOW = A(2) + B * A(1)
       THIGH = TLOW + A(1)
       AMUAD = A(ISUB) + (TEMP - TLOW) / (THIGH - TLOW)
      1       * (A(ISUB+1) - A(ISUB))
       AMUAD = AMUAD + 1.0E-3
       RETURN
       END
C  ------------------------------
       FUNCTION AMULD(TEMP)
C  ------------------------------
C  CALCULATION OF VISCOSITY OF LIQUID (WATER)
C
       DIMENSION  A(11)
       DATA A/20.,  0., 1.787, 1.0019, 0.653, 0.4665, 0.3548, 0.2821,
      1       0.2319, 0.1941, 0.1677/
       ISUB = 3. + (TEMP -A(2)) / A(1)
       B = ISUB - 3
       TLOW = A(2) + B * A(1)
       THIGH = TLOW + A(1)
       AMULD = A(ISUB) + (TEMP - TLOW) / (THIGH - TLOW)
      1       * (A(ISUB+1) - A(ISUB))
       AMULD = AMULD + 1.0E-3
       RETURN
       END
C  ------------------------------
```

```
      DATA  A / 5.,      5.,    2489.6, 2477.7, 2465.8, 2454.1,
     1          2442.3, 2430.5, 2418.6, 2406.7, 2394.8, 2382.7,
     2          2370.7, 2358.5, 2346.2, 2333.8, 2321.4, 2308.8,
     3          2296.0, 2283.2, 2270.2, 2257.0, 2243.7, 2230.2,
     4          2216.5, 2202.6, 2188.5, 2174.2, 2159.6, 2144.7,
     5          2129.6/
      ISUB = 3. + (TEMP -A(2)) / A(1)
      B = ISUB - 3
      TLOW = A(2) + B * A(1)
      THIGH = TLOW + A(1)
      HEVAPD = A(ISUB) + (TEMP - TLOW) / (THIGH - TLOW)
     1       * (A(ISUB+1) - A(ISUB))
      HEVAPD = HEVAPD * 1000.0
      RETURN
      END
C  ------------------------------
      FUNCTION HSTEAM(TEMP)
C  ------------------------------
C  CALCULATION OF STEAM ENTHALPY
C
      DIMENSION  A(36)
      DATA A/5.,  5., 2510.6, 2519.8, 2528.9, 2538.1, 2547.2, 2556.3,
     1       2563.3,  2574.3, 2583.2, 2592.1, 2600.8, 2609.6, 2618.3,
     2       2626.8,  2635.3, 2643.7, 2651.8, 2660.1, 2668.1, 2676.1,
     3       2683.8,  2691.5, 2699.0, 2706.3, 2713.5, 2720.5, 2727.3,
     4       2733.8,  2740.3, 2746.5, 2752.4, 2758.1, 2763.5, 2768.7/
      ISUB = 3. + (TEMP -A(2)) / A(1)
      B = ISUB - 3
      TLOW = A(2) + B * A(1)
      THIGH = TLOW + A(1)
      HSTEAM = A(ISUB) + (TEMP - TLOW) / (THIGH - TLOW)
     1       * (A(ISUB+1) - A(ISUB))
      HSTEAM = HSTEAM * 1000.0
      RETURN
      END
C  ------------------------------
      FUNCTION SVSD(TEMP)
C  ------------------------------
C  CALCULATION OF SPECIFIC VOLUME OF STEAM
C
      DIMENSION  A(37)
      DATA A    / 5.,      0.,    206.14, 147.12, 106.38, 77.83, 57.79,
     1          43.36,  32.89,   25.22,  19.52,  15.26,  12.03, 9.558,
     2            7.671,  6.197,  5.042,  4.131,  3.407,  2.828,
     3            2.361,  1.982,  1.6729, 1.4194, 1.2102, 1.0380,
     4            0.8919, 0.7706, 0.6685, 0.5822, 0.5089, 0.4463,
     5            0.3928, 0.3468, 0.3071, 0.2727, 0.2428/
      ISUB = 3. + (TEMP -A(2)) / A(1)
      B = ISUB - 3
      TLOW = A(2) + B * A(1)
      THIGH = TLOW + A(1)
      SVSD = A(ISUB) + (TEMP - TLOW) / (THIGH - TLOW)
     1       * (A(ISUB+1) - A(ISUB))
      RETURN
      END
```

```
      PREF=P(IPREF,JPREF)
      DO 83 J=1,M1
      DO 83 I=1,L1
   83 P(I,J)=P(I,J)-PREF
   96 CONTINUE
C
      WRITE(14,50)
      IEND=0
  301 IF(IEND.EQ.L1) GO TO 310
      IBEG=IEND+1
      IEND=IEND+7
      IEND=MIN0(IEND,L1)
      WRITE(14,50)
      WRITE(14,51) (I, I=IBEG,IEND)
      IF(MODE.EQ.3) GO TO 302
      WRITE(14,52) (X(I),I=IBEG,IEND)
      GO TO 303
  302 WRITE(14,53) (X(I),I=IBEG,IEND)
  303 GO TO 301
  310 JEND=0
      WRITE(14,50)
  311 IF(JEND.EQ.M1) GO TO 320
      JBEG=JEND+1
      JEND=JEND+7
      JEND=MIN0(JEND,M1)
      WRITE(14,50)
      WRITE(14,54) (J,J=JBEG,JEND)
      WRITE(14,55) (Y(J),J=JBEG,JEND)
      GO TO 311
  320 CONTINUE
C
      DO 999 NF=1,NGAM
      IF(.NOT.LPRINT(NF)) GO TO 999
      WRITE(14,50)
      WRITE(14,10) TITLE(NF)
      IFST=1
      JFST=1
      IF(NF.EQ.1.OR.NF.EQ.3) IFST=2
      IF(NF.EQ.2.OR.NF.EQ.3) JFST=2
      IBEG=IFST-7
  110 CONTINUE
      IBEG=IBEG+7
      IEND=IBEG+6
      IEND=MIN0(IEND,L1)
      WRITE(14,50)
      WRITE(14,20) (I,I=IBEG,IEND)
      WRITE(14,30)
      JFL=JFST+M1
      DO 115 JJ=JFST,M1
      J=JFL-JJ
      WRITE(14,40) J,(P(I,J,NF),I=IBEG,IEND)
  115 CONTINUE
      IF(IEND.LT.L1) GO TO 110
  999 CONTINUE
      RETURN
```

```
      DATA G, BETA, FACTOR /9.8, 0.00367, 0.5/
      DATA FRATIO, CRWERE /0.8, 100.0/
C-----------------------------------------------------------------------
      ENTRY GRID
C-----------------------------------------------------------------------
      MODE = 2
      YL = 0.83
      XL = 0.144
      WRITE(*,*) 'PLS TYPE LASTM1,  GAMMA FOR NODE SPACING?'
      READ(*,*) LASTM1, GAMMA
      L1 = 33
      IF (GAMMA. EQ. 1) THEN
       CALL UGRID
      ELSE
       YY(2) = 0.181
       DO 8 I = 3, 8
        YY(I) = YY(I-1) + 0.4415
    8  CONTINUE
       DO 9 I = 8,7
        YY(I) = YY(I-1) + 0.4415/2.
    9  CONTINUE
       DO 10 I = 8,10
        YY(I) = YY(I-1) + 0.4415/3.
   10  CONTINUE
       YSPACE = (0.4415) * (GAMMA-1.)/(GAMMA**(LASTM1)-1.)
       WRITE(14,*) 'LASTM1, YSPACE=', LASTM1, YSPACE
       YSPACE = YSPACE*(GAMMA**(LASTM1-1))
       DO 11 I = 11, 10+LASTM1
        YY(I) = YY(I-1) + YSPACE
        YSPACE = YSPACE/GAMMA
   11  CONTINUE
        M1 = 10 + LASTM1
       XU(2) = 0.
       XU(3) = 2.8 E-3
       DX = 0.3048
       DO 13 I = 4,L1
        XU(I) = XU(I-1) + DX
   13  CONTINUE
       XL = XU(L1)
      END IF
      RETURN
C-----------------------------------------------------------------------
      ENTRY START
C-----------------------------------------------------------------------
      WRITE(*,*) 'PLS TYPE LAST, LASOUT'
      READ (*,*)  LAST, LASOUT
      TWALL = 87.4
      TS = 194.8
      TI = 98.8
      PTOTAL = 0.1536
      CALL SAT (TS,PS,DPS)
      PA = PTOTAL - PS
      AMFSS = (PS*AMWS)/(PS*AMWS+PA*AMWA)
      WRITE (14,100) TWALL, TS, TI, VIN, PTOTAL, LAST, LASOUT
  100 FORMAT ( ' INPUT DATA', /, ' TWALL=', E12.3,'  TS=',E12.3,
```

```
      117 CONTINUE
          TICAL(1) = TWALL
C---------CALCULATE THE RATE OF INFLOW AND OUTFLOW
C           AND MATCH THE INFLOW RATE TO THE OUTFLOW RATE--------
          FIY = 0.0
          FIX = 0.0
          DO 118 I=13,22
      118 FIY = FIY + RHO(I,1)*V(I,2)*XCV(I)*R(1)
          DO 119 J=2,M2
      119 FIX = FIX + RHO(1,J)*U(2,J)*YCVR(J)
          DO 120 I = 2, 12
      120 FIX = FIX + RHO(I,1)*V(I,2)*XCV(I)*R(1)
          DO 121 I = 23, L2
      121 FIX = FIX + RHO(I,1)*V(I,2)*XCV(I)*R(1)
          FOY = 0.
          FOX = 0.
          DO 122 I=2,L2
      122 FOY = FOY + RHO(I,M1)*V(I,M1)*XCV(I)*R(M1)
          DO 123 J=2,M2
      123 FOX = FOX + RHO(L1,J)*U(L1,J)*YCVR(J)
          FIN = FIY
          FOUT = FOX-FIX+FOY
          ALPHA = FOUT/FIN
          DO 124 I = 13, 22
           V(I,2) = V(I,2) * ALPHA
      124 CONTINUE
           DO 125 J=1,M1
           DO 125 I=1,L1
           RHO(I,J) = DENSOB
           TKE(I,J) = 0.0001 * V(I,2)**2.
      125  DIS(I,J) = 0.1 * TKE(I,J)**2.
          TICAL(1) = TWALL
          CD = 0.09
          C1 = 1.44
          C2 = 1.92
          PRT = 0.85 + 0.01/PRNUM
          SCT = 0.85 + 0.01/SCNUM
          PRK = 1.
          PRD = 1.3
          PR = PRNUM
          SC = SCNUM
          PRPRT = PR/PRT
          PPFN = 9.*(PRPRT-1.)/PRPRT**0.25
          SCSCT = SC/SCT
          SSFN = 9.*(SCSCT-1.)/SCSCT**0.25
          CD4 = CD**0.25
          DO 130 I = 1, L1
           PFN(I) = PPFN
           SFN(I) = SSFN
           ACON(I) = 0.
      130 CONTINUE
          WRITE(*,*) 'DO YOU WANT TO READ THE RESULT OF THE PREVIOUS CALT'
          WRITE(*,*) '(YES = 1,  NO = 2)'
          READ(*,*) IREAD
          IF (IREAD .EQ. 1) THEN
```

```
1156            AMF(I,1) = AMFSS
1157           TKE(I,1) = 0.0001*V(I,2)**2.
1158           DIS(I,1) = 0.1 * TKE(I,1)**2.
1159       231 CONTINUE
1160       C ----------CALCULATE THE BOUNDARY CONDITION FOR TOP SURFACE----------
1161           DO 251 J = 2, M2
1162            T(L1,J) = T(L2,J)
1163            IF (J .LE. 8) T(L1,J) = TS
1164            AMF(L1,J) = AMF(L2,J)
1165            IF (J .LE. 8) AMF(L1,J) = AMFSS
1166            TKE(L1,J) = TKE(L2,J)
1167            DIS(L1,J) = DIS(L2,J)
1168       251 CONTINUE
1169
1170       C----------CALCULATE THE RATE OF INFLOW AND OUTFLOW----------
1171           FOY= 0.0
1172           DO 256 I = 2, L2
1173       256 FOY = FOY + RHO(I,M1)*V(I,M1)*XCV(I)*R(M1)
1174           IF (ABS(FOY/FIN).LE. 1.0) THEN
1175           FIN = FIY
1176           FOUT = FOX - FIX + FOY
1177           ALPHA = FOUT/FIN
1178           DO 258 I = 13, 22
1179           V(I,2) = UORIG(I) * ALPHA
1180       258 CONTINUE
1181           ELSE
1182            WRITE(*,*) 'FOY, FIN', FOY, FIN
1183            WRITE(12,*) 'WARNINIG: FOY IS LARGER THAN 1.0*FOUT'
1184           END IF
1185           WRITE(*,*)'FOY=',FOY,'FIN=',FIN,'U(3,M2)=',U(3,M2),'ALPHA=',ALPHA
1186           WRITE(*,*) 'U(L1,M3)=', U(L1,M3)
1187       C   ------------------------------------------------------------------
1188       C   CALCULATE THE BOUNDARY CONDITION FOR RIGHT (CONDENSATE FILM)
1189       C   SURFACE AT THE END OF INNER CALCULATION
1190       C   ------------------------------------------------------------------
1191           IF (ITER .NE. LAST) RETURN
1192           DO 260 I = 2, L1
1193           IF (XPLUS(I) .LE. 11.5) THEN
1194            AKTG = AKG
1195           ELSE
1196            AKTG = CPG * AMUG*XPLUS(I)
1197          1         / (PRT*(2.5*LOG(ACON(I)*XPLUS(I))+PFN(I)))
1198           END IF
1199       260 Q(I) = HPRIM*(AMDOT(I))*AKTG*(T(I,M2)-T(I,M1))*XCV(I)/YDIF(M1)
1200           CALL FILM1N
1201           CALL FILM1A
1202           DO 261 I=1,L1
1203            CALL SAT(TICAL(I), PSI, DPSI)
1204            PAI = PTOTAL - PSI
1205            AMFSIC(I) = (PSI*AMWS) / (PSI*AMWS+PAI*AMWA)
1206            AMF(I,M1) = AMFSIC(I)
1207       261 T(I,M1) = TICAL(I)
1208           GAMF = 0.0
1209           DO 262 I=2,L2
1210           REK(I) = 4.* DEL(I) * CD**0.25*TKE(I,M2)**0.5
```

```
      DO 331 I = 2, L2
       IF (XPLUS(I) .LE. 11.5) THEN
        AKTS = AK0
       ELSE
        AKTS = CP0 * AMUO*XPLUS(I)
     1        / (PRT*(2.5*LOG(ACON(I)*XPLUS(I))+PFN(I)))
       END IF
       Q(I) = HPRIM*(AMDOT(I))*AKTS*(T(I,M2)-T(I,M1))*XCV(I)/YDIF(M1)
       HNU= (DENSL*(DENSL-DENSGB)*(G)*HPRIM*AKL**3/(4.*AMUL*X(I)
     1       *(TS-TWALL)))**(0.25)
       QNU = HNU * (TS-TWALL) * XCV(I)
       QTOT = QTOT + Q(I)
       QNUTOT = QNUTOT + QNU
       HGAS = Q(I) / XCV(I) / (TS-T(I,M1))
       HFILM = Q(I) / XCV(I) / (T(I,M1)-TWALL)
       HOVER = HFILM*HGAS / (HFILM+HGAS)
       WRITE(12,333) X(I), Q(I), HFILM, HGAS, HOVER, XPLUS(I)
       WRITE(16,*) X(I), HOVER
  331 CONTINUE
  333 FORMAT(6E15.7)
      RTOT = QTOT / QNUTOT
      WRITE (12,*) ' RATE OF THE TOTAL CALCULATED TO NUSSELT=', RTOT
      WRITE (12,*) ' TOTAL HEAT TRANSFERED BY NUSSELT CAL   =', QNUTOT
      DO 332 J = 1, M1
       WRITE(22,*) Y(J), T(15,J)
       WRITE(23,*) Y(J), AMF(15,J)
       WRITE(24,*) Y(J), U(15,J)
  332 CONTINUE
      WRITE(12,334)
  334 FORMAT(///,5X, 'X(I)', 11X, 'TICAL(I)', 7X, 'VDELTA(I)',
     1       6X, 'VLAVG(I)', 7X, 'AMDOT(I)', 6X, 'DEL(I)')
      DO 338 I = 2, L2
       WRITE(12,333) X(I),TICAL(I),VDELTA(I),VLAVG(I),AMDOT(I),DEL(I)
  338 CONTINUE
      WRITE(12,336)
  336 FORMAT(///,5X, 'X(I)', 11X, 'REX(I)', 9X, 'REFILM(I)', 6X,
     1              'ACON(I)', 8X, 'PFN(I)', 9X, 'SFN(I)')
      DO 337 I = 2, L2
       WRITE(12,333) X(I), REX(I), REFILM(I), ACON(I), PFN(I), SFN(I)
  337 CONTINUE
      WRITE(12,338)
  338 FORMAT(///,5X, 'X(I)', 11X, 'APLUS(I)', 8X, 'XMPLUS(I)')
      DO 339 I = 2, L2
       WRITE(12,3381) X(I), APLUS(I), XMPLUS(I)
  339 CONTINUE
 3381 FORMAT(3E15.7)
      WRITE(12,3382)
 3382 FORMAT(16X, 'Y(J)', 16X, 'YPLUS(J)')
      DO 3383 J = 2, M2
       WRITE(12,3384) Y(J), YPLUS(J)
 3383 CONTINUE
 3384 FORMAT(2(E14.8, 1X))
C ------------WRITE THE RESULT FOR THE RESTART OPTION----------------
      DO 350 I = 1, L1
       DO 360 J = 1, M1
```

```
1376          GO TO 436
1377       436 CONTINUE
1378          DO 435 J = 2, 9
1379          GO TO (432,432,431,433,434,431,431) NF
1380       431 GAM(1,J)=0.
1381          GO TO 435
1382       432 YPLUS(J)=RO40(2,J)*SQRT(TKE(2,J))*CD4*XDIF(2)/AMUG
1383          GAM(1,J)=AMUG
1384          IF(YPLUS(J).GT.11.5) GAM(1,J)=AMUG*YPLUS(J)/(2.5*
1385         1LOG(9.0*YPLUS(J)))
1386          GO TO 435
1387       433 GAM(1,J)=AMUG/PR
1388          IF(YPLUS(J).GT.11.5) GAM(1,J)=AMUG/PRT*YPLUS(J)/(2.5*
1389         1LOG(9.0*YPLUS(J))+PPFN)
1390          GO TO 435
1391       434 GAM(1,J)=AMUG/SC
1392          IF(YPLUS(J).GT.11.5) GAM(1,J)=AMUG/SCT*YPLUS(J)/(2.5*
1393         1LOG(9.0*YPLUS(J))+SSFN)
1394          GO TO 435
1395       435 CONTINUE
1396          IF (NF .NE. 1) GO TO 409
1397          DO 440 J = 2,M2
1398          DO 440 I=3,L2
1399          CON(I,J)=(GAM(I,J)*(U(I+1,J)-U(I,J))/XCV(I)-
1400         1GAM(I-1,J)*(U(I,J)-U(I-1,J))/XCV(I-1))/XDIF(I)
1401          GAMP=GAM(I,J+1)*GAM(I-1,J+1)*XDIF(I)/(GAM(I,J+1)*
1402         1XCV(I)*GAM(I-1,J+1)*XCV(I-1)+1.E-30)
1403          GAMP=GAMP+GAM(I,J)*GAM(I-1,J)*XDIF(I)/(GAM(I,J)*
1404         1XCV(I)*GAM(I-1,J)*XCV(I-1)+1.E-30)
1405          GAMM=GAM(I,J-1)*GAM(I-1,J-1)*XDIF(I)/(GAM(I,J-1)*
1406         1XCV(I)*GAM(I-1,J-1)*XCV(I-1)+1.E-30)
1407          GAMM=GAMM+GAM(I,J)*GAM(I-1,J)*XDIF(I)/(GAM(I,J)*
1408         1XCV(I)*GAM(I-1,J)*XCV(I-1)+1.E-30)
1409          CON(I,J)=CON(I,J)+(RHN(J+1)*GAMP*(V(I,J+1)-V(I-1,J+1))
1410         1-RHN(J)*GAMM*(V(I,J)-V(I-1,J)))/(YCVR(J)*XDIF(I))
1411       440 CONTINUE
1412          RETURN
1413       409 IF(NF.NE.2) GO TO 410
1414          DO 466 J=3,M2
1415          DO 466 I=2,L2
1416          CON(I,J)=(R(J)*GAM(I,J)*(V(I,J+1)-V(I,J))/YCV(J)-R(J-1)*
1417         1GAM(I,J-1)*(V(I,J)-V(I,J-1))/YCV(J-1))/(RHN(J)*YDIF(J))
1418          GAMP=GAM(I+1,J)*GAM(I+1,J-1)*YDIF(J)/(GAM(I+1,J)*YCV(J)+
1419         1GAM(I+1,J-1)*YCV(J-1)+1.E-30)
1420          GAMP=GAMP+GAM(I,J)*GAM(I,J-1)*YDIF(J)/(GAM(I,J)*YCV(J)+
1421         1GAM(I,J-1)*YCV(J-1)+1.E-30)
1422          GAMM=GAM(I-1,J)*GAM(I-1,J-1)*YDIF(J)/(GAM(I-1,J)*
1423         1YCV(J)+GAM(I-1,J-1)*YCV(J-1)+1.E-30)
1424          GAMM=GAMM+GAM(I,J)*GAM(I,J-1)*YDIF(J)/(GAM(I,J)*YCV(J)+
1425         1GAM(I,J-1)*YCV(J-1)+1.E-30)
1426          CON(I,J)=CON(I,J)+(GAMP*(U(I+1,J)-U(I+1,J-1))-GAMM*(U(I,J)
1427         1-U(I,J-1)))/(XCV(I)*YDIF(J))
1428          IF(MODE.EQ.2) AP(I,J)=AP(I,J)-4.*GAM(I,J)*GAM(I,J-1)*
1429         1YDIF(J)/(GAM(I,J)*YCV(J)+GAM(I,J-1)*YCV(J-1)+1.E-30)
1430         2/RHN(J)**2
```

```
      428 IF(MF.NE.7) RETURN
          DO 490 J=2,M2
          DO 490 I=2,L2
          CON(I,J)=C1*GEN(I,J)*CD*RHO(I,J)*TKE(I,J)
          AP(I,J)=-C2*RHO(I,J)*DIS(I,J)/(TKE(I,J)+1.E-30)
      490 CONTINUE
          DO 491 I = 2, L2
          DISS=CD*TKE(I,M2)**1.5/(0.4*CD4*YDIF(M1))
          CON(I,M2)=(1.E+30)*DISS
          AP(I,M2)=-1.E+30
      491 CONTINUE
          DO 492 J = 2, 9
          DISS=CD*TKE(2,J)**1.5/(0.4*CD4*XDIF(2))
          CON(2,J)=(1.E+30)*DISS
          AP(2,J)=-1.E+30
      492 CONTINUE
          DO 510 J = 1,M1
           IF(J .GE. 10 .AND. MF .EQ. 4) GAM(L1,J) = 0.0
           IF(J .GE. 10 .AND. MF .EQ. 5) GAM(L1,J) = 0.0
           IF(J .GE. 10 .AND. MF .EQ. 1) GAM(L1,J) = 0.0
      510 CONTINUE
          DO 511 I = 1,12
           IF (MF .EQ. 1) GAM(I,1) = 0.0
      511 CONTINUE
          DO 512 I = 24, L1
           IF (MF .EQ. 1) GAM(I,1) = 0.0
      512 CONTINUE
          DO 513 J = 10, M1
           IF (MF .NE. 1) GAM(1,J) = 0.0
      513 CONTINUE
          RETURN
          END
C-----------------------------------------------------------------------
          SUBROUTINE FILM1N
C-----------------------------------------------------------------------
C
C  THIS SUBROUTINE IS PROGRAMED TO CALCULATE THE HEAT TRANSFER
C  COEFFICIENT OF THE CONDENSATE FILM AT THE FIRST NODE.
C
          IMPLICIT DOUBLE PRECISION (A-H, O-Z)
          PARAMETER (NN=100)
          COMMON F(NN,NN,9),P(NN,NN),RHO(NN,NN),GAM(NN,NN),CON(NN,NN),
         1 AIP(NN,NN),AIM(NN,NN),AJP(NN,NN),AJM(NN,NN),AP(NN,NN),
         2 X(NN),XU(NN),XDIF(NN),XCV(NN),XCVS(NN),
         3 Y(NN),YV(NN),YDIF(NN),YCV(NN),YCVS(NN),
         4 YCVR(NN),YCVRS(NN),ARX(NN),ARXJ(NN),ARXJP(NN),
         5 R(NN),RSN(NN),SX(NN),SIGMN(NN),XCVI(NN),XCVIP(NN)
          COMMON/INDX/MF,MFMAX,MP,NPHO,NGAM,L1,L2,L3,M1,M2,M3,
         1 IST,JST,ITER,LAST,TITLE(13),RELAX(13),TIME,DT,XL,YL,
         2 IPREF,JPREF,LSOLVE(11),LPRINT(13),MODE,NTIMES(11),RHOCON
          COMMON /PROP/ TBALL, TS, TREF1, TI, AMFSS, AMFSI, DENSO, DENSL,
         1              AMUG, AMUL, AKG, AKL, SAB, CPG, CPS, CPA, CPL,
         2              HPRIM, PTOTAL, AMWS, AMWA, DENSGS, AMUGS,
         3              PRNUM, SCNUM
          COMMON /FILM/ TICAL(NN), VDELTA(NN), G(NN), AJ(NN), AMDOT(NN),
```

```
      VDELTA(L2) = DENSL*GRAVG/AMUL*DEL(L2)**2/2. + TAUDEL
     1          /AMUL*DEL(L2)
C     2     '   + AKL*(TICAL(L2)-TBALL)*VIN/(AMUL*HPRIM)
      VLAVG(L2) = -DENSL*GRAVG/(6.*AMUL)*DEL(L2)**2
     1           + (DENSL*GRAVG*DEL(L2)+TAUDEL) * DEL(L2)/(2.*AMUL)
      WRITE(*,*) 'TICAL(L2)=', TICAL(L2), 'VDELTA(L2)=', VDELTA(L2),
     1           'DEL(L2)=', DEL(L2), 'FX8=', FX8, 'DELTAX= ', DELTAX,
     2           'IITER=', IITER
      RETURN
      END
C
C-----------------------------------------------------------------------
      SUBROUTINE FILMLA
C-----------------------------------------------------------------------
C
C     THIS SUBROUTINE IS PROGRAMED TO CALCULATE THE HEAT TRANSFER
C     COEFFICIENT OF THE LAMINAR CONDENSATE FILM
C
C-----------------------------------------------------------------------
      IMPLICIT DOUBLE PRECISION (A-H, O-Z)
      PARAMETER (MM=100)
      COMMON F(MM,MM,9),P(MM,MM),RHO(MM,MM),GAM(MM,MM),CON(MM,MM),
     1 AIP(MM,MM),AIM(MM,MM),AJP(MM,MM),AJM(MM,MM),AP(MM,MM),
     2 X(MM),XU(MM),XDIF(MM),XCV(MM),XCVS(MM),
     3 Y(MM),YV(MM),YDIF(MM),YCV(MM),YCVS(MM),
     4 YCVR(MM),YCVRS(MM),ARX(MM),ARXJ(MM),ARXJP(MM),
     5 R(MM),RMM(MM),SX(MM),SXMM(MM),XCVI(MM),XCVIP(MM)
      COMMON/INDX/NF,NFMAX,MP,MRHO,NGAM,L1,L2,L3,M1,M2,M3,
     1 IST,JST,ITER,LAST,TITLE(13),RELAX(13),TIME,DT,XL,YL,
     2 IPREF,JPREF,LSOLVE(11),LPRINT(13),MODE,NTIMES(11),RHOCON
      COMMON /PROP/ TBALL, TS, TREF1, TI, AMFSB, AMFSI, DENSG, DENSL,
     1              AMUG, AMUL, AKG, AKL, DAB, CPG, CPS, CPA, CPL,
     2              HPRIM, PTOTAL, AMFS, AMRA, DENSGB, AMUGB,
     3              PRNUM, SCNUM
      COMMON /FILM/ TICAL(MM), VDELTA(MM), G(MM), AJ(MM), AMDOT(MM),
     1               DEL(MM), FACTOR, XPLUS(MM), REX(MM), REFILM(MM),
     2               ACON(MM), PFN(MM), SFN(MM), VLAVG(MM), IBAYE, VIN
      DIMENSION U(MM,MM),V(MM,MM),PC(MM,MM)
      EQUIVALENCE(F(1,1,1),U(1,1)),(F(1,1,2),V(1,1)),(F(1,1,3),PC(1,1))
      GRAVG = -9.8
      DO 900 II=2,L3
       I = L1-II
       ACONST = DENSL**2. * GRAVG / (AMUL)
       IF (XPLUS(I) .LE. 11.5) THEN
        AMUTG = AMUG
       ELSE
        AMUTG = AMUG * XPLUS(I)/(2.5*LOG(ACON(I)*XPLUS(I)))
       END IF
       TAUDEL = AMUTG * (U(I,M2) - U(I,M1))/YDIF(M1)
       BCONST =  DENSL * TAUDEL / AMUL
C       CCONST = DENSL*AKL*(TICAL(I)-TBALL)*VIN/(2.*AMUL*HPRIM)
       CCONST = 0.0
       DENOM = (ACONST*DEL(I+1)**2 + BCONST*DEL(I+1) + CCONST)
       DELTAD = -AMDOT(I) / DENOM
       DEL(I) = DEL(I+1) + DELTAD
```

```
1706          DENSSB = 1. / SVSD(TS)
1707          DENSA = (PTOTAL-PSREF1)*1.0E6 * AMWA / (8314.*(TREF1 + 273.))
1708          DENSAB = (PTOTAL-PS) * 1.0E6 * AMWA / (8314. * (TS + 273.))
1709          DENSG = DENSS + DENSA
1710          DENSGB = DENSSB + DENSAB
1711          DENSL = 1. / 0.001
1712      C
1713      C CALCULATE VISCOSITY
1714      C
1715          AMUS = 5.84E-6 + 4.67E-8 * TREF1 - DENSS * (1.858E-7 - 5.9E-10
1716         1        *TREF1)
1717          AMUA = AMUAD(TREF1)
1718          PISA = (1 + (AMUS / AMUA)**0.5 * (AMWA / AMWS)**0.25)**2 /
1719         1        (8 * (1 + AMWS / AMWA))**0.5
1720          PIAS = (1 + (AMUA / AMUS)**0.5 * (AMWS / AMWA)**0.25)**2 /
1721         1        (8 * (1 + AMWA / AMWS))**0.5
1722          AMFS = PSREF1 * AMWS / (PSREF1 * AMWS + (PTOTAL - PSREF1) * AMWA)
1723          AMFA = 1 - AMFS
1724          AMOLES = AMFS / AMWS
1725          AMOLEA = AMFA / AMWA
1726          XS = AMOLES / (AMOLES + AMOLEA)
1727          XA = AMOLEA / (AMOLES + AMOLEA)
1728          AMUG = XS * AMUS / (XS + XA*PISA) + XA * AMUA / (XA + XS*PIAS)
1729          AMUL = AMULD (TREF2)
1730      C VISCOSITY OF GAS AT BULK
1731          AMUSB = 5.84E-6 + 4.67E-8 * TS - DENSSB * (1.858E-7 - 5.9E-10
1732         1        *TS)
1733          AMUAB = AMUAD(TS)
1734          PISAB = (1 + (AMUSB / AMUAB)**0.5 * (AMWA / AMWS)**0.25)**2 /
1735         1        (8 * (1 + AMWS / AMWA))**0.5
1736          PIASB = (1 + (AMUAB / AMUSB)**0.5 * (AMWS / AMWA)**0.25)**2 /
1737         1        (8 * (1 + AMWA / AMWS))**0.5
1738          AMFSB = PS * AMWS / (PS * AMWS + (PTOTAL - PS) * AMWA)
1739          AMFAB = 1 - AMFSB
1740          AMOLSB = AMFSB / AMWS
1741          AMOLAB = AMFAB / AMWA
1742          XSB = AMOLSB / (AMOLSB + AMOLAB)
1743          XAB = AMOLAB / (AMOLSB + AMOLAB)
1744          AMUGB = XSB * AMUSB / (XSB + XAB*PISAB) + XAB * AMUAB
1745         1        / (XAB + XSB*PIASB)
1746      C
1747      C CALCULATE CONDUCTIVITY
1748      C
1749          AKS = AKSD (TREF1)
1750          AKA = AKAD (TREF1)
1751          AKG = XS * AKS / (XS + XA * PISA) + XA * AKA / (XA + XS * PIAS)
1752          AKL = AKLD(TREF2)
1753      C
1754      C CALCULATE SPECIFIC HEAT
1755      C
1756          CPS = CPSD (TREF1)
1757          CPA = CPAD (TREF1)
1758          CPG = AMFS * CPS + AMFA * CPA
1759          CPL = CPLD (TREF2)
1760      C
```

```
      SUM = 0.
      DSUM = 0.
      X = 0.65 - 0.01 * TSAT
      TAU = 1000. / (TSAT + 273.15)
      DELT = 374.136 - TSAT
      DO 1 I = 1, 8
      J = 8 - I
      IF (J .EQ. 1) GO TO 1
      DSUM = DSUM * X + (J - 1) * F(J)
    1 SUM = SUM * X + F(J)
      RES = TAU * 1.E-05 * DELT *SUM
      PSAT = EXP(RES) * 22.068
      DSUM = - 0.01 * DSUM
      RED = -1.E-05 * (TAU**2 * DELT * SUM / 1000. + TAU * SUM - TAU
     1      * DELT * DSUM)
      DPSAT = PSAT * RED
      RETURN
      END
C
C-----------------------------------------------------------------------
      SUBROUTINE SATMP (PSAT,TSAT)
C-----------------------------------------------------------------------
C
C   THIS SUBROUTINE CALCULATE SATURATION TEMPERATURE WITH GIVEN
C   SATURATION PRESSURE.
C
      IMPLICIT DOUBLE PRECISION (A-H, O-Z)
      ACCURA = 1.0E-8
      TSAT = 200.
    2 CALL SAT (TSAT, PSATA, DPSAT)
      DELP = PSAT - PSATA
      IF (ABS(DELP/PSAT).LT.ACCURA) GO TO 3
      TSAT = TSAT + DELP / DPSAT
      IF (TSAT.GT.374.136) TSAT = 374.136
      GO TO 2
    3 RETURN
      END
C     ------------------------
      FUNCTION AKAD(TEMP)
C     ------------------------
C   CALCULATION OF THERMAL CONDUCTIVITY OF AIR
C
      IMPLICIT DOUBLE PRECISION (A-H, O-Z)
      DIMENSION  A(15)
      DATA A    / 10.0,   10.0,   0.0249, 0.0256, 0.0264,
     1            0.0271, 0.0278, 0.0285, 0.0292, 0.0299,
     2            0.0306, 0.0313, 0.0320, 0.0327, 0.0334 /
      ISUB = 3. + (TEMP -A(2)) / A(1)
      B = ISUB - 3
      TLOW = A(2) + B * A(1)
      THIGH = TLOW + A(1)
      AKAD = A(ISUB) + (TEMP - TLOW) / (THIGH - TLOW)
     1       * (A(ISUB+1) - A(ISUB))
      RETURN
      END
```

```
      FUNCTION AMULD(TEMP)
C     ------------------------------
C     CALCULATION OF VISCOSITY OF LIQUID (WATER)
C
      IMPLICIT DOUBLE PRECISION (A-H, O-Z)
      DIMENSION  A(11)
      DATA A/20.,  0., 1.787, 1.0010, 0.653, 0.4665, 0.3548, 0.2821,
     1       0.2318, 0.1941, 0.1677/
      ISUB = 3. * (TEMP -A(2)) / A(1)
      S = ISUB - 3
      TLOW = A(2) + S * A(1)
      THIGH = TLOW + A(1)
      AMULD = A(ISUB) + (TEMP - TLOW) / (THIGH - TLOW)
     1       * (A(ISUB+1) - A(ISUB))
      AMULD = AMULD * 1.0E-3
      RETURN
      END
C     ------------------------------
      FUNCTION CPAD(TEMP)
C     ------------------------------
C     CALCULATION OF SPECIFIC HEAT OF AIR
C
      IMPLICIT DOUBLE PRECISION (A-H, O-Z)
      DIMENSION  A(10)
      DATA A    / 10.0,   20.0,   1004.0, 1005.0, 1006.0,
     1            1006.0, 1009.0, 1011.0, 1013.0, 1018.0 /
      ISUB = 3. * (TEMP -A(2)) / A(1)
      S = ISUB - 3
      TLOW = A(2) + S * A(1)
      THIGH = TLOW + A(1)
      CPAD = A(ISUB) + (TEMP - TLOW) / (THIGH - TLOW)
     1       * (A(ISUB+1) - A(ISUB))
      RETURN
      END
C     ------------------------------
      FUNCTION CPSD(TEMP)
C     ------------------------------
C     CALCULATION OF SPECIFIC HEAT OF STEAM
C
      IMPLICIT DOUBLE PRECISION (A-H, O-Z)
      DIMENSION  A(15)
      DATA A    / 10.0,  15.0,  1870., 1880., 1890., 1900.,
     1            1912., 1926., 1940., 1970., 1999., 2034.,
     2            2070., 2125., 2190. /
      ISUB = 3. * (TEMP -A(2)) / A(1)
      S = ISUB - 3
      TLOW = A(2) + S * A(1)
      THIGH = TLOW + A(1)
      CPSD = A(ISUB) + (TEMP - TLOW) / (THIGH - TLOW)
     1       * (A(ISUB+1) - A(ISUB))
      RETURN
      END
C     ------------------------------
      FUNCTION CPLD(TEMP)
C     ------------------------------
```

```
2036          HSTEAM = HSTEAM * 1000.0
2037          RETURN
2038          END
2039    C     ------------------------------
2040          FUNCTION SVSD(TEMP)
2041    C     ------------------------------
2042    C  CALCULATION OF SPECIFIC VOLUME OF STEAM
2043    C
2044          IMPLICIT DOUBLE PRECISION (A-H, O-Z)
2045          DIMENSION  A(37)
2046          DATA A    / 5.,      0.,    206.14, 147.12, 106.38, 77.93, 57.79,
2047         1           43.36,  32.89,    25.22,  19.52,  15.26,  12.03, 9.658,
2048         2             7.671,  6.197,  5.042,  4.131,  3.407,  2.828,
2049         3             2.361,  1.982,  1.6729, 1.4194, 1.2102, 1.0366,
2050         4             0.8919, 0.7706, 0.6685, 0.5822, 0.5089, 0.4463,
2051         5             0.3928, 0.3468, 0.3071, 0.2727, 0.2428/
2052          ISUB = 3. + (TEMP -A(2)) / A(1)
2053          B = ISUB - 3
2054          TLOW = A(2) + B * A(1)
2055          THIGH = TLOW + A(1)
2056          SVSD = A(ISUB) + (TEMP - TLOW) / (THIGH - TLOW)
2057         1       * (A(ISUB+1) - A(ISUB))
2058          RETURN
2059          END
```

Transfer, Vol. 10, pp. 1677-1692, (1967).

[11] J.C. Koh, E.M. Sparrow and J.O. Hartnett, "The Two-Phase Boundary Layer in Laminar Film Condensation," Int. J. Heat Mass Transfer, Vol. pp. 69-82, (1961).

[12] M.M. Chen, "An Analytical Study of Laminar Film Condensation Part I - Flat Plates," J. Heat Transfer, Vol. 83, Series C, pp. 48-55, (1961).

[13] R.D. Cess, "Laminar Film Condensation on a Flat Plat in the absence of body force," Zeitschrift fur Angewandte und Physik, 11, pp. 426-433, (1960).

[14] H.W. Emmons and D.C. Leigh, "Tabulation of the Blasius Function with Blowing and Suction," Fluid Motion Sub-committee, Aeronaut. Res. Coun., Report No. FM 1915, (1953).

[15] I.G. Shekriladze and V.I. Gomelauri, "Theoretical Study of Laminar Film Condensation of Flowing Vapor," Int. J. Heat Mass Transfer, Vol. 9, pp. 581-591, (1966).

[16] Y.R. Mayhew, D.J. Griffiths and J.W. Phillips, "Effect of Vapor Drag on Laminar Film Condensation on a Vertical Surface," Proc. Instn. Mech. Engrs., Vol. 180, Part 3J, pp. 280-289, (1965-1966).

[17] Y.R. Mayhew, "Comments on the paper 'Theoretical Study of Laminar Film Condensation of Flowing Vapor' (by I.G. Shekriladze and V.I. Gomelauri)," Int. J. Heat Mass Transfer, Vol. 10, pp. 107-108, (1967).

[18] Y.R. Mayhew and J.K. Aggarwal, " Laminar Film Condensation with Vapor Drag on a Flat Surface," Int. J. Heat Mass Transfer, Vol. 16, pp. 1944-1949, (1973).

[19] V. South III and V.E. Denny, "The Vapor Shear Boundary Condition for Laminar Film Condensation," Trans. ASME, 94, pp. 248-249, (1972).

[20] H.R. Jacobs, "An Integral Treatment of Combined Body

of a Noncondensing Gas," Int. J. Heat Mass Transfer, Vol. 12, pp. 233-237, (1969)

[29] E.M. Sparrow, W.J. Minkowycz and M. Saddy, "Forced Convection in the Presence of Noncondensables and Interfacial Resistance," Int. J. Heat Mass Transfer., Vol. 10, pp. 1829-1845, (1967).

[30] J.C.Y. Koh, " Laminar Film Condensation of Condensable Gases and Gaseous Mixture on a Flat Plate," Proc. 4th U.S.A. Nat. Cong. Appl. Mech., 2, pp. 1327-1336, (1962).

[31] T. Fujii, M. Uehara, K. Mihara and Y. Kato, "Forced Convection in the Presence of Non-condensables - a Theoretical Treatment for Two-phase Laminar Boundary Layer (In Japanese)," University of Kyushu Research Institute of Industrial Science, Report No. 66, pp 53-80, (1977).

[32] J.W. Rose, "Approximate Equations for Forced - Convection Condensation in the Presence of a Noncondensing Gas on a Flat Plate and Horizontal Tube," Int. J. Heat Mass Transfer, Vol. 23, pp. 539-546, (1980).

[33] J.W. Rose, "Boundary Layer Flow with Transpiration on an Isothermal Flat Plate," Int. J. Heat Mass Transfer, Vol. 22, pp. 1243-1244,(1979).

[34] V.E. Denny, A.F. Mills and V.J. Jusionis, "Laminar Film Condensation from a Steam-Air Mixture UndergoingForced Flow Down a Vertical Surface," J. Heat Transfer, Vol. 93, pp. 297-304, (1971).

[35] V.E. Denny and V.J. Jousionis, "Effects of noncondensable gas and forced flow on laminar film condensation," Int. J. Heat Mass Transfer, Vol. 15, pp. 315-326, (1972).

[36] K. Asano and Y. Nakano, "Fored Convection Film Condensation of Vapors in the Presence of

[46] L. Sleger and R.A. Seban, "Laminar Film Condensation of Steam Containing Small Concentrations of Air," Int. J. Heat Mass Transfer, Vol. 13, pp. 1941-1947, (1970).

[47] M.M. Al-Diwany and J.W. Rose, "Free Convection Film Condensation of Steam in the Presence of Noncondensing Gases," Int. J. Heat Mass Transfer, Vol. 16, pp. 1359-1369, (1973).

[48] A.C. DeVuono and R.N. Christensen, "Experimental Investigation of the Pressure Effects on Film Condensation of Stem-Air Mixtures at Pressure above Atmospheric," Fundamentals of Phase Change: Boiling and Condensation, The Winter Annual Meeting of ASME, New Orleans, Louisiana, HTD-Vol. 38, (1984).

[49] J.W. Rauscher, A.F. Mills and V.E. Denny, "Experimental Study of Film Condensation from Steam-Air Mixtures Flowing Downward over a Horizontal Tube," J. Heat transfer, Vol. 96, pp. 83-88, (1974).

[50] V.E. Denny and V. South III, "Effects of Forced Flow, Noncondensable and Variable Properties on Film Condensation of Pure and Binary Vapors at the Forward Stagnation Point of a Horizontal Cylinder," Int. J. Heat Mass Transfer, Vol. 15, pp. 2133-2142, (1972).

[51] V.G. Levich, Physicochemical Hydrodynamics, Prentice-Hall, Inc., (1962).

[52] T.B. Benjamin, "Wave Formation in Laminar Flow Down an Inclined Plane," J. Fluid Mechnics, Vol. 2, pp. 554-574, (1957).

[53] P.L. Kapitza, "Wave Flow of Thin Layers of a Viscous Fluid," Collected Papers of P.L. Kapitza, Vol. II, Macmillan, New York, (1964).

[54] C. Massot, F. Irani and E.N. Lightfoot, "Modified

Element Method," Int. J. Heat Mass Transfer, Vol. 27, pp. 815-827, (1984).

[64] L.S. Cohen and T.J. Hanratty, "Effect of Waves at a Gas-Liquid Interface on a Turbulent Air Flow," J. Fluid Mech. Vol. 31, pp. 467-479, (1968).

[65] G.B. Wallis, "Annular Two-Phase Flow - Part 1: A Simple Theory," Paper No. 69-FE-45, 69-FE-46, ASME Applied Mech.-Fluids Engg. Conf., Northwestern University, (1969).

[66] L.F. Moody and M.J. Princeton, "Friction Factors for Pipe Flow," Trans. ASME, Vol. 66, pp. 671-684, (1944).

[67] C.G. Kirkbride, "Heat Transfer by Condensing Vapor on Vertical Tubes," Trans. AIChE, Vol. 30, pp. 170, (1933-1934).

[68] A.P. Colburn, "The Calculation of Condensation Where a Portion of the Condensate Layer is in Turbulent Motion," Trans. AIChE, Vol. 30, pp. 187, (1933-1934).

[69] E.F. Carpenter and A.P. Colburn, "The Effect of Vapor Velocity on Condensation inside Tubes," Proc. of General Discussion on Heat Transfer, IMechE/ASME, pp. 20-26, (1951).

[70] R.A. Seban, "Remarks on Film Condensation with Turbulent Flow," Trans. ASME, Vol. 76, pp. 299-303, (1954).

[71] W.M. Rohsenow, J.H. Webber and A.T. Ling, "Effect of Vapor Velocity on Laminar and Turbulent Film Condensation," Trans. ASME, Vol. 78, pp. 1637-1643, (1956).

[72] A.E. Dukler, "Fluid Mechanics and Heat Transfer in Vertical Falling Film Systems," Chem. Eng. Progr. Symposium Ser., No. 30, pp. 1-10, (1960).

[73] Jon Lee, "Turbulent Film Condensation," AIChE

of Turbulence," Int. J. Heat Mass Transfer, Vol. 16, pp. 1119-1130, (1973).

[84] C.C. Chieng and B.E. Launder, "On the Calculation of Turbulent Heat Transport Downstream from an Abrupt Pipe Expansion," Numer. Heat Transfer, Vol. 3, pp. 189-207, (1980).

[85] P.L. Stephenson, "A Theoretical Study of Heat Transfer in Two-Dimensional Turbulent Flow in a Circular Pipe and between Parallel and Diverging Plates," Int. J. Heat Mass Trans., Vol. 19, pp. 413-423, (1975).

[86] R.S. Amano and K.F. Neusen, "A Numerical and Experimental Investigation of High Velocity Jets Impinging on a Flat Plate," Proc. 6th Int. Symp. Jet Cutting Technol., pp. 107-122, (1982).

[87] R.S. Amano, "Development of a Turbulence Near-Wall Model and Its Application to Separated and Reattached Flows," Numerical Heat Transfer, Vol. 7, pp. 59-75, (1984).

[88] T. Cebeci, "Behavior of Turbulent Folw near a Porous Wall with Pressure Gradient," AIAA Journal, Vol. 8, pp. 2152-2156, (1970).

[89] W.M Kays, "Heat Transfer to the Transpired Turbulent Boundary Layer," Int. J. Heat Mass Transfer, Vol. 15, pp. 1023-1044 (1972).

[90] B.E. Launder and C.M. Priddin, "The Near Wall Mixing Length Profile - A Comparison of Some Variants of Van Driest's Proposal," Dept. Mech. Engineering, Imperial College, London, TM/TN/A/15, (1971).

[91] S.V. Patankar and D.B. Spalding, Heat and Mass Transfer in Boundary Layers, Morgan-Grampian, London, (1967).

[92] U. Renz and H.P. Odenthal, "Numerical Prediction of Heat and Mass Transfer during Condensation from a

C-Series Test Results, NUREG/CR-2177, LA-8866-MS, (1981).

[103] K. Almenas and Un Chul Lee, "A Statistical Evaluation of the Heat Transfer Data Obtained in the HDR Containment Tests," University of Maryland, (1984).

[104] B.E. Anshus, "Finite Amplitude Wavy Flow on a Thin Film on a Vertical Wall," Ph. D. Dissertation, Univ. of Calif., Berkeley, (1965).

[105] K. Javdani and S.L. Goren, "Finite Amplitude Wavy Flow on Thin Films," Intern. Symp. Two-Phase System, Haifa, Israel, (1971).

[106] A.P. Colburn, T.H. Chilton, "Mass Transfer(Absorption) Coefficients - Prediction from Data on Heat Transfer and Fluid Friction," Ind. Eng. Chem., Vol. 26, pp. 1183- 1187, (1934).

[107] J.P. Holman, Heat Transfer, New York, McGraw-Hill (1976).

[108] A.J. Reynolds, "The Prediction of Turbulent Prandtl and Schmidt Number," Int. J. Heat Mass Transfer, Vol. 18, pp. 1055-1069 (1975).

[109] M. Jischa and H. B. Rieke, "About the Prediction of Turbulent Prandtl and Schmidt Number from Modeled Transport Equations," Int. J. Heat Mass Transfer, Vol. 22, pp. 1547-1555 (1979).

[110] W. M. Rohsenow and H. Choi, Heat, Mass and Momentum Transfer, Prentice-Hall Publishers, New Jersey (1961).

[111] M Graber, "Der Warmeubergang in Glatten Rohren, Zwischen Parallelen Platterm, in Ringspalten und Langs Rohrbundeln bei Exponentieller Warmeflu Vertet Mass Transfer, Vol. 18, pp. 1055-1069 (1975).

[112] R.B. Bird, W.E. Stewart and E.N. Lightfoot, Transport Phenomena, John Wiley & Sons, (1960).

XX

an Impinging Round Hot Gas Jet of Low Reynolds Number," Int. J. Heat Mass Transfer, Vol. 23 pp. 1055-1068, (1980).